AD-A196 878

(4)

David Taylor Research Center
Bethesda, MD 20084-5000

DTIC FILE COPY

DTRC/SME-86/108 April 1988

Ship Materials Engineering Department
Research and Development Report

Electrochemical Impedance of Organic Coated Steel: Correlation of Impedance Parameters with Long Term Coating Deterioration

by
John R. Scully

DTIC
ELECTE
JUN 27 1988
S D

DTRC/SME-86/108 Electrochemical Impedance of Organic Coated Steel: Correlation of Impedance Parameters with Long Term Coating Deterioration

Approved for public release; distribution unlimited.

88

MAJOR DTRC TECHNICAL COMPONENTS

CODE 011 DIRECTOR OF TECHNOLOGY, PLANS AND ASSESSMENT

12 SHIP SYSTEMS INTEGRATION DEPARTMENT

14 SHIP ELECTROMAGNETIC SIGNATURES DEPARTMENT

15 SHIP HYDROMECHANICS DEPARTMENT

16 AVIATION DEPARTMENT

17 SHIP STRUCTURES AND PROTECTION DEPARTMENT

18 COMPUTATION, MATHEMATICS & LOGISTICS DEPARTMENT

19 SHIP ACOUSTICS DEPARTMENT

27 PROPULSION AND AUXILIARY SYSTEMS DEPARTMENT

28 SHIP MATERIALS ENGINEERING DEPARTMENT

DTRC ISSUES THREE TYPES OF REPORTS:

1. **DTRC *reports*, *a formal series*,** contain information of permanent technical value. They carry a consecutive numerical identification regardless of their classification or the originating department.

2. **Departmental reports, a semiformal series,** contain information of a preliminary, temporary, or proprietary nature or of limited interest or significance. They carry a departmental alphanumerical identification.

3. **Technical memoranda, an informal series,** contain technical documentation of limited use and interest. They are primarily working papers intended for internal use. They carry an identifying number which indicates their type and the numerical code of the originating department. Any distribution outside DTRC must be approved by the head of the originating department on a case-by-case basis.

NDW-DTNSRDC 5602-51 (Rev 2-88)

UNCLASSIFIED

SECURITY CLASSIFICATION OF THIS PAGE

REPORT DOCUMENTATION PAGE

1a. REPORT SECURITY CLASSIFICATION	1b RESTRICTIVE MARKINGS
2a. SECURITY CLASSIFICATION AUTHORITY	3 DISTRIBUTION / AVAILABILITY OF REPORT Approved for public release; distribution unlimited.
2b. DECLASSIFICATION / DOWNGRADING SCHEDULE	
4. PERFORMING ORGANIZATION REPORT NUMBER(S) DTRC/SME-86/108	5 MONITORING ORGANIZATION REPORT NUMBER(S)
6a NAME OF PERFORMING ORGANIZATION David Taylor Research Center 6b OFFICE SYMBOL (If applicable)	7a NAME OF MONITORING ORGANIZATION
6c ADDRESS (City, State, and ZIP Code) Bethesda, MD 20084-5000	7b ADDRESS (City, State, and ZIP Code)
8a NAME OF FUNDING / SPONSORING ORGANIZATION David Taylor Research Center 8b OFFICE SYMBOL (If applicable) Code 0.12	9 PROCUREMENT INSTRUMENT IDENTIFICATION NUMBER
8c. ADDRESS (City, State, and ZIP Code) Bethesda, MD 20084-5000	10 SOURCE OF FUNDING NUMBERS PROGRAM ELEMENT NO: 62761N PROJECT NO: TASK NO: SF 61-541-491 WORK UNIT ACCESSION NO:

11. TITLE (Include Security Classification)
Electrochemical Impedance of Organic Coated Steel: Correlation of Impedance Parameters with Long-Term Coating Deterioration

12. PERSONAL AUTHOR(S)
John R. Scully

13a. TYPE OF REPORT	13b TIME COVERED	14 DATE OF REPORT (Year, Month, Day)	15 PAGE COUNT
Research & Development	FROM _____ TO _____	1988 April	103

16. SUPPLEMENTARY NOTATION

17. COSATI CODES			18 SUBJECT TERMS (Continue on reverse if necessary and identify by block number)
FIELD	GROUP	SUB-GROUP	AC ~~impedance~~ Corrosion Electrochemical impedance Anti-corrosion coating Organic coating ~~Impedance~~

19. ABSTRACT (Continue on reverse if necessary and identify by block number)

Electrochemical impedance results are presented for 550 day exposures of organic coated carbon steel samples. Coatings consisted of translucent pigmented and unpigmented epoxy and conventional opaque epoxy polyamide systems. Coating thicknesses ranged from 20 to 185 microns. Specimens were exposed under freely corroding conditions and at two cathodic polarization levels (-805 mV and -1250 mV versus SCE) in ASTM artificial ocean water. The objective was to identify impedance parameters which measure subcritical coated-metal system property changes at early exposure times that are indicators of significant long term coating deterioration. Impedance data developed at early times, including coating resistance, coating capacitance, the increase in frequency associated with the coating's resistive-capacitive (RC) 45 degree phase angle, and low frequency impedance data, are compared to the coating system's performance evaluated after 550 days exposure. Coating performance at 550 days is visually evaluated using ASTM Method D-610, ~~and~~ a modification of ASTM D-714.

(continued on reverse side)

20 DISTRIBUTION / AVAILABILITY OF ABSTRACT	21 ABSTRACT SECURITY CLASSIFICATION
☐ UNCLASSIFIED/UNLIMITED ☒ SAME AS RPT ☐ DTIC USERS	UNCLASSIFIED
22a NAME OF RESPONSIBLE INDIVIDUAL John R. Scully	22b TELEPHONE (Include Area Code) / 22c OFFICE SYMBOL

DD FORM 1473, 84 MAR 83 APR edition may be used until exhausted
All other editions are obsolete

SECURITY CLASSIFICATION OF THIS PAGE

☆U.S. Government Printing Office: 1985—639-012

0102-LF-014-6602

UNCLASSIFIED

Block 19 (continued)

In particular, coating resistance, 45 degree coating phase angle frequency data, and low frequency impedance magnitude data determined at exposure times ranging from 2 to 200 days were found to predict the 550 day coating performance. Relative increases in the electrochemically active surface area were correlated with the frequency at which the coating RC phase angle was equal to 45 degrees.

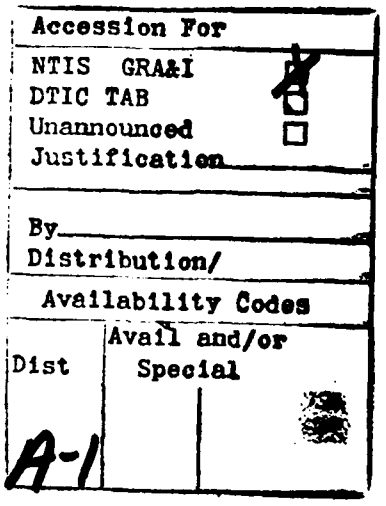

CONTENTS

	Page
ABBREVIATIONS AND SYMBOLS	x
ABSTRACT	1
ADMINISTRATIVE INFORMATION	1
INTRODUCTION	1
MATERIALS	3
EXPERIMENTAL PROCEDURE	4
EXPOSURE CONDITIONS	4
INSTRUMENTATION AND TESTING	4
CELL DESIGN	5
METHODS OF ANALYSIS	5
THE ELECTROCHEMICAL IMPEDANCE OF A COATED METAL SYSTEM	5
COATING RESISTANCE	9
IMPEDANCE MAGNITUDE	10
COATING CAPACITANCE	10
DETERMINATION OF ELECTROCHEMICALLY ACTIVE AREA	11
ASTM METHODS FOR VISUAL COATING EVALUATION	14
RESULTS	14
EPOXY POLYAMIDE COATINGS OF VARIOUS THICKNESSES	14
CATHODICALLY POLARIZED	18
TRANSLUCENT UNPIGMENTED COATINGS	19
TRANSLUCENT PIGMENTED COATINGS	20
PREDICTIONS OF LONG TERM BEHAVIOR	21
DISCUSSION	23
CONCLUSIONS	26

CONTENTS (continued)

Page

REFERENCES..... 87

FIGURES

1a. General electrical equivalent circuit model for coated metal system..... 31

1b. Diffusional impedance parameters utilized to model Z..... 31

2. Transmission line model for Z_m..... 32

3. Examples of area percentages in ASTM D-610..... 33

4. Bode magnitude and phase data for 20-μm-thick epoxy polyamide coated steel..... 34

5. Bode magnitude and phase data for 25-μm-thick epoxy polyamide coated steel..... 35

6. Coating resistance as a function of exposure time for 20-26-μm-thick epoxy polyamide coated steel..... 36

7. Low frequency impedance data for 20-μm-thick epoxy polyamide coated steel..... 36

8. Low frequency impedance data for 25-μm-thick epoxy polyamide coated steel..... 37

9. Visual appearance of 20-25-μm-thick epoxy polyamide coated steel after 5-days exposure in ASTM artificial ocean water..... 38

10. Visual appearance of 20-25-μm-thick epoxy polyamide coated steel after 34-days exposure in ASTM artificial ocean water..... 39

11. Visual appearance of 20-25-μm-thick epoxy polyamide coated steel after 267-days exposure in ASTM artificial ocean water..... 40

12. Bode magnitude and phase data for 54-55-μm-thick epoxy polyamide steel..... 41

13. Bode magnitude and phase data for 54-55-μm-thick epoxy polyamide coated steel..... 42

14. Coating resistance as a function of exposure time for 54-55-μm-thick epoxy polyamide coated steel..... 43

FIGURES (continued)

Page

15. Coating resistance versus time behavior for epoxy polyamide coated steel of 20-25 and 54-55-μm-thicknesses..... 43

16. Coating resistance and capacitance data for 54-μm-thick epoxy polyamide coated steel..... 44

17. Coating resistance and capacitance data for 55-μm-thick epoxy polyamide coated steel..... 44

18. Low frequency impedance behavior for 54-μm-thick epoxy polyamide coated steel..... 45

19. Low frequency impedance behavior for 55-μm-thick epoxy polyamide coated steel..... 45

20. Relative increases in electrochemically active area for 54-55 μm thick epoxy polyamide coated steel..... 46

21. Visual appearance of 54-55-μm-thick epoxy polyamide coated steel after 158-days exposure in ASTM artificial ocean water..... 47

22. Visual appearance of 54-55-μm-thick epoxy polyamide coated steel after 400-days exposure in ASTM artificial ocean water..... 48

23. Bode magnitude and phase data for 116-μm-thick epoxy polyamide coated steel..... 49

24. Coating resistance and capacitance behavior as a function of exposure time for 121-μm-thick epoxy polyamide coated steel..... 50

25. Coating resistance and capacitance behavior as a function of exposure time for 116-μm-thick epoxy polyamide coated steel..... 50

26. Low frequency impedance behavior as a function of exposure time for 121-μm-thick epoxy polyamide coated steel..... 51

27. Low frequency impedance behavior as a function of exposure time for 116-μm-thick epoxy polyamide coated steel..... 51

28. Relative increases in electrochemically active area for 116-121-μm-thick epoxy polyamide coated steel..... 52

29. Visual appearance of 116-121-μm-thick epoxy polyamide coated steel after 267-days exposure in ASTM artificial ocean water..... 53

30. Visual appearance of 116-121-μm-thick epoxy polyamide coated steel after 400-days exposure in ASTM artificial ocean water..... 54

FIGURES (continued)

Page

31. Coating resistance and capacitance behavior as a function of exposure time for 183-μm-thick epoxy polyamide coated steel..... 55

32. Coating resistance and capacitance behavior as a function of exposure time for 180-μm-thick epoxy polyamide coated steel..... 55

33. Low frequency impedance behavior as a function of exposure time for 183-μm-thick epoxy polyamide coated steel..... 56

34. Low frequency impedance behavior as a function of exposure time for 180-μm-thick epoxy polyamide coated steel..... 56

35. Relative increases in electrochemically active area for 180-183-μm-thick epoxy polyamide coated steel..... 57

36. Visual appearance of 180-183-μm-thick epoxy polyamide coated steel after 267-days exposure in ASTM artificial ocean water..... 58

37. Comparison of coating resistance behavior as a function of exposure time for for various thicknesses of epoxy polyamide coated steel..... 59

38. Coating resistance as a function of exposure time for 146-160-μm-thick epoxy polyamide coated steel..... 59

39. Low frequency impedance behavior as a function of exposure time for 160-μm-thick epoxy polyamide coated steel..... 60

40. Low frequency impedance behavior as a function of exposure time for 157-μm-thick epoxy polyamide coated steel..... 60

41. Low frequency impedance behavior as a function of exposure time for 146-μm-thick epoxy polyamide coated steel..... 61

42. Relative increases in electrochemically active area for 146-160-μm-thick epoxy polyamide coated steel..... 61

43. Visual appearance of 146-160-μm-thick epoxy polyamide coated steel after 366-days exposure in ASTM artificial ocean water..... 62

44. Comparison of coating resistance behavior as a function of exposure time for various thicknesses of epoxy polyamide coated steel..... 63

45. Coating resistance, capacitance and total cathodic charge for cathodically polarized epoxy polyamide coated steel..... 63

FIGURES (continued)

Page

46. Coating resistance, capacitance and total cathodic charge for polarized epoxy polyamide coated steel..... 64

47. Coating resistance, capacitance and total cathodic charge for cathodically polarized epoxy polyamide coated steel..... 64

48. Coating resistance, capacitance and total cathodic charge for cathodically polarized epoxy polyamide coated steel..... 65

49. Coating capacitance versus time..... 65

50. Coating capacitance versus time..... 66

51. Relative increases in electrochemically active area for cathodically polarized epoxy polyamide coated steel..... 66

52. Visual appearance of 145-155-μm-thick epoxy polyamide coated steel after 345-days exposure in ASTM artificial ocean water..... 67

53. Visual appearance of 155-160-μm-thick epoxy polyamide coated steel after 345-days exposure in ASTM artificial ocean water..... 68

54. Coating resistance and capacitance behavior as a function of exposure time for translucent epoxy coated steel..... 69

55. Coating resistance and capacitance behavior as a function of exposure time for translucent epoxy coated steel..... 69

56. Coating resistance and capacitance behavior as a function of exposure time for translucent epoxy coated steel..... 70

57. Low frequency impedance behavior as a function of exposure time for translucent epoxy coated steel..... 70

58. Low frequency impedance behavior as a function of exposure time for translucent epoxy coated steel..... 71

59. Low frequency impedance behavior as a function of exposure time for translucent epoxy coated steel..... 71

60. Relative increases in electrochemically active area for translucent epoxy coated steel..... 72

61. Relative increases in electrochemically active area for translucent epoxy coated steel..... 72

62. Visual appearance of translucent epoxy coated steel after 110-days exposure in ASTM artificial ocean water..... 73

FIGURES (continued)

Page

63. Visual appearance of translucent epoxy coated steel after 475-days exposure in ASTM artificial ocean water..... 74

64. Coating resistance and capacitance behavior as a function of exposure time for translucent pigmented epoxy coated steel..... 75

65. Coating resistance and capacitance behavior as a function of exposure time for translucent pigmented epoxy coated steel..... 75

66. Low frequency impedance behavior as a function of exposure time for translucent pigmented epoxy coated steel..... 76

67. Low frequency impedance behavior as a function of exposure time for translucent pigmented epoxy coated steel..... 76

68. Relative increases in electrochemically active area for translucent pigmented epoxy coated steel..... 77

69. Visual appearance of translucent pigmented epoxy coated steel after 110-days exposure in ASTM artificial ocean water..... 78

70. Visual appearance of translucent pigmnented epoxy coated steel after 475-days exposure in ASTM artificial ocean water..... 79

71. Correlation between impedance data determined at short exposure time and 550-day ASTM visual evaluation: coating resistance at 2 days..... 80

72. Correlation between impedance data determined at short exposure time and 550-day ASTM visual evaluation: coating resistance at 10 days..... 80

73. Correlation between impedance data determined at short exposure time and 550-day ASTM visual evaluation: coating resistance at 50 days..... 81

74. Correlation between impedance data determined at short exposure time and 550-day ASTM visual evaluation: coating resistance at 200 days..... 81

75. Correlation between impedance data determined at short exposure time and 550-day ASTM visual evaluation: 10 mHz impedance at 2 days..... 82

76. Correlation between impedance data determined at short exposure time and 550-day ASTM visual evaluation: 10 mHz impedance at 10 days..... 82

FIGURES (continued)

Page

77. Correlation between impedance data determined at short exposure time and 550-day ASTM visual evaluation: 10 mHz impedance at 50 days..... 83

78. Correlation between impedance data determined at short exposure time and 550-day ASTM visual evaluation: 10 mHz impedance at 200 days..... 83

79. Correlation between impedance data determined at short exposure time and 550-day ASTM visual evaluation: 45-degree phase shift frequency at 2 days..... 84

80. Correlation between impedance data determined at short exposure time and 550-day ASTM visual evaluation: 45-degree phase shift frequency at 10 days..... 84

81. Correlation between impedance data determined at short exposure time and 550-day ASTM visual evaluation: 45-degree phase shift frequency at 50 days..... 85

82. Correlation between impedance data determined at short exposure time and 550-day ASTM visual evaluation: 45-degree phase shift frequency at 200 days..... 85

83. Electrolyte permeation for epoxy polyamide coatings: H_2O, O_2..... 86

84. Electrolyte permeation for epoxy polyamide coatings: Na^+, Cl^-..... 86

TABLES

1. Materials and exposure conditions..... 28

2. Scale and description of rust grades for ASTM D-610..... 29

3. Correlation of impedance parameters with 550-day visual evaluations for 20-185 μm-thick epoxy coatings on steel..... 30

4. Transport properties in organic coatings..... 30

ABBREVIATIONS AND SYMBOLS

A	Area (cm^2)
C	Capacitance (farads/cm^2)
C_c	Coating capacitance (farads/cm^2)
D_{dl}	Double layer capacitance (farads/cm^2)
C_d	Pseudo-capacitance (farads/cm^2)
C_o	Concentration of oxidizing species
C_r	Concentration of reducing species
δ	Nernst diffusional boundary layer thickness (cm)
D	Diffusion coefficient (cm^2/sec)
D_o	Diffusion coefficient - oxidizing species (cm^2/sec)
D_R	Diffusion coefficient - reducing species (cm^2/sec)
d	Film or coating thickness (cm)
ε	Dielectric constant
ε_o	Permittivity of free space (8.85×10^{-14} farads/cm)
E	Voltage of potential (mV)
E_{oc}	Open circuit potential (mV)
E_{corr}	Corrosion potential (mV)
E	Applied potential difference (mV)
η	Overpotential or polarization ($E-E_{corr}$) (mV)
F	Faraday's constant (96,496 coulombs/equivalent)
f	Frequency in cycles per second (Hz)
$f_b f_{45^\circ}$	Break point frequency
I	Applied current (amps)
i	Applied current density (amps/cm^2)
i_{corr}	Corrosion current density (amps/cm^2)

i	Applied current density difference (amps/cm^2)
j	Imaginary number, $j2 = 1$ (-)
R	Ideal gas constant (1.98 cal/mole-K)
R	Resistance (ohm-cm^2)
R_c	Electrochemical charge transfer resistance in transmission line model
R_{ct}	Also electrochemical charge transfer resistance in some models
R_D	Diffusional resistance
R_p	Coating pore resistance (ohm-cm^2)
R_t	Electrochemical charge transfer resistance (ohm-cm^2)
R_s	Solution resistance (ohm-cm^2)
R_Ω	Ohmic resistance (ohm-cm^2)
SCE	Standard calomel electrode (-)
σ	Warburg impedance coefficient (ohm-cm^2-$sec^{-1/2}$)
θ	Fractional surface coverage
T	Temperature (°C)
t	Time (seconds)
τ	Time constant, $\tau = RC$ for parallel resistive capacitive electrical currents
V	Voltage (volts)
W	Warburg impedance parameter (ohm-cm^2-$sec^{-1/2}$)
w	Rate constant
Z	General impedance magnitude (ohm-cm^2); also impedance modulus
Z'	Real component of impedance (ohm-cm^2)
Z''	Imaginary component of impedance (ohm-cm^2)
Z_D	Diffusional impedance (ohm-cm^2)
Z'_D	Real component of diffusional impedance (ohm-cm^2)
Z''_D	Imaginary component of diffusional impedance (ohm-cm^2)

ϕ Phase angle (degrees)

ω Frequency (radians/second) where $\omega = 2\pi f$

ABSTRACT

Electrochemical impedance results are presented for 550 day exposures of organic coated carbon steel samples. Coatings consisted of translucent pigmented and unpigmented epoxy and conventional opaque epoxy polyamide systems. Coating thicknesses ranged from 20 to 185 microns. Specimens were exposed under freely corroding conditions and at two cathodic polarization levels (-850 mV, and -1250 mV versus SCE) in ASTM artificial ocean water. The objective was to identify impedance parameters which measure subcritical coated-metal system property changes at early exposure times that are indicators of significant long term coating deterioration. Impedance data developed at early times, including coating resistance, coating capacitance, the increase in frequency associated with the coating's resistivecapacitive (RC) 45 degree phase angle, and low frequency impedance data, are compared to the coating system's performance evaluated after 550 days exposure. Coating performance at 550 days is visually evaluated using ASTM Method D-610, and a modification of ASTM D-714. In particular, coating resistance, 45 degree coating phase angle frequency data, and low frequency impedance magnitude data determined at exposure times ranging from 2 to 200 days were found to predict the 550 day coating performance. Relative increases in the electrochemically active surface area were correlated with the frequency at which the coating R-C phase angle was equal to 45 degrees.

ADMINISTRATIVE INFORMATION

This project was supported by the DTRC Ship and Submarine Materials Block Program under the administration of DTRC Code 0115. The program coordinator is Mr. Ivan Caplan. The work described was performed under Work Unit 1-2803-137-02 and satisfies milestone CT6/3. The work was conducted at DTRC in the Marine Corrosion Branch, Code 2813, under the direction of Mr. Terry Morton.

INTRODUCTION

The electrochemical impedance technique is capable of probing the electrochemical interface of an organic coated metal, providing information concerning the influence of corrosive environments on protective coatings and metallic substrates [13]. Impedance methods have advantages over DC electrochemical

methods, including the ability to measure electrochemical impedances despite large organic coating resistances, the non-destructive nature of the test, and the capability to provide spectrographic coated metal impedance data when a sufficient frequency bandwidth is utilized.

However, it remains to be established whether measurements of coated metal system property changes can be made early in the degradation process which correlate with long term significant coating deterioration for relatively slowly deteriorating coated metal systems where visually detectable damage is modest at early exposure times. In order for a predictive capability to be feasible, the impedance parameters providing the best correlation must be determined.

The objective of this research is to identify key electrochemical impedance parameters whose behavior early in the exposure period give advanced indication of significant coating deterioration determined after a one to two year exposure duration.

Electrochemical impedance results are reported for long term (550 day) exposures of various translucent epoxy, opaque epoxy polyamide, and opaque primer and top-coat epoxy polyamide coated carbon steel samples. Specimens were exposed in ASTM artificial seawater. Translucent coatings were specially developed so that visual signs of corrosion attack could be monitored more reliably at earlier exposure times than possible for opaque coatings. Four thicknesses of epoxy polyamide primer were tested so that the variation in coating thickness could be correlated with impedance paramaters. Epoxy polyamide primer and topcoat panels were studied at open circuit, -850 mV, and -1250 mV versus Standard Calomel Reference Electrode (SCE) to include the effects of cathodic polarization on the deterioration process.

MATERIALS

Cold rolled low carbon steel panels (SAE 1010; 1/4 hard) with a 15-25 micro-inch ground surface were utilized in all tests. Steel panels (5 by 7 inches) were degreased with xylene and coated with either epoxy polyamide or translucent coatings by a dip application method as in ASTM Standard D-823 [4]. All coatings were fully cured prior to exposure. Coating thicknesses ranging from approximately 20 μm to 185 μm were investigated. These coatings are nominally defect free but may contain many latent discontinuities. Details for each coating type are given below:

1. Epoxy Polyamide Primer Coatings of Various Thicknesses: These coatings were applied using the MIL-24441 series epoxy primer with ethylene glycol monoethyl ether solvent. Final thicknesses ranged from 20 microns to 185 microns. Coating thicknesses are given in Table 1.

2. Epoxy Polyamide Primer/Top Coat Coating Systems: These panels were coated with epoxy MIL-24441 series primer and topcoat coatings to total thicknesses ranging from 145 to 160 microns. Coating thicknesses are given in Table 1. These coatings contained the glycol monoethyl ether solvent, as well.

3. Translucent Coatings: These coatings were formulated with the same ingredients as the MIL-24441 epoxy except for the substitution of finely divided quartz (Cabosil) for the normal pigments. A second translucent coating was formulated from the same materials but with no particulate added. Coating thicknesses are given in Table 1.

EXPERIMENTAL PROCEDURE

EXPOSURE CONDITIONS

Panels from all three categories were exposed under freely corroding conditions in ASTM artificial ocean water at room temperature with aeration provided with gas bubbling (6 ppm dissolved oxygen concentration). Panels from category 2 were also cathodically polarized to -850 mV, and -1250 mV vs SCE during the full exposure period using mini-potentiostats.

INSTRUMENTATION AND TESTING

Impedance experiments were conducted using a Solartron 1250 frequency response analyzer, Stonehart BC 1200 potentiostat, and Tektronix 4052 computer. The impedance of the electrochemical system was probed using a swept sine voltage perturbation with data obtained using a correlation method of analysis. Impedance data was collected at frequencies ranging from 1 mHz to 65 KHz at voltage amplitudes ranging from 10 to 300 mV rms about the open circuit potential or the protection potential. For very good coatings, where no stable open circuit measurement was obtainable, a 300 mV amplitude was utilized. Samples behaving in this manner were potentiostatically polarized to -400 mV and -600 mV vs. SCE for these measurement. Results were identical in either case. For coatings where open circuit potentials were measurable but where the low frequency (10 mHz) impedance magnitude maximum was greater than 10^7 ohm-cm^2, a 60 mV amplitude was applied. For coatings with both a stable open circuit potential and low frequency impedance of less than 10^7 ohm-cm^2 a 10 mV amplitude was applied. Voltage amplitude was increased in order to improve gain and allow for a decrease in the current measuring resistor utilized. However, potentiostat phase shifts in the frequency range of 10 Khz to 65 Khz were still obtained for high impedance

coatings producing possibly greater than 50% measurement error [5]. This precluded utilization of the impedance data over this frequency range.

CELL DESIGN

At the time of impedance measurements, panels were momentarily removed from seawater tanks, surfaces were dried, and cylindrical PTFE cells containing ASTM artificial ocean water were positioned on panel surfaces. This cell contained a platinized screen auxiliary electrode oriented parallel to the painted metal surface. An aperture in the screen contained a glass lined Ag/AgCl tipped reference electrode which was positioned between the painted surface and the counter electrode along the center line of the cylindrical cell. This arrangement minimizes a variety of frequency and orientation related current non-uniformity effects on the impedance results and minimizes other edge effects from the panel [5]. The Ag/AgCl/0.6 M Cl^- reference electrode system in ASTM artificial ocean water is +8 mV vs. SCE at 25 C. The Ag/AgCl electrode was chosen to minimize high frequency phase shift of reference electrode origin by lowering the reference electrode RC time constant to a value below that usually associated with glass frit reference electrodes.

METHODS OF ANALYSIS

THE ELECTROCHEMICAL IMPEDANCE OF AN ORGANIC COATED METAL

The electrochemical impedance of a defect free organic coated metal exposed in aqueous sodium chloride solution will initially behave as a capacitor. Impedance will vary inversely in proportion to frequency of the applied voltage signal. At frequencies near 1 mHz, the resistance of the organic coating phase both perpendicular to the plane of the surface and tangential will likely be quite large for a well coated sample in exposure for a short period of time.

Consequently, the rate of any electrochemical reactions occurring on the metallic substrate will be very low. However, many organic coated metals contain latent discontinuities or defects which give rise to ionically conducting low resistive paths perpendicular to the coated surface which may penetrate to the metallic substrate. The resistivity of these paths, according to a direct concentration dependent degradation mechanism [6], will decrease as a function of exposure time as H_2O and oxygen are transported through the polymer and as anionic and cationic species permeate the pathways in the organic phase [6]. At this time, low resistance paths tangential to the metallic substrate may form. Such pathways of tangential ionic conduction are usually followed by the initiation of underfilm corrosion reactions. For organic coated steels in neutral or alkaline environments, the high frequency resistive capacitive (RC) relaxation of the coated metal system usually becomes distinguishable from intermediate and low frequency relaxations owing to the differences in the interfacial and coating RC time constants once the coating resistance decreases. That is to say, the RC time constant of the coating becomes smaller than that of the pseudocapacitance-faradaic resistance time constant for the metal electrolyte interface. This allows direct determination of the coating capacitance, C_c, and the in phase (phase angle approaching zero) perpendicular coating resistance, R_p, from high frequency impedance data. If this deterioration process were to continue to proceed in a strictly homogeneous fashion with no localized corrosion, the impedance of the electrochemical interface could behave in general as depicted in the equivalent circuit shown in Figure 1a, where Z_m describes the general impedance of the metal/electrolyte interface. Z_m may include terms associated with the solution/metal interfacial or double layer capacitance, charge transfer processes and diffusional processes. Several models have been developed to describe these as shown in Figure 1b [7-12].

definitions for all symbols and terms are given at the end of the text). However, the corrosion processes at latter times usually result in anodic and cathodic site separation as evidenced by rust spots, cathodic blistering, decohesion, and delamination which occur in a very heterogeneous fashion. The near DC (below 10 mHz in frequency) impedance of, particularly, a coated, but even an uncoated electrochemical interface is usually, therefore, considerably more complex.

Theoretically, the low frequency impedance of bare steel corroding in aerated alkaline chloride solution can be described by a Nernst diffusion layer diffusional impedance or heterogeneous pore diffusional impedance since the cathodic reduction of oxygen is diffusion controlled. The slope of the logarithm of the impedance modulus as a function of the logarithm of frequency would be -0.5 and the phase angle 45 degrees over the appropriate low frequency range [7,8]. However, such impedance behavior cannot be attributed to diffusional impedance over a similar frequency range for a thick coating on steel in alkaline or neutral sodium chloride where diffusion through the coating phase is considered. For these conditions the primary diffusion limited reaction at open circuit is still the cathodic oxygen reduction reaction but molecular diffusion of oxygen through the coating must occur before oxygen reduction can occur at the coated metal interface. Under this assumption, the diffusional time constant concept utilized by Buck [13] and modified by Dawson and John [12] illustrates that 1-100 mHz impedance data is not strongly influenced by this diffusional impedance. By setting the thickness of the diffusional boundary layer equal to the coating thickness (100 um), and the diffusivity of oxygen through the coating as equal to 5×10^{-8} cm^2/sec [14] (the range given in reference 14 is 10^{-10} to 10^{-8} $cm^2/second$), the frequency, ω, at which the finite imaginary (diffusional)

impedance reaches a maximum is given by:

$$w=5.081/\tau \quad (1)$$

where $\tau = 2d^2/D$, d is the coating thickness and D is the diffusivity for oxygen in the coating. For a 100 um coating, Z_d", the imaginary component of diffusional impedance, reaches a maximum at less than 0.25 mHz. A lower diffusivity such as given in the range above would result in an even lower frequency. An applied frequency of less than 1 mHz is, therefore, required in order for diffusional impedance to strongly influence the measured low frequency impedance modulus. Instead, the heterogeneous deterioration of the polymer/metals system is most accurately simulated by a transmission line as illustrated in Figure 2, were Z_m is replaced by "n" unit cells, each containing an interfacial R-C process [3]. In this model, the low frequency impedance behavior is most accurately depicted by a series of "n" RC unit cell processes, where R_c describes the unit cell faradaic process, shorted together by a series tangential coating resistance, R, representative of ionic conduction paths parallel to the coating metal interface. R_p, the perpendicular coating resistance has its usual meaning. In the particular model shown, the transmission line gives rise to a $w^{-0.5}$ frequency dependence at intermediate frequencies, and frequency independent impedance at low frequency (for R_c greater than R tangential). For organic coated steels in aerated neutral or alkaline sodium chloride environments the slope of the logarithm of impedance modulus versus logarithm of frequency behavior in the context of this model can be rationalized to behave in any one of the following manner at frequencies well below those given by $1/R_{pc} C$:

1) Vary from -0.5 to 0 with decreasing frequency as the transmission line model described in reference 3 and shown in Figure 2 for finite values of R, and R less than R_c such as with thick coatings.

2) Contain a slope of -1, over a range of frequency, and approach a slope of near zero at low frequency. For low resistivity coatings, with corrosion occurring homogeneously, R may be much smaller than R_c and approach the tangential resistance in an electrolyte with no coating. In this case the net interfacial resistance and capacitance for "n" unit cells may be replaced by an appropriate single RC parallel circuit analog for one lumped unit cell.

3) Behave as in (2) but contain a frequency dependent pseudocapacitance yielding a slope which varies as a function of frequency.

4) Show almost no slope at all at frequencies below $1/R_pC_c$ when the tangential resistance, R, is much less than R_c and R_c is almost equal to or less than R_p.

Given the complex range of behaviors possible, rigorous quantification of the terms described above was not undertaken in this study. The deterioration process is, instead, quantitatively characterized by the use of the following parameters:

COATING RESISTANCE

The in-phase magnitude of the coating resistance was determined from Bode magnitude and phase information as a function of exposure time. Adequate separation of the coating R_pC_c response from that of the metal/electrolyte interface was observed. Coating resistance was determined from the phase minimum observed at intermediate but lower frequency than the near 90 degree shift associated with the coating capacitance. R_p data was reduced to a scale of 0-10 for direct comparison with 0-10 ASTM visual rating systems. The following

formula was utilized in order to convert such data:

$$\text{Numeric Rating} = 10 - \log\ (10^8\ \text{ohm-cm}^2/R_p\ \text{ohm-cm}^2) \quad (2)$$

The 10^8 ohm-cm^2 value was representative of the maxium initial in-phase impedance value obtained for well coated systems.

IMPEDANCE MAGNITUDE

The magnitude of the complex imedance was determined from Bode magnitude data as a function of exposure time at 1 mHz, and 10 mHz. The similar numeric scale as shown was utilized:

$$\text{Numeric Rating} = 10 - \log\ (10^9\ \text{ohm-cm}^2/Z_{\tau\ 1\ \text{mHz}}) \quad (3)$$

or:

$$\text{Numeric Rating} = 10 - \log\ (10^9\ \text{ohm-cm}^2/Z_{\ 10\text{mHz}}) \quad (4)$$

The 10^9 ohm-cm^2 value was representative of the maxium initial near DC impedance value obtained for well coated systems.

COATING CAPACITANCE

This approach is contingent on the presence of a region where impedance is dependent on ω^{-1} over a range of high frequencies. The coating capacitance is calculated directly from the known complex impedance and frequency:

$$Z = -j/\omega\, C_c \quad (5)$$

Where Z is the impedance in ohm-cm^2, ω is the frequency in radians/second, and C_c the coating capacitance in farads/cm^2. The coating capacitance may by related to the volum of electrolyte absorbed by the coating [15]:

$$X_v = \log\ (C_c/C_o)/\log\ 80 \quad (6)$$

where X_v is the volume fraction of water, C_c is the coating capacitance at a

given time, and C_o is the estimated dry coating capacitance based upon the dieletric constant and coating thickness. C_o is given by:

$$C_o = \varepsilon \ \varepsilon_o/d \quad (\text{Farads/cm}^2) \tag{7}$$

where ε is the dielectric constant (3.8 for epoxy), d the coating thickness, and ε_o the permittivity of free space, 8.85×10^{-14} farads/cm.

In order to convert capacitance changes to a scale of 0-10 for direct comparison with ASTM visual rating systems, the following formula was utilized:

$$\text{Numeric Rating} = 10 - C_c/C_o \tag{8}$$

DETERMINATION OF THE ELECTROCHEMICALLY ACTIVE AREA

Determination of the percentage of area actively undergoing electrochemical processes can be undertaken using several approaches. Two approaches are dependent on the existence of a relationship between specific interfacial capacitance per unit area and a electrochemical capacitance term determined from the impedance experiment:

$$\text{Area} = C_{meas.}/C_x \tag{9}$$

where C_x is an area specific capacitance (in this case, for the underfilm electrolyte-metallic interface) in farads/cm^2 while C_{meas} is determined by one of the following methods:

Method 1: This approach is derived directly from either of the breakpoint frequencies, f_b, for the case where the interfacial process Z_m shown in Figure 1 behaves as a simple parallel resistive capacitive (RC) process:

$$\text{Area} = 1/(2\pi f_b Z C_x) \tag{10}$$

The breakpoint frequencies, f_{1b}, and f_{2b}, or frequencies associated with a 45 degree phase shift, are defined as the frequencies where at f_{1b}: $Z = R_p + R_\Omega$ and Z also equals $1/2\pi f_{1b}C$, or at f_{2b} $Z = R + R_p + R_\Omega$ and Z also equals $1/2\pi f_2 C$. In these expressions R is the faradaic resistance, R_Ω is the solution resistance, and C is the interfacial, double layer, or pseudocapacitance. Rearrangement of these expressions in terms of C and substitution of C in Equation 9 for the measured capacitance yields equation 10. Since a 45 degree phase shift may be near the maximum phase shift shown for the transmission line model such data does not satisfy equation 10 derived for a system containing a simple RC process. Therefore, this method is usually not possible except in the most ideal circumstances.

Method 2: This approach is derived directly from data from the low frequency transmission line unit cell R_cC process:

$$\text{Area} = T/(R_c\ C_x) \qquad (11)$$

where $T=R_cC$, where T is the time constant for the "n" unit cells in the transmission model, R_c is the faradaic unit cell resistance and C is the interfacial, double layer, or pseudo capacitance. Rearrangement of the time constant expression in terms of C and substitution of C in equation 9 for the measured capacitance yields equation 11. Since T and R_c must both be determined as well as C_x, this method is inherently difficult.

Method 3: In this method, the frequency at which a 45 degree phase angle is obtained in the coating high frequency RC relaxation process is monitored over the time of exposure as discussed by Haruyama [16]. This frequency (the breakpoint frequency) is utilized to follow the relative rate of increase of

electrochemically active surface area. The coating break point frequency is the frequency at which R_p equals the impedance magnitude, $Z=1\ \omega C_c=R_p$. The advantage of this method lies in the ability to clearly separate the high frequency break point from the remainder of the impedance spectra, particularly the complex behavior occurring at lower frequency. This is usually possible for coatings containing latent defects. It is assumed that the intrinsic bulk volume coating resistivity changes little during certain stages of exposure, i.e. when localized areas of the coating perpendicular to the coated metal interface become highly defective. Decreases in the average measured coating resistance with time reflect increases in the percentage of highly defective areas instead of changes in intrinsic volume resistivity. These areas will most likely develop into areas of increased corrosion activity. The following expression relates this break point frequency with such an area increase:

$$f_{45} = K\ (A_t/A_o) \qquad (12)$$

and $K = (1/2\pi\rho\varepsilon\ \varepsilon_o)$

where A_t is the time dependent defective area, A_o is the fixed total specimen area, ρ is the intrinsic coating resistivity, ε is the dielectric constant for the water laden coating (which approaches 80 compared to 3.8 for epoxy), and ε_o is the permittivity of free space. When electrolyte penetrates the coating, ε decreases by an order of magnitude while ρ increases similarly. This offset makes K a constant compared to f_{45} which may increase by several orders of magnitude with defective area growth. The relative increase in area can be determined from the increase of f_{45} with exposure time. The method is not contingent on determination of an area specific capacitance and was utilized in this study. In order to convert the relative increases in the defective area

to a scale of 0-10 for direct comparison with ASTM visual rating systems, the following formula was utilized:

$$\text{Numeric Rating} = 10 - 2\times\log(f_{45}) \qquad (13)$$

where f_{45} is the frequency (Hz) associated with a 45 degree phase shift and the factor of 2 is used to give ratings from 0 to 10.

ASTM METHHODS FOR VISUAL COATING EVALUATION

ASTM Standard D-610, and a modification of ASTM D-714 were utilized to visually evaluate the state of deterioration of the various organic coated steel panels [17,18]. ASTM standard 610 contains a rust standard rating scale which converts the percentage of area rusting to a scale from 0 to 10 [17]. This scale is reproduced on Table 2, and in Figure 3. ASTM Standard D-714 employs photographic reference standards of blister size on a numerical scale from 0 to 10 [18]. The lowest numeric rating corresponds to the largest blister size. The density of blisters at each size are given by dense, medium dense, medium and few. D-714 was modified to create a scale of 0 to 10, where 0 to 10 now corresponds to the percentage of area blistered regardless of blister sizes. Thus the same area percentages as in D-610 are utilized. These techniques could be used more efficiently with the translucent coatings since rusting at the metal/coating interface could be visually detected prior to rust or blistering at the coating/electrolyte surface.

RESULTS

EPOXY POLYAMIDE PRIMER COATINGS OF VARIOUS THICKNESSES

Figures 4 and 5 show selected Bode magnitude and phase data at various

exposure times for 20-26 micron thick epoxy polyamide coatings. Initial impedance values are below 10^5 ohm-cm^2 at all frequencies. Low frequency phase angle are present at early exposure times indicative of the development of corroded areas. The high frequency phase information shifts to higher frequencies with exposure time as the coating resistance decreases and the areas of corrosion increase. The time dependent behavior of the coating resistance is shown in Figure 6. ASTM D-610 and D-714 ratings are directly annotated on Figure 6. The frequency at which the high frequency phase angle is equal to 45 degrees is greater than 10^5 hz at all exposure times indicative of the presence of large electrochemically active areas. Figures 7 and 8 show 1 and 10 mHz impedance data and open circuit potentials as a function of exposure time. The low values of impedance are indicative of early rapid corrosion as are electronegative open circuit potentials. Figures 9 to 11 show extensive corrosion visually confirming the impedance data since blistered and rusted areas are observed at early exposure times.

Figures 12 and 13 show selected Bode magnitude and phase plots for 54-55 micron thick epoxy polyamide coated steel. Initial impedance values are above 10^5 ohm-cm^2 but decrease with time. The low frequency phase angle peaks both increase and broaden with time as electrochemically active areas develop. The high frequency phase angle peaks shift to higher frequency with exposure time as the defective areas in the coating increase. Figure 14 shows coating resistance data as a function of exposure time. ASTM ratings from D-610 and D-714 are annotated directly on the plot. Visual evidence of corrosion is not observed until after 50 to 100 days but impedance decreases are observed at much earlier times. Figure 15 illustrates a comparison of coating resistance data for 20-25 micron thick epoxy polyamide to 54-55 micron thick coatings.

For both systems widespread corrosion is observed when the coating resistance is below 10^4 ohm-cm^2. Figures 16 and 17 show coating resistance and coating capacitance data for 54-55 micron thick epoxy polyamide coated steel. Increases in coating capacitance are observed as a function of exposure time. Capacitance was determined from impedance data above 10^4 Hz and therefore are considered questionable in this case. Figures 18 and 19 show 10 mHz and 1 mHz frequency impedance data and open circuit potentials as a function of exposure time. Low values of impedance and electronegative potentials indicate active corrosion. Figure 20 shows the frequency at which 45 degree phase shift occurs in the coating R-C process as a function of exposure time. ASTM visual ratings are annotated directly on the plot. Increases in frequency indicate increases in electrochemically active area as confirmed by ASTM ratings which drop to 4.5/4.5 after 400 days. Figures 21 and 22 show development of blisters and rust areas after various exposure times confirming the validity of this frequency data in predicting the actively corroding area. Bode magnitude and phase data for 115-120 micron coatings were similar to data illustrated above except that initial impedance data was capacitive in behavior over a four decade range in frequency (6.5 Hz to 65 KHz). Selected impedance magnitude and phase data are illustrated in Figure 23. A second low frequency R-C process was obtained at 44 days signifying the onset of corrosion. Localized areas of corrosion were not visually observed until greater than 100 days. Figures 24 and 25 show coating resistance and coating capacitance data as a function of exposure time. Two order of magnitude decreases in coating resistance are evident. Capacitive data, however, does not change systematically. Figures 26 and 27 illustrate low frequency impedance changes for duplicate coated panels. No stable open circuit potential could be measured from 8 to 50 days for one panel. In all cases when the low frequency impedance decreased to below 10^6 ohm-cm^2 an open circuit potential became measurable. Figure 28 illustrates the frequency at which a 45 degree

obtained for this panel increased slightly with time (Figure 35) but did not exhibit the large systematic increases in electrochemically active area as observed for thin coatings. ASTM ratings confirmed this findings as shown in Figures 35 and 36. ASTM ratings of 8/9 are obtained in the test area even after over 300 days of exposure.

Figure 37 shows a comparison of coating resistance data for all of the epoxy polyamide coatings of the various thicknesses discussed above. Epoxy Polyamide Primer/Top Coat Coating Systems Freely Corroding 146 to 160 micron epoxy polyamide primer and top coat systems were exposed both under freely corroding conditions and at two cathodic polarization levels in ASTM artificial ocean water. Bode magnitude and phase data were similar to data illustrated for thich coatings described above in that initial impedance data was capacitive over a five decade range in frequency (.65 Hz to 65 kHz) but changed to a multi-time constant process when localized corrosion began. Coating resistance data for three replicate samples exposed under freely corroding conditions are shown in Figure 38. Coating capacitance data showed only very slight increases with exposure time and is not shown. Initial coating resistance values were greater than 10^8 ohm-cm^2, but decreased over two orders of magnitude with time. ASTM ratings have been annotated directly on the coating resistance versus time plots. There was no visual evidence of corrosion even after 400 days of exposure. Fluctuations in coating resistance are observed after 50 days and this behavior is believed to reflect the transient development of microscopic localized areas of attack. As with the 180-183 micron coatings discussed above, when impedance values were high no stable potential or electropositive potentials were measured. When impedance values decreased, electronegative open circuit potentials were measured. This behavior is shown

in Figures 39-41. Figure 42 shows the frequency at which a 45 degree phase shift is obtained. This frequency increases with exposure time, but to a lesser extent than for thin coatings discussed above, consistent with ASTM visual ratings of 9.7/10 as shown in Figure 43. Figure 44 shows a comparison of coating resistance data for 146-160, 54-55, and 20-24 micron thick epoxy polyamide coatings on steel.

Cathodically Polarized

145 to 159 micron thick coated panels were cathodically polarized to -850 and -1250 mV vs. SCE. Bode magnitude and phase data were similar to data illustrated above in that initial impedance data was capacitive in behavior over a five decade range in frequency but changed to a multi-time constant process at much greater times when localized blistering began. Figures 45-48 show coating resistance, capacitance, and the total accumulated cathodic charge for the -850 and -1250 mV polarization conditions. Coating resistance data decreased from greater than 10^7 ohm-cm^2 to belol 10^6 ohm-cm^2. Low frequency impedance data behaved in a similar manner. Coating resistance data was more sensitive measure of deterioration than coating capacitance which increased only slightly. However, coating capacitance did indicate cathodic polarization since coating capacitance increases for cathodically protected panels exceeded coating capacitance increases for the three 146 to 150 micron thick epoxy polyamide coated exposed under freely corroding conditions. This is shown in Figures 49 and 50. Figure 51 illustrates the increase with time in the frequency at which a 45 degree phase angle occurs, indicative of an increase in the electrochemically active surface area. Visible signs of blistering were still quite limited at 315 days as indicated by ASTM ratings directly annotated on Figure 51. ASTM D-610 and D-714 ratings of 10/10 were obtained at 315 days. However, by 345

days one of the panels cathodically polarized to -1250 mV vs. Ag/AgCl developed large blister areas. Smaller blister areas became visible on other cathodically polarized panels (Figures 52 and 53).

TRANSLUCENT UNPIGMENTED COATINGS

68 to 74 micron thick translucent epoxy coating systems were exposed under freely corroding conditions in ASTM artificial ocean water. Bode magnitude and phase data were similar to data illustrated above in that initial impedance data was capacitive in behavior over a five decade range in frequency. This data remained capacitive over a large frequency range for a period of time greater than 400 days for 201 and 202, suggesting limited localized corrosion attack. Coating resistance and capacitance data for three samples are shown in Figures 54-56. Coating capacitance data showed only very slight increases with exposure time. Initial coating resistance values were near 10^8 ohm-cm^2, and in two cases decreased over one order of magnitude with time. One sample (206) was anodically polarized to -200 mV vs Ag/AgCl for 8 hours, initially, and this sample showed large decreases in coating resistance and the greatest increases in coating capacitance. Figures 57-59 illustrate low frequency impedance data and open circuit potential data for the three specimens. Fluctuations in coating resistance, low frequency impedance, and open circuit potential are observed. This behavior is believed to reflect the transient development of microscopic localized areas of attack. Localized corrosion product development may increase the resistance of the coating in very small defective regions. As with 146-160 and 180-183 micron thick coatings discussed above, when impedance values were high, no stable potential or electropositive potentials were measured.When impedance values decreased, electronegative open circuit potentials were measured. Figures 60 and 61 show the frequency at which a 45 degree phase

shift is obtained for 201, exposed at open circuit, and for 206, the anodically polarized sample. For 201, this frequency actually decreases after some exposure time consistent with the increasing impedance data presented above. The anodically polarized 206 had a more systematic increase in the 45 degree frequency and in electrochemically active area. These findings are confirmed by ASTM visual ratings which are annotated directly on Figures 60 and 61. Photographs of these panels are shown in Figures 62 and 63. Note the grind marks still visible beneath the translucent coating 201 after 476 days. Panel 206, which was anodically polarized, shows significant more underfilm staining at this time.

TRANSLUCENT PIGMENTED COATINGS

76 to 77 micron thick translucent epoxy coating systems were exposed under freely corroding conditions in ASTM artificial ocean water. Bode magnitude and phase data were similar to data illustrated above in that initial impedance data was capacitive in behavior over a five decade range in frequency. This data remained capacitive over a large frequency range for a period of time greater than 500 days, suggesting limited localized corrosion attack. Coating resistance and capacitance data for replicate samples are shown in Figures 64-65. Coating capacitance data showed only very slight increases with exposure time. Initial coating resistance values were near 10^8 ohm-cm2, and decreased over one order of magnitude with time. Figures 66-67 illustrate low frequency impedance data and open circuit potential data. Fluctuations in coating resistance, low frequency impedance, and open circuit potential are observed. Again, this behavior is believed to reflect the transient development and repair of microscopic localized areas of attack. As with 146-160 and 180-183 micron

thick coatings discussed above, when impedance values were high, no stable potential or electropositive potentials were measured. When impedance values decreased, electronegative open circuit potentials were measured. Figure 68 shows the frequency at which a 45 degree phase shift is obtained for one panel exposed at open circuit. For this sample, this frequency increases erratically with exposure time. This data is consistent with the impedance data presented above. Photographs of these panels are shown in Figures 69 and 70. Virtually no attack is observed after 110 days. Some underfilm staining is visible after 475 days of exposure.

PREDICTIONS OF LONG TERM BEHAVIOR

In order for impedance parameters to be predictive, they must measure subcritical property changes at early times that provide advanced indication of more significant property changes to occur later.

Impedance parameters measured at 1-5, 20, 50, and 200 days were compared to ASTM D-610 and modified D-714 visual ratings obtained at 550 days. A systematic correlation between impedance results converted to a 0-10 scale and ASTM ratings presented on a 0-10 scale indicates the extent of predictive capability. Representative plots of ASTM D-601 and D-714 ratings versus coating resistance, 10 mHz impedance, and frequency of 45 degree phase shift are shown in Figures 71-74, 75-78, and 79-82, respectively. Bands of data are bounded by lines added to aid the reader. Linear relationships on the 0-10 scale are generally not obtained. In almost all cases impedance data is more capable of predicting the performance of coatings showing 33% corrosion (2 on ASTM Scale) or greater after 550 days, or coatings showing 0.3% corrosion (7 on ASTM Scale) or less after 550 days. Impedance parameters are somewhat insensitive for coatings with 550 day deterioration ratings within the range from 0.3% and 33%.

Figure 72 shows that a coating resistance of 10^8 ohm-cm^2 or greater determined at 10 days ensures a 550 day corrosion area of 0.1% or less. However, a day 10 coating resistance of less than 10^6 ohm-cm^2 indicates that anywhere from 0.1% to 50% of the coating may be corroded after 550 days. Figures 75-78 show that a 10_{mHz} impedance of 10^9 ohm-cm^2 determined over a 2 to 200 day exposure period is required to insure a 550 day corrosion area of less than 0.3 percent. Figures 79 to 82 illustrate that a frequency associated with a 45 degree phase shift of 10 Hz or less determined over a period of 2-200 days (for a 13 cm^2 coated surface area) ensures a 0.1% corroded area after 550 days. Table 3 summarizes all results. A good correlation is defined as data that when plotted on 0-10 scales produces distinct bands of data even if this includes portions of data of near zero or infinity slope when any 3-4 integer range is considered on both the ordinate and abscissa. The term correlation is used when bands of data are 4-5 integers wide on both scales over a range of data. No correlation indicates that no bands could be drawn showing trends. For low frequency impedance and coating resistance data the plot bands decrease in integer width as the time of the measurement increases but the slopes are very large indicating a sensitive range of impedances below which 550 damage was great. For the 45 degree frequency data, bands are wide but the slope appraoches 1 if 0-10 data is considered on both the ordinate and abscissa. Low frequency impedance and coating resistance data are somewhat more predictive at time periods of ten days or greater. Coating capacitance information shows no predictive capability at any time. Open circuit potential measurement, while not predictive in a quantitative sense, qualitatively correlates with coating condition in that well coated systems do not have measurable open circuit potentials.

DISCUSSION

Impedance parameters determined over time periods from 1-5, 10, 50, and 200 days correlate to various degrees with the long term (550 day) visual evaluations of coating damage obtained with ASTM Standards D-610 and modified D-714. Coating capacitance changes tracked with water uptake rates but was unsuccessfully correlated with eventual deterioration rates under all circumstances. Other impedance data taken in the 1-5 day time period were slightly less successfully correlated with 550 day deterioration assessments than impedance data taken at later times. It remains to be determined why this is the case.

Deterioration of coated metal systems has been characterized by several stages which must occur in series in order for corrosion reactions and loss of coating adhesion to become possible at the coated metal interface. These stages are water and oxygen permeation, sometimes called an incubation stage, cationic and anionic transport, the development of anodic and cathodic sites, electrochemical reactions, and catholyte and anolyte generation. Oxygen reduction at cathodic sites and associated alkalinity have been cited as a strong factor in coating delamination [6]. Alkaline metal cations have been cited to be a solution concentration dependent factor in determining the nature of the deterioration process, and the rate determining species in the overall process for polybutadiene [6,19]. An important question relative to this overall process is the time required for each stage. Since the first two stages involve transport of species to the reaction site, the times required to complete those stages can be examined.Water and oxygen are reported to be transported through coatings rapidly in comparison with the transport of Na^+ and Cl^-, even with consideration of migration in an electric field as well as concentration gradient dependent molecular diffusion [20]. The time necessary for molecular diffusion of oxygen

through the coating to the coated metal interface, where oxygen is electrochemically reduced, is given be the following expression:

$$t = 0.0653x(L)^2/D \quad (14)$$

where L is the coating thickness and D is the diffusivity of the species considered.The constant 0.0653 corresponds to a condition where the permeation flux at the coated metal interface is one tenth of the final steady state permeation flux, assuming complete reaction of the oxygen at the coated metal interface. Since water, Na^+, and Cl^- will accumulate at the metal/coating interface, the appropriate expression is of a more complex form at later times for these species. Nevertheless, use of this simple expression permits direct comparison of the time required for initial permeation of each species to the coated metal interface. Table 4 gives diffusivity values for exygen, water, Na^+ and Cl^- in epoxy coatings compiled from various references [14,20-22]. Figures 83 and 84 illustrate the relationship between permeation time and coating thickness for Na^+, Cl^-, H_2O, and O_2. Figure 83 illustrates that O_2 and H_2O are transported to the coated metal interface in less than one day for the range of coating thicknesses shown. Figure 84 illustrates that from 1 to 10 days is required for Na^+ to permeat to the coated metal interface depending upon coating thickness and still longer times are required for Cl^-. Longer time is required for sufficient Na^+ to accumulate to support the cathodic reaction process by maintaining charge neutrality. For polybutadiene [6] it has been pointed out that the permeation rates for O_2 and H_2O are considerably in excess of that required to sustain cathodic reduction of oxygen and cathodic delamination and are therefore not rate determining. It was therefore suggested that the transport of Na^+ (the major ionic charge transport carrier in the coating) was rate controlling in the corrosion process [6]. In the present study, $Z_{10\ mHz}$ impedance measurements conducted in the 1-5 day time frame were slightly less

capable of predicting 550 day degradation assessment. This time period corresponds to the minimum time required for Na^+ permeation for the thicker (100 μm) coatings. Z_{10} mHz impedance measurements conducted after 10 days were found to correlate better with 550 day deterioration rates, and this corresponds well with the times required to permeate Na^+ to the coated metal interface. For 20 um coatings, impedance results indicating significant later damage were obtained within the 1-5 day time period (see data points on Figures 75-78) corresponsing to a 550 day ASTM rating of 0). This is again consistent with the Na^+ transport theory since Figure 84 illustrates that less than one day is required for Na^+ transport to the coated metal interface in the case of a 20 μm coating. Cl^- ions must undoubtably be present at the metal interface to disrupt the passivity of the carbon steel, but extremely small concentrations may accomplish this and these may already be present at the interface.

Since all coatings studies permeated large quantities of H_2O and O_2 regardless of thickness and eventual performance, coating capacitance data increased with time but was not a discriminating parameter in assessing long term coating deterioration. This shortcoming can be accounted for by the fact that increases in coating capacitance indicate only water uptake. Water uptake alone is not apparently a significant indicator of eventual coating deterioration for the epoxy polyamide-steel systems studies. Since significant water uptake may occur in days it is unclear why coating capacitance continues to increase after hundreds of days of exposure. Deterioration of the coating with time permitting a gradual increase in water solubility may explain this effect.

In regard to the frequency at which a 45 degree phase angle was determined, this parameter does correlate well with increases in the relative electrochemically active area evaluated with the ASTM standards. Localized areas of corrosion

and cathodic delamination mechansim for "concentrated" alkali metal cation electrlytes [19] applicable for the 0.6 molar NaCl concentration utilized. For this method to correlate with active area, localized decreases in the coating resistivity at defective sites are required (as opposed to bulk homogeneous changes in the intrinsic volume resistivity of the coating) and this requirement has been met.

CONCLUSIONS

Impedance parameters Z_{10mhz}, the low frequency complex impedance, and R, the coating resistance, were found to provide predictive information on the corrosion and coating deterioration of epoxy and epoxy polyamide coated steel systems in ASTM artificial ocean water. Positive predictive correlations with 550 day corrosion damage were obtained only when these measurements were made at times sufficient to permit permeation of specifically H_2, O_2, Na_+, and to a lesser extent Cl^-, through the coating to the reacting metallic interface. In this regard, Na^+ diffusion and migration may be rate determining in the corrosion initiation process. Measurements of impedance paramaters Z_{10mhz}, and the coating resistance, R_p, at exposure times less than the time required for molecular diffusion of Na^+ to the coating-metal interface were less successfully correlated with long term coating deterioration rates.

Coating capacitance data was useful in monitoring the acceleration of water uptake such as with cathodic polarization. However, coating capacitance was not found to correlate in a systematic manner with eventual long term deterioration rates for the coated metal systems studied.

Electrochemically active area increases based on the utilization of coating 45 degree phase angle frequency data correlated well with the percentage of area visually identified to be electrochemically active by ASTM D-610 and D-714.

This parameter is quite sensitive to the development of localized low resistivity defects and, therefore, actively corroding areas and is a good predictive paramater.

Finally, the electrochemical impedance methods is shown to provide a predictive capability for assessing coating deterioration and the initiation of corrosion on organic coated metals when appropriate impedance parameters and measurement times are utilized.

ACKNOWLEDGEMENTS

The authors would like to thank Dr. George Loeb and Dr. Jim Mimm for providing coated steel panels, and their technical assistance throughout the experimental investigation. Bryan Pearce is thanked for technician support.

Table 1. Coating thicknesses and exposure conditions for coated steel specimens.

Plate No.	Mean Coat Thick (μm)	Standard Deviation (μm)	Coating Type	Exposure Conditions
		Translucent		
101	75.92	1.84	Quartz pigment	Open circuit
102	77.03	1.67	Quartz pigment	Open circuit
201	68.3	1.45	Epoxy only	Open circuit
202	69.42	1.69	Epoxy only	Open circuit
206	73.93	3.69	Epoxy only	Open circuit
		Epoxy Polyamide Primer		
401	54.18	1.71	MIL-24441	Open circuit
402	55.03	1.23	MIL-24441	Open circuit
406	20.04	6.41	MIL-24441	Open circuit
407	24.56	2.06	MIL-24441	Open circuit
326	182.87	2.70	MIL-24441	Open circuit
327	180.32	1.70	MIL-24441	Open circuit
331	120.79	2.12	MIL-24441	Open circuit
332	115.98	1.69	MIL-24441	Open circuit
		Epoxy Polyamide Primer/Topcoat		
316	159.73	2.80	MIL-24441	Open circuit
317	156.91	1.61	MIL-24441	Open circuit
318	146.47	2.08	MIL-24441	Open circuit
319	145.33	2.00	MIL-24441	-850 mV vs SCE
320	155.21	1.88	MIL-24441	-850 mV vs SCE
321	155.49	2.33	MIL-24441	-1250 mV vs SCE
322	158.6	1.74	MIL-24441	-1250 mV vs SCE

Table 2. Scale and description of rust grades for ASTM D-610.

RUST GRADES[A]	DESCRIPTION	ASTM-SSPC COLORED PHOTOGRAPHIC STANDARD
10	NO RUSTING OR LESS THAN 0.01% OF SURFACE RUSTED	UNNECESSARY
9	MINUTE RUSTING, LESS THAN 0.03% OF SURFACE RUSTED	NO. 9
8[B]	FEW ISOLATED RUST SPOTS, LESS THAN 0.1% OF SURFACE RUSTED	NO 8
7	LESS THAN 0.3% OF SURFACE RUSTED	NONE
6[C]	EXTENSIVE RUST SPOTS BUT LESS THAN 1% OF SURFACE RUSTED	NO. 6
5	RUSTING TO THE EXTENT OF 3% OF SURFACE RUSTED	NONE
4[D]	RUSTING TO THE EXTENT OF 10% OF SURFACE RUSTED	NO. 4
3[E]	APPROXIMATELY ONE SIXTH OF THE SURFACE RUSTED	NONE
2	APPROXIMATELY ONE THIRD OF THE SURFACE RUSTED	NONE
1	APPROXIMATELY ONE HALF OF THE SURFACE RUSTED	NONE
O[F]	APPROXIMATELY 100% OF SURFACE RUSTED	UNNECESSARY

[A] CORRESPOND TO SWEDISH PICTORIAL STANDARDS FOR RUSTING (1955) (BLACK AND WHITE).
[B] CORRESPONDS TO SSPC INITIAL SURFACE CONDITIONS E AND BISRA (BRITISH IRON AND STEEL RESEARCH ASSN.) 0.1%.
[C] CORRESPONDS TO SSPC INITIAL SURFACE CONDITIONS F AND BISRA 1.0%.
[D] CORRESPONDS TO SSPC INITIAL SURFACE CONDITIONS G.
[E] RUST GRADES BELOW 4 ARE OF NO PRACTICAL IMPORTANCE IN GRADING PERFORMANCES OF PAINTS.
[F] CORRESPONDS TO SSPC INITIAL SURFACE CONDITION H.

Table 3. Correlation of impedance parameters with 550-day ASTM visual evaluations for 20-185-μm epoxy and epoxy polyamide coatings on steel.

Impedance Parameter	Time of Impedance Measurement			
	1-5 Days	10 Days	50 Days	200 Days
Low Frequency Impedance	Correlation	Good Correlation	Good Correlation	Good Correlation
Coating Resistance	Correlation	Good Correlation	Good Correlation	Cood Correlation
Coating Capacitance	No Correlation	No Correlation	No Correlation	No Correlation
Frequency of 45 Degree Phase Shift for High Frequency Data	Correlation	Correlation	Correlation	Correlation
Open Circuit Potential	Weak Correlation	Weak Correlation	Weak Correlation	Weak Correlation

Table 4. Transport properties in organic coatings.

Species of Interest	Diffusion Coefficient (cm^2/sec)	Reference
O_2	10^{-10} to 10^{-8}	Brandrup and Immergut (Reference 14)
H_2O	1.0×10^{-8}	Ruggeri and Beck (Reference 21)
Na^+	0.31×10^{-10}	Glass and Smith* (Reference 22)
Cl^-	0.47×10^{-11}	Glass and Smith* (Reference 22)

*Data for epoxy polyamide.

GENERAL ELECTRICAL EQUIVALENT CIRCUIT MODEL

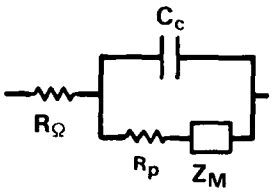

where

C_c = COATING CAPACITANCE

R_p = COATING RESISTANCE

R_Ω = SOLUTION RESISTANCE

Z_M = GENERAL IMPEDANCE CHARACTERIZING ELECTROCHEMICAL REACTIONS AT METAL/COATING INTERFACE

Fig. 1a. General electric equivalent circuit model for coated metal system.

Z_M	DIFFUSIONAL IMPEDANCE	INVESTIGATOR
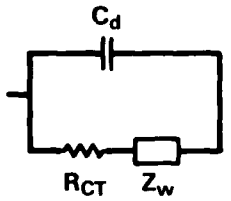	$Z_{re} = R_\Omega + R_{CT} + \sigma\omega^{-1/2}$ $Z_{IM} = \sigma\omega^{-1/2} + 2\sigma^2 C_d$ $\sigma = \frac{RT}{n^2F^2A\sqrt{2}}\left(\frac{1}{D_o^{1/2}C_o} + \frac{1}{D_R^{1/2}C_R}\right)$	A. BARD L. FAULKNER
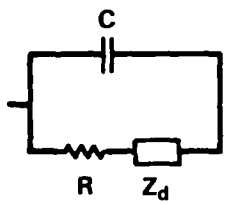	$Z_d = \frac{RT}{nF(i_L - i)}\frac{\tanh(\sqrt{j\mu})}{\sqrt{j\mu}}$ $\mu = \omega\delta^2/D$ δ = NERNST DIFFUSION THICKNESS	D. MacDONALD M. McKUBRE
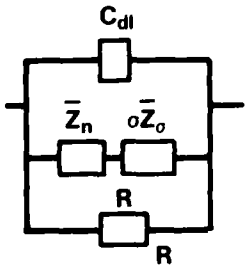	$\bar{Z}(j\omega) = \bar{Z}_n + \sigma\bar{Z}_o$ $\quad \sigma = \theta/1\text{-}\theta$ θ – COVERAGE $\bar{Z}_n = \frac{RT}{n^2F^2C^o}\frac{1}{\sqrt{j\omega D}}\tanh(\delta\sqrt{j\omega/D})$ $\bar{Z}_o = \frac{RT}{n^2F^2C^o}\frac{1}{\sqrt{(j\omega + W)D}}\tanh\left(\frac{\delta\sqrt{j\omega + W}}{D}\right)$ W = RATE CONSTANT	K. JUTTNER W. LORENZ
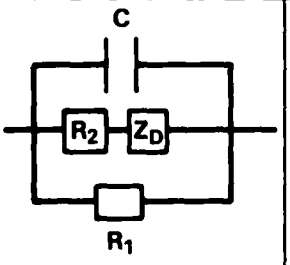	$Z_D = R_D\frac{\tanh\left(\frac{j\omega\delta^2}{D}\right)^{1/2}}{\left(j\omega\frac{\delta^2}{D}\right)^{1/2}}$	M. KEDDAM et. al.

Fig. 1b. Diffusional impedance parameters utilized to model Z.

GENERAL ELECTRICAL EQUIVALENT CIRCUIT MODEL

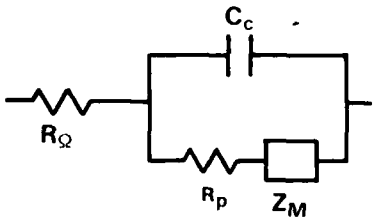

where

C_c = COATING CAPACITANCE

R_p = COATING RESISTANCE

R_Ω = SOLUTION RESISTANCE

Z_M = GENERAL IMPEDANCE CHARACTERIZING ELECTROCHEMICAL REACTIONS AT METAL/COATING INTERFACE

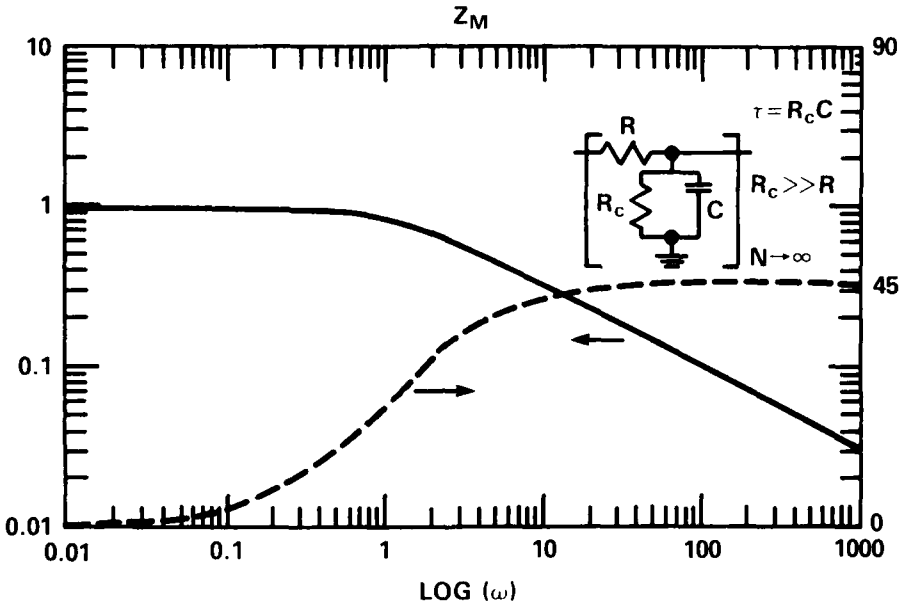

AT LOW FREQUENCIES =

$$Z_M = \frac{R}{2} + \sqrt{\frac{R^2}{4} + \frac{R \cdot R_c}{1 - \omega j R_c C}}$$

FOR A COATED METAL SYSTEM AS $\omega \rightarrow 0$:

$$Z = R_\Omega + R_p + \frac{R}{2} + \sqrt{\frac{R^2}{4} + \frac{R \cdot R_c}{1 - \omega j R_c C}}$$

Fig. 2. Transmission line model for Z_m.

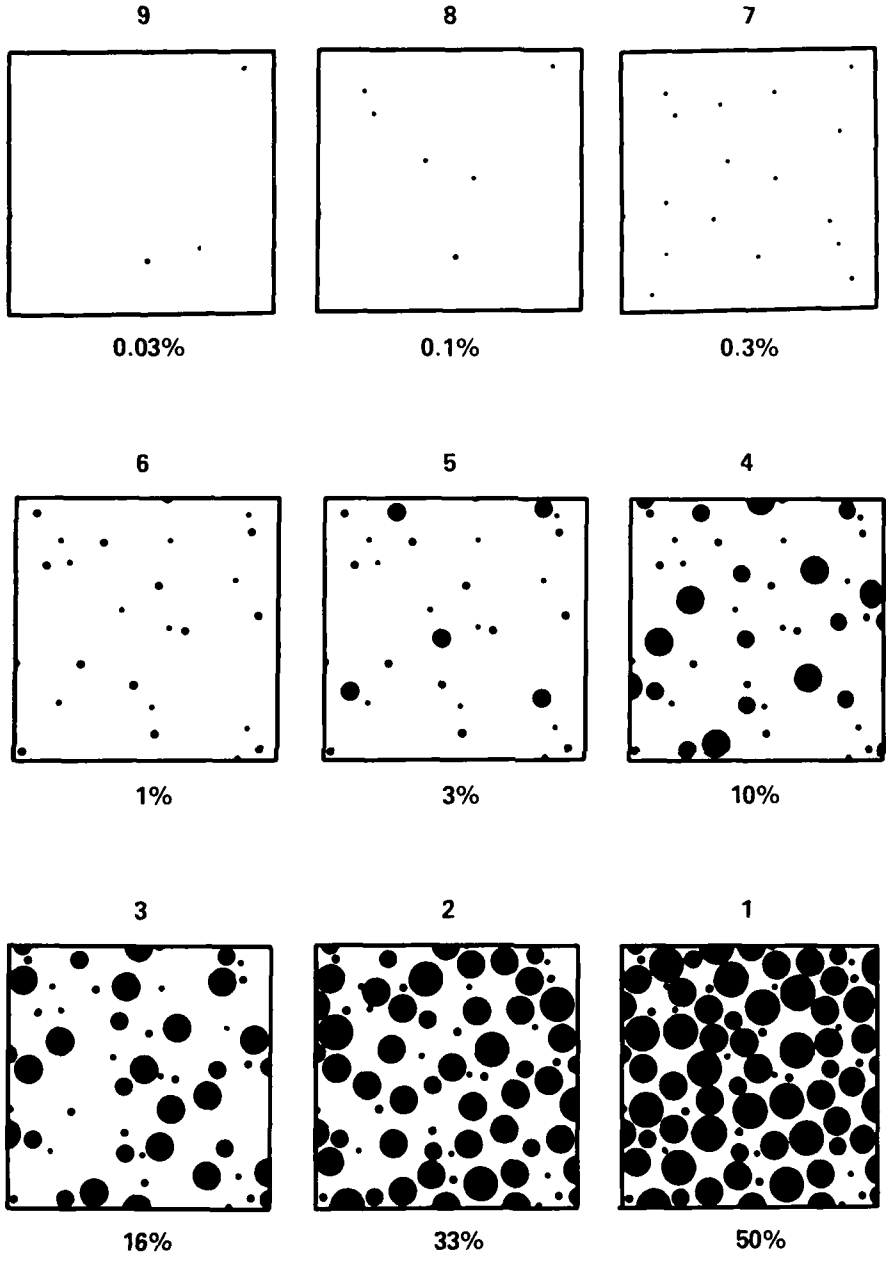

Fig. 3. Examples of area percentages in ASTM D-610.

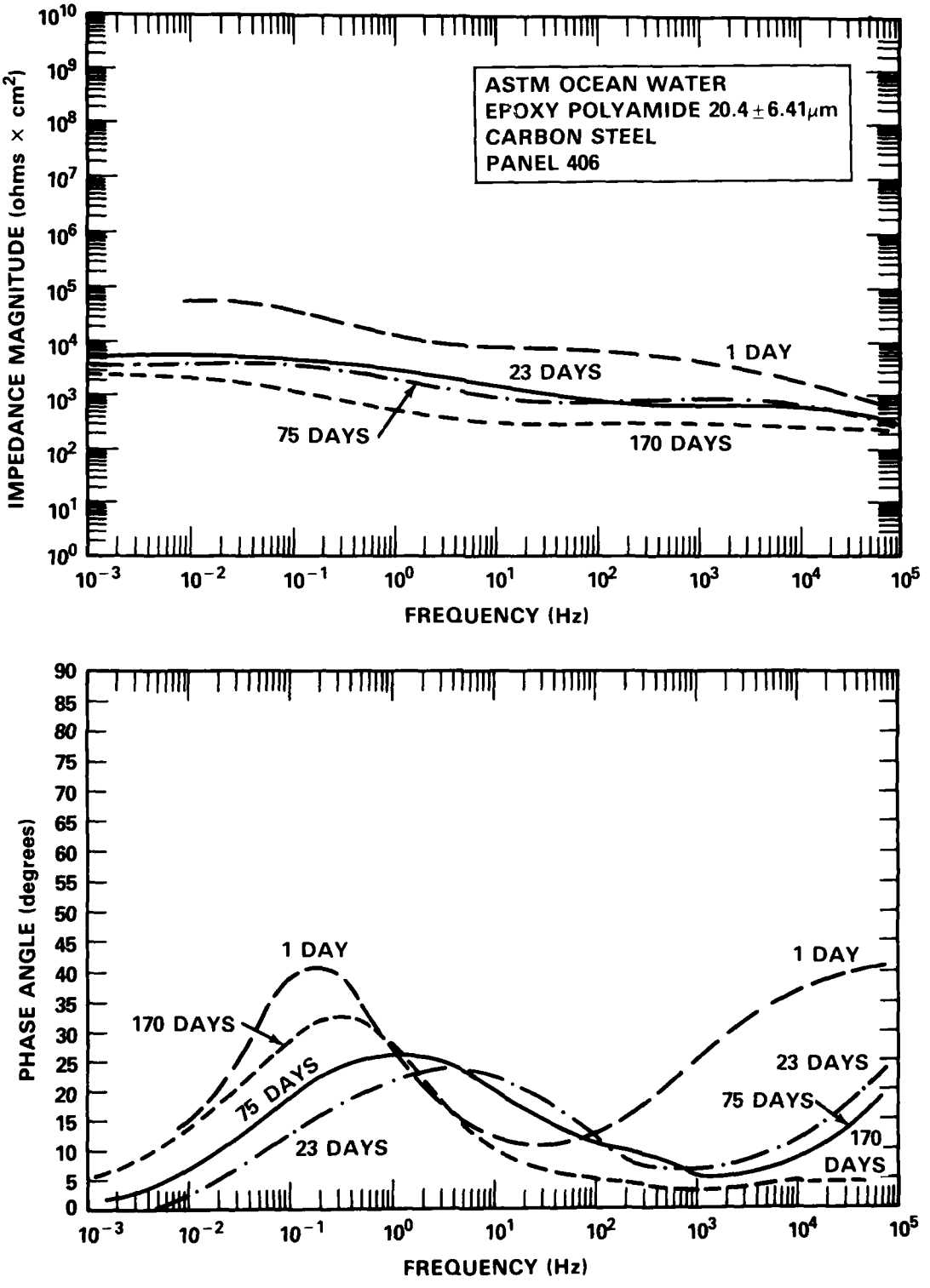

Fig. 4. Bode magnitude and phase data for 20-μm-thick epoxy polyamide coated steel.

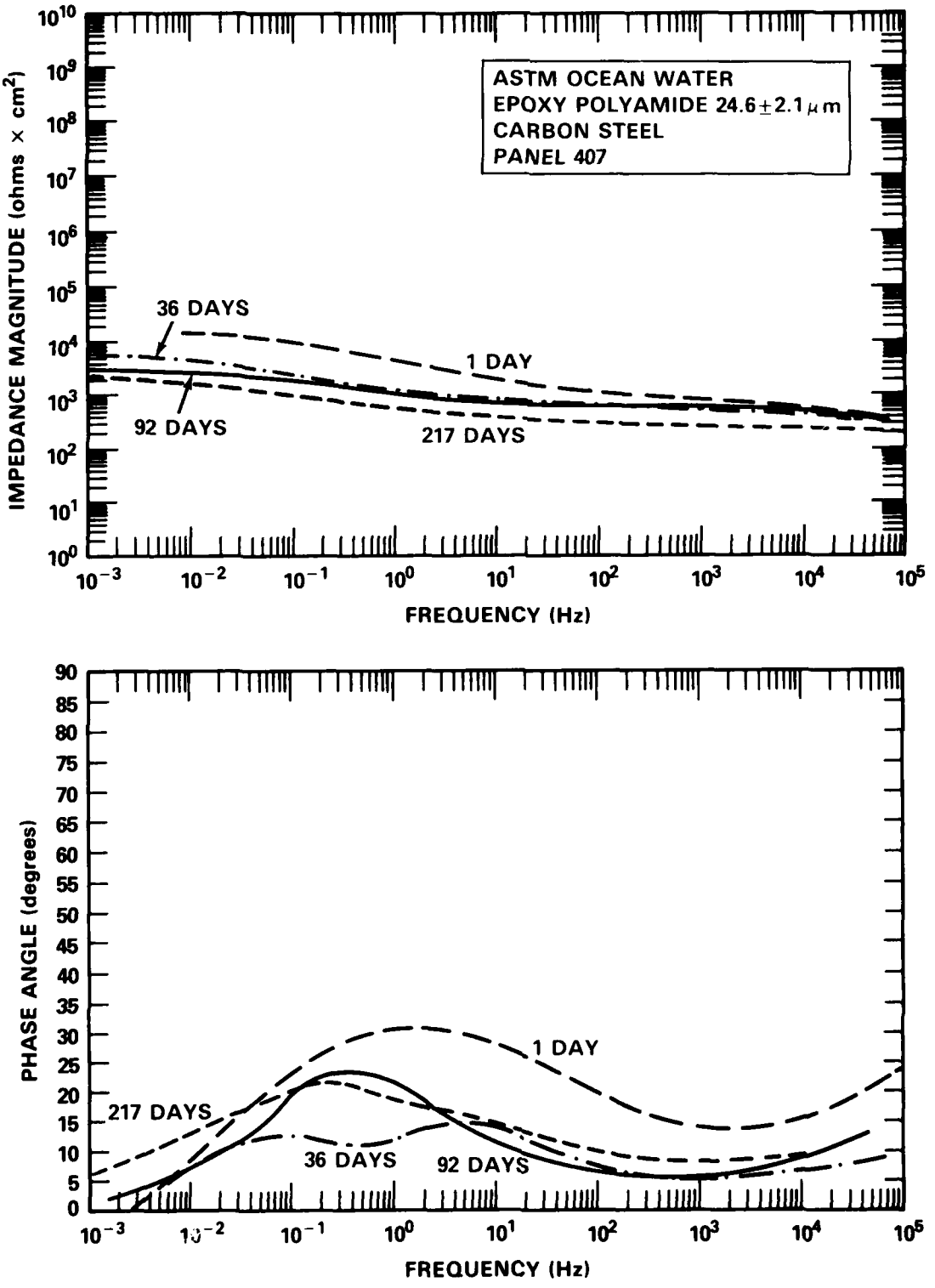

Fig. 5. Bode magnitude and phase data for 25-μm-thick epoxy polyamide coated steel.

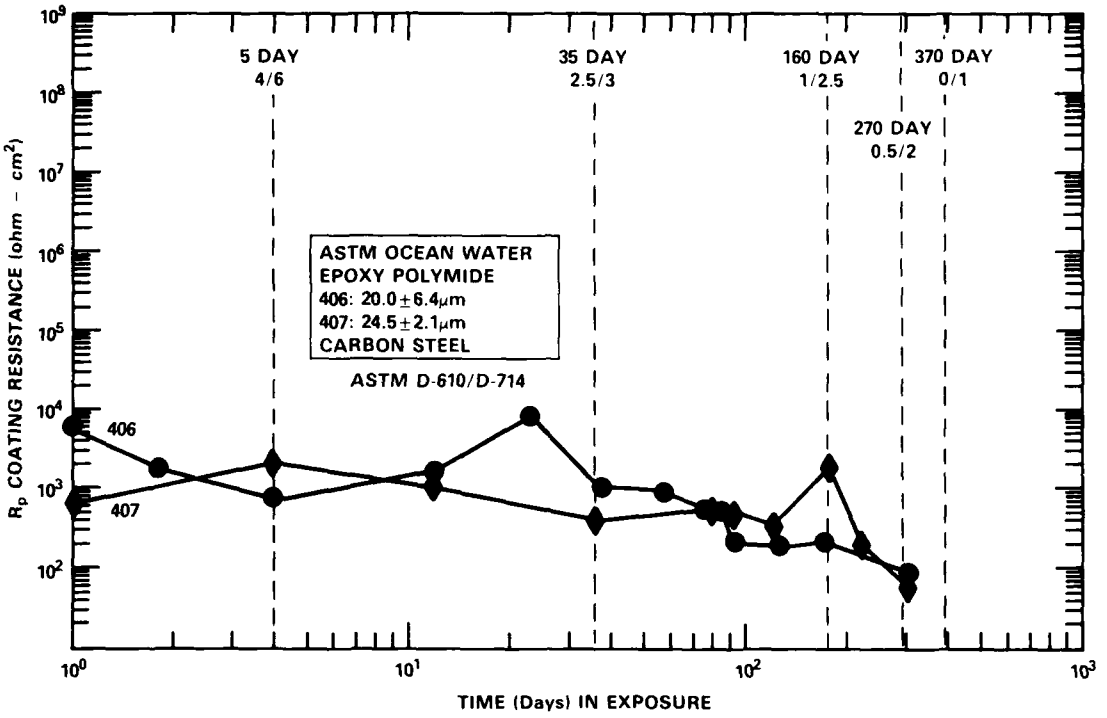

Fig. 6. Coating resistance as a function of exposure time for 20-26-μm-thick epoxy polyamide coated steel.

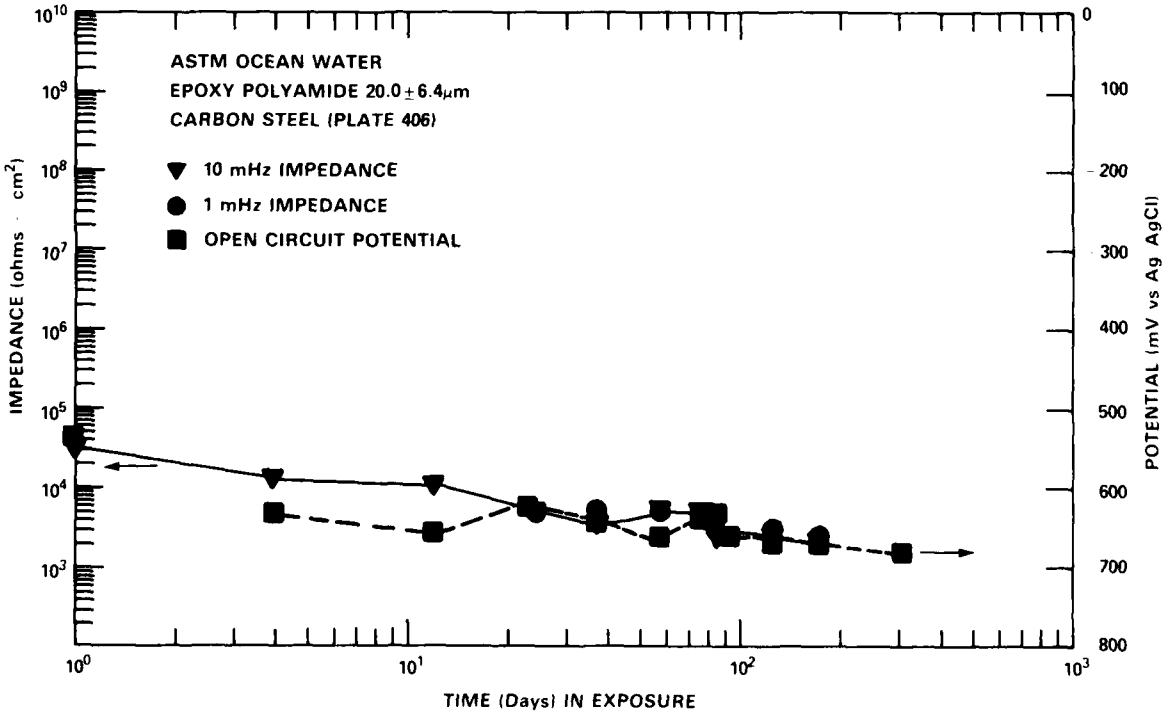

Fig. 7. Low frequency impedance data for 20-μm-thick epoxy polyamide coated steel.

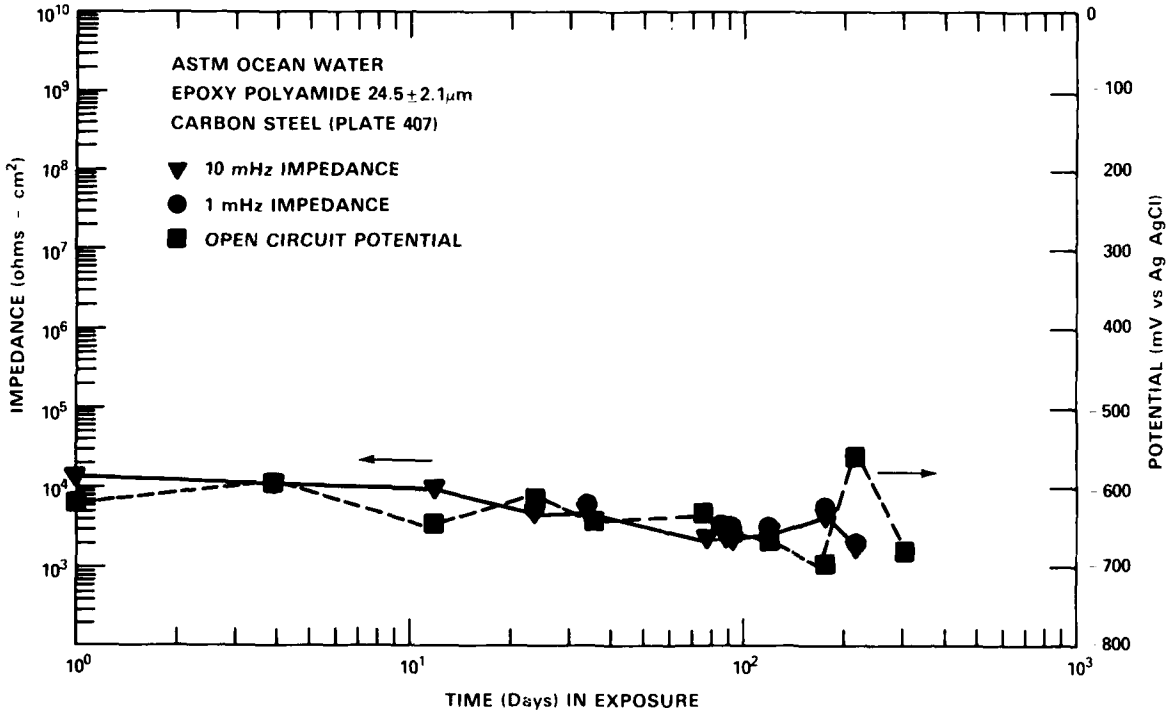

Fig. 8. Low frequency impedance data for 25-μm-thick epoxy polyamide coated steel.

Fig. 9. Visual appearance of 20-25-μm-thick epoxy polyamide coated steel after 5-days exposure in ASTM artificial ocean water.

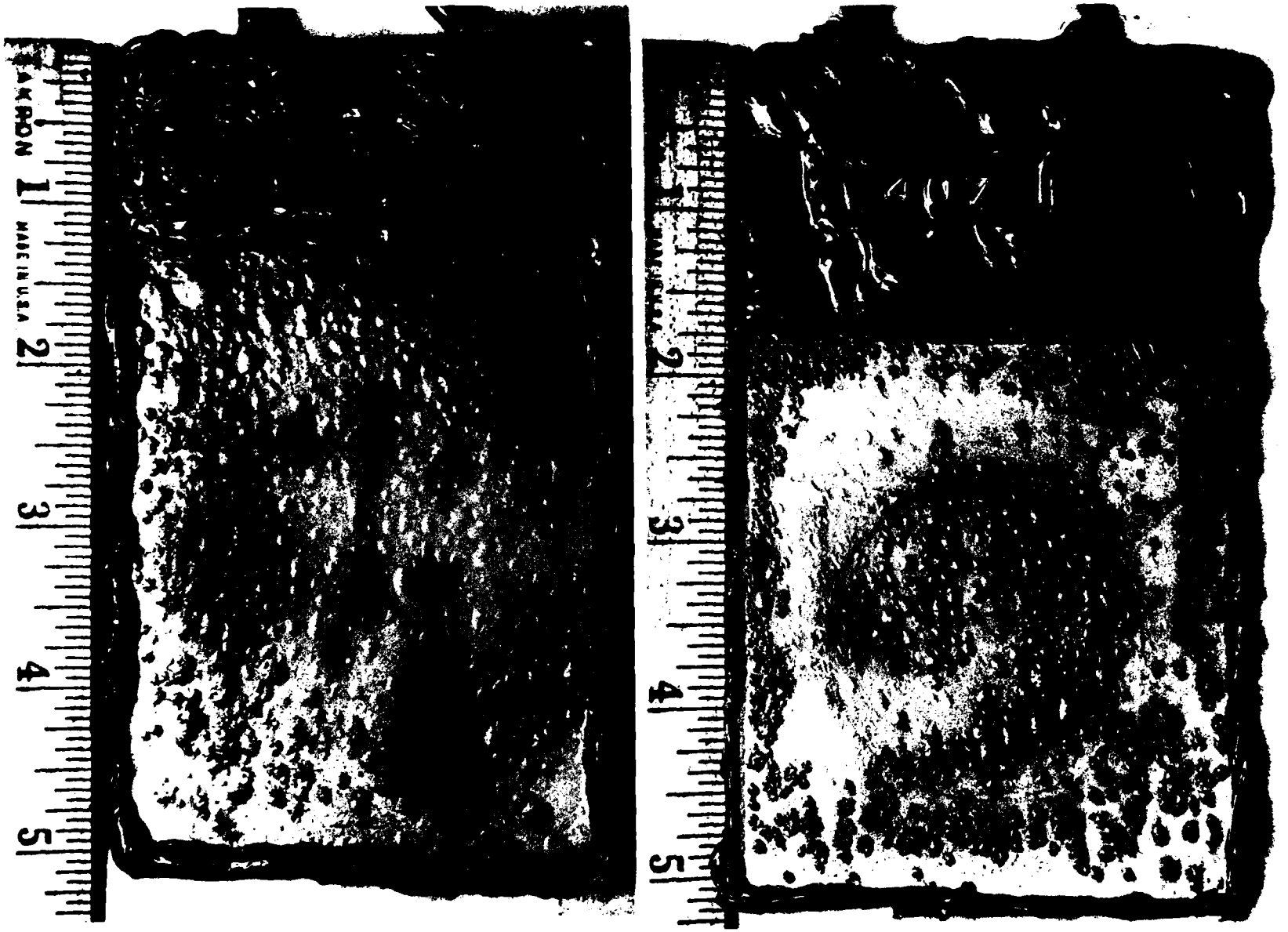

Fig. 10. Visual appearance of 20-25-μm-thick epoxy polyamide coated steel after 34-days exposure in ASTM artificial ocean water.

Fig. 11. Visual appearance of 20-25-μm-thick epoxy polyamide coated steel after 267-days exposure in ASTM artificial ocean water.

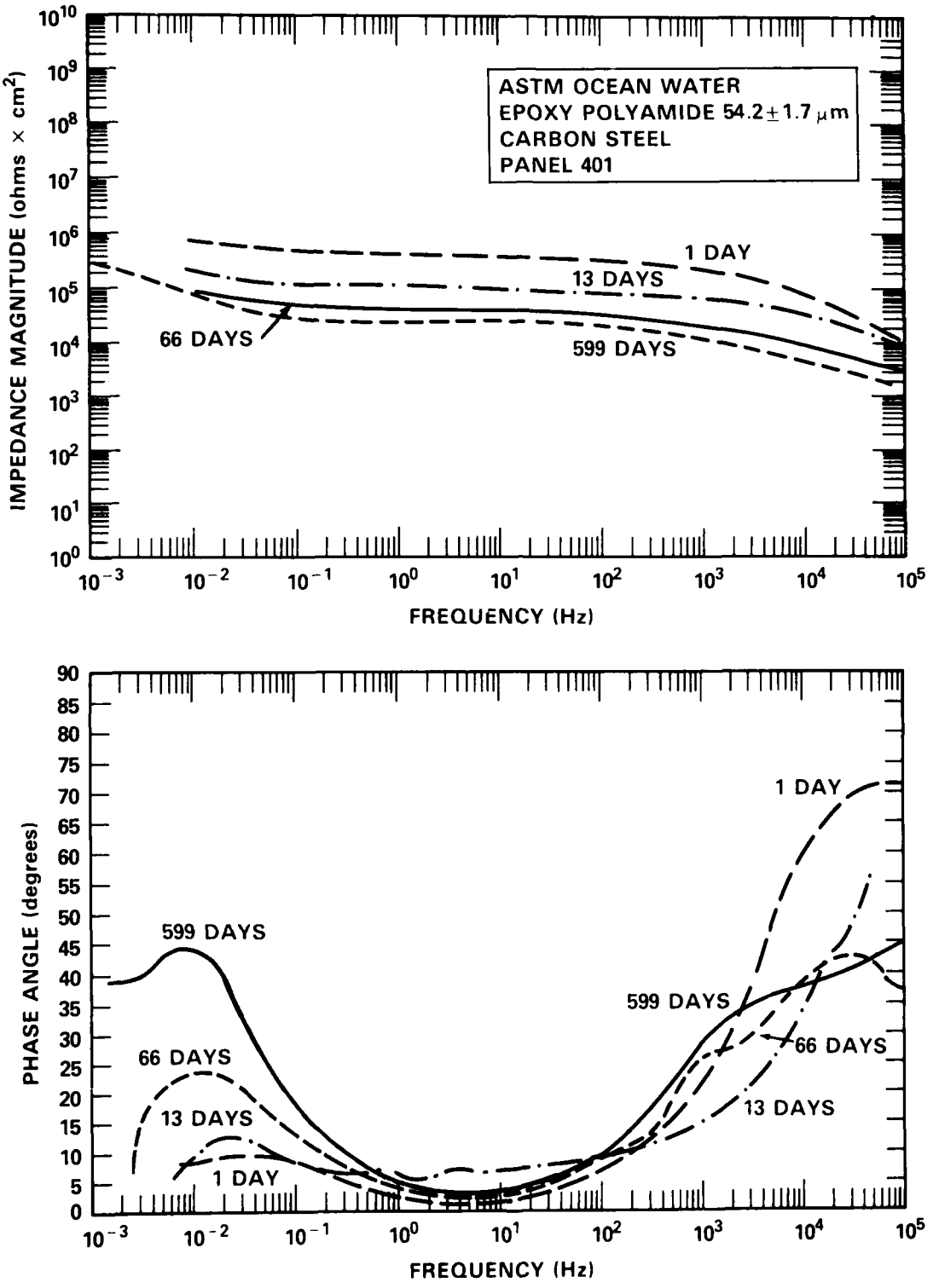

Fig. 12. Bode magnitude and phase data for 54-55-μm-thick epoxy polyamide coated steel.

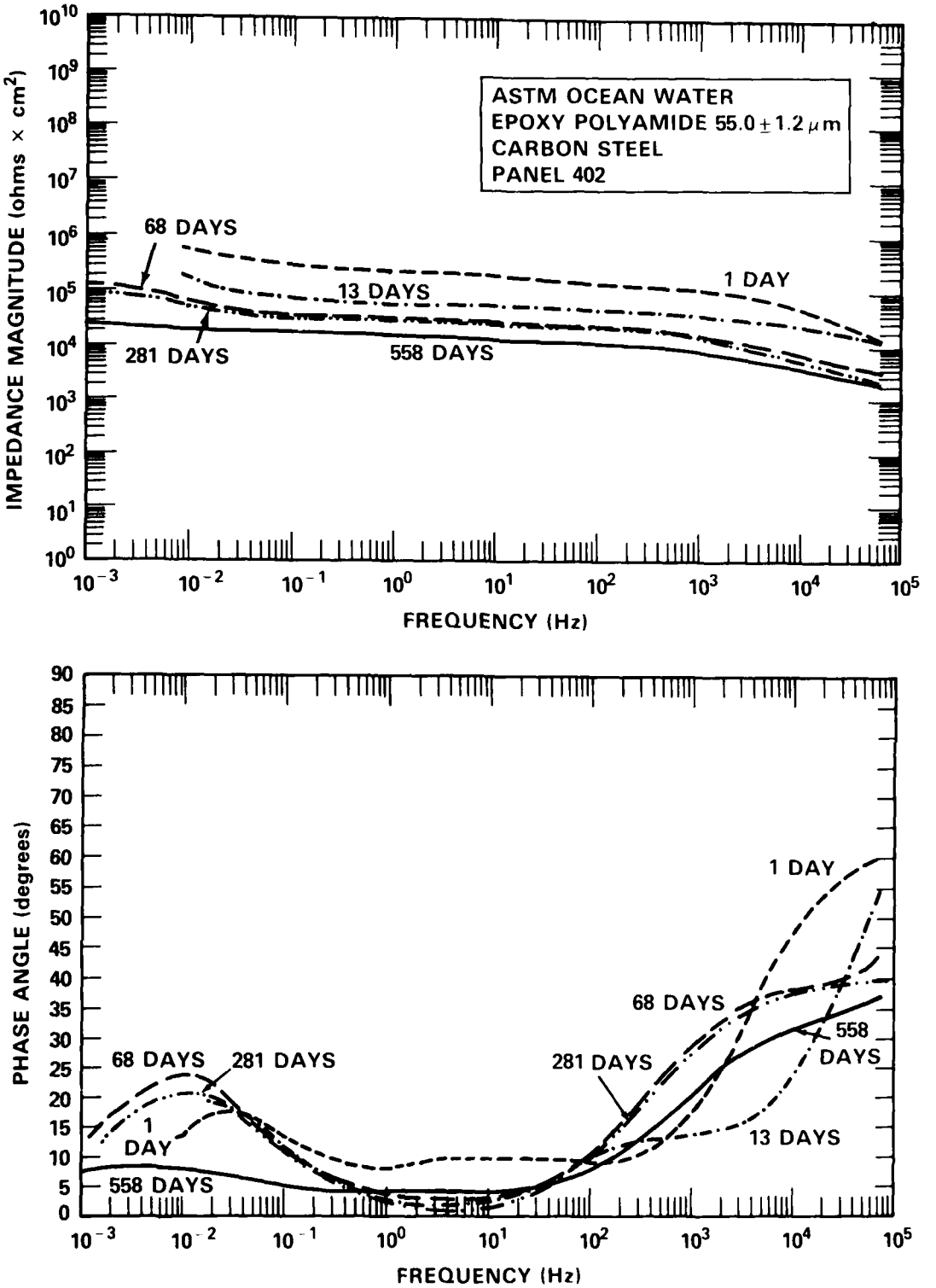

Fig. 13. Bode magnitude and phase data for 54-55-μm-thick epoxy polyamide coated steel.

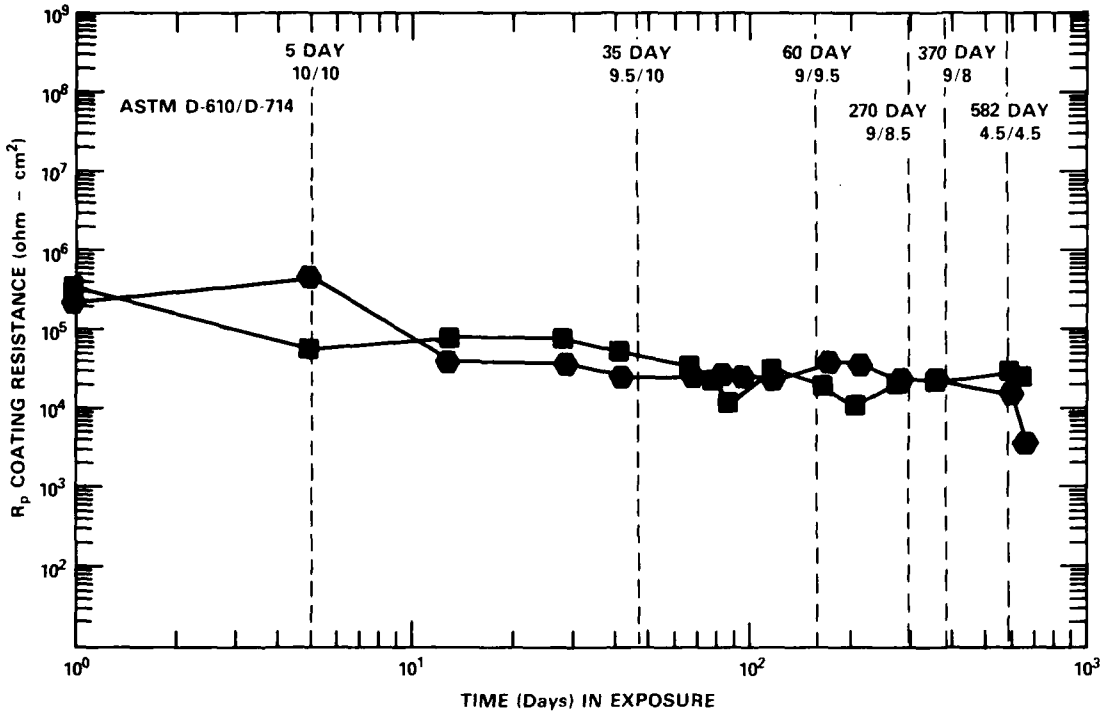

Fig. 14. Coating resistance as a function of exposure time for 54-55-μm-thick epoxy polyamide coated steel.

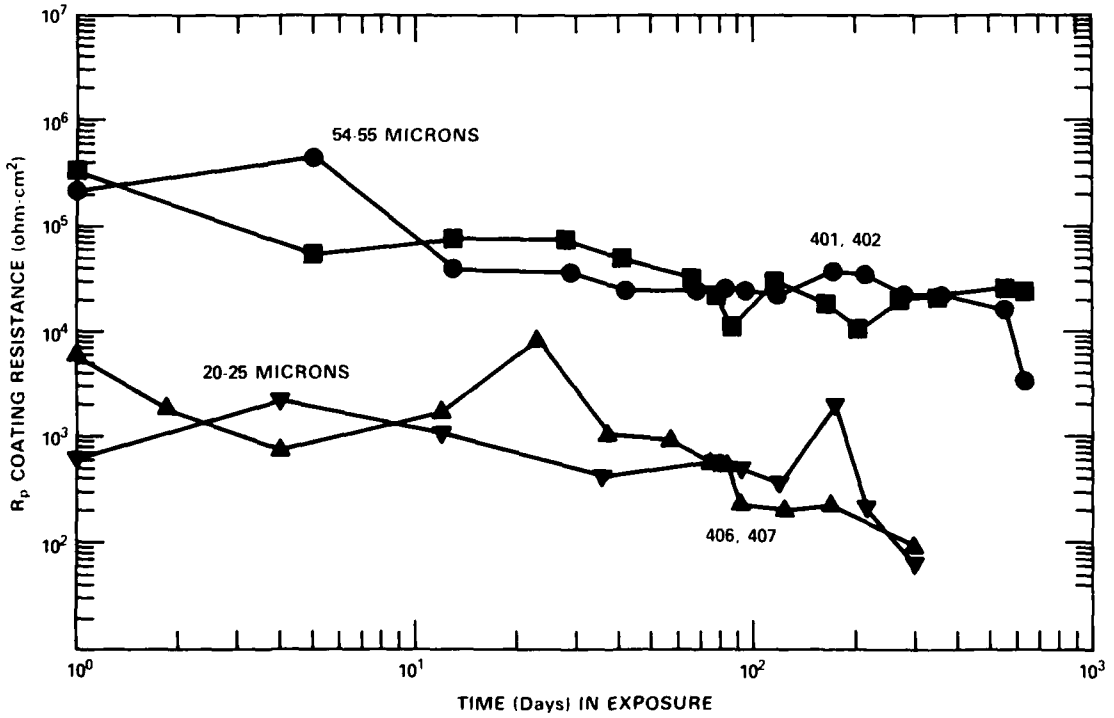

Fig. 15. Coating resistance versus time behavior for epoxy polyamide coated steel of 20-25 and 54-55 μm thicknesses.

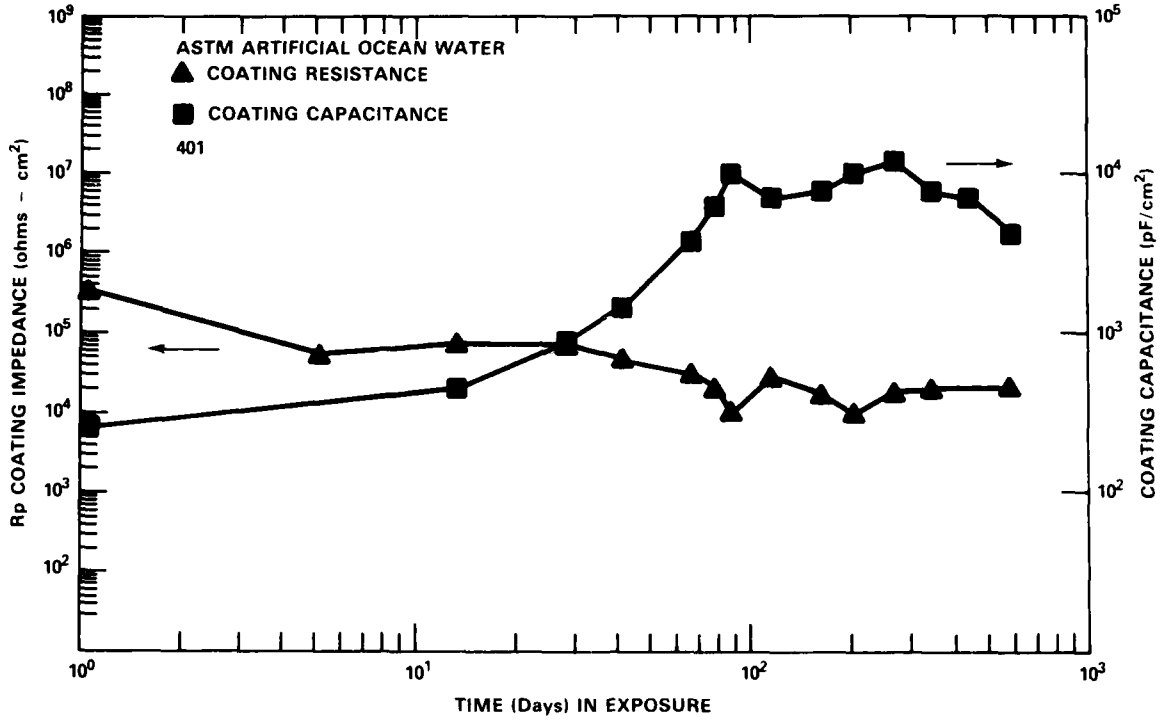

Fig. 16. Coating resistance and capacitance data for 54-μm-thick epoxy polyamide coated steel.

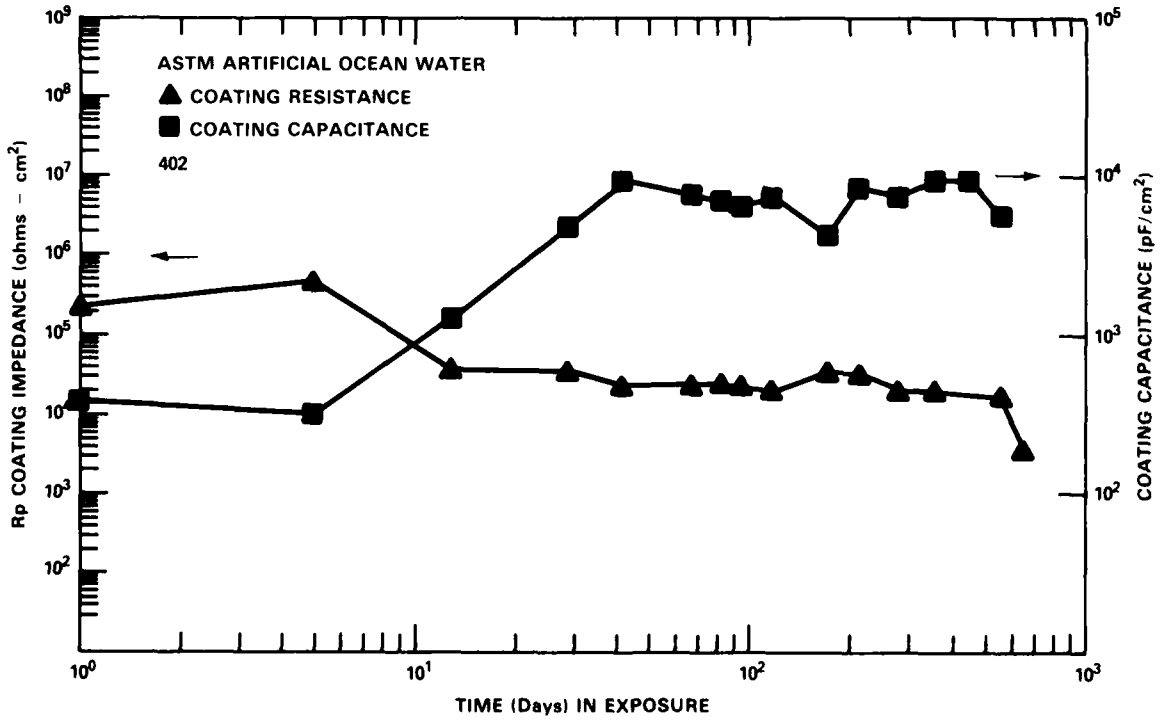

Fig. 17. Coating resistance and capacitance data for 55-μm-thick epoxy polyamide coated steel.

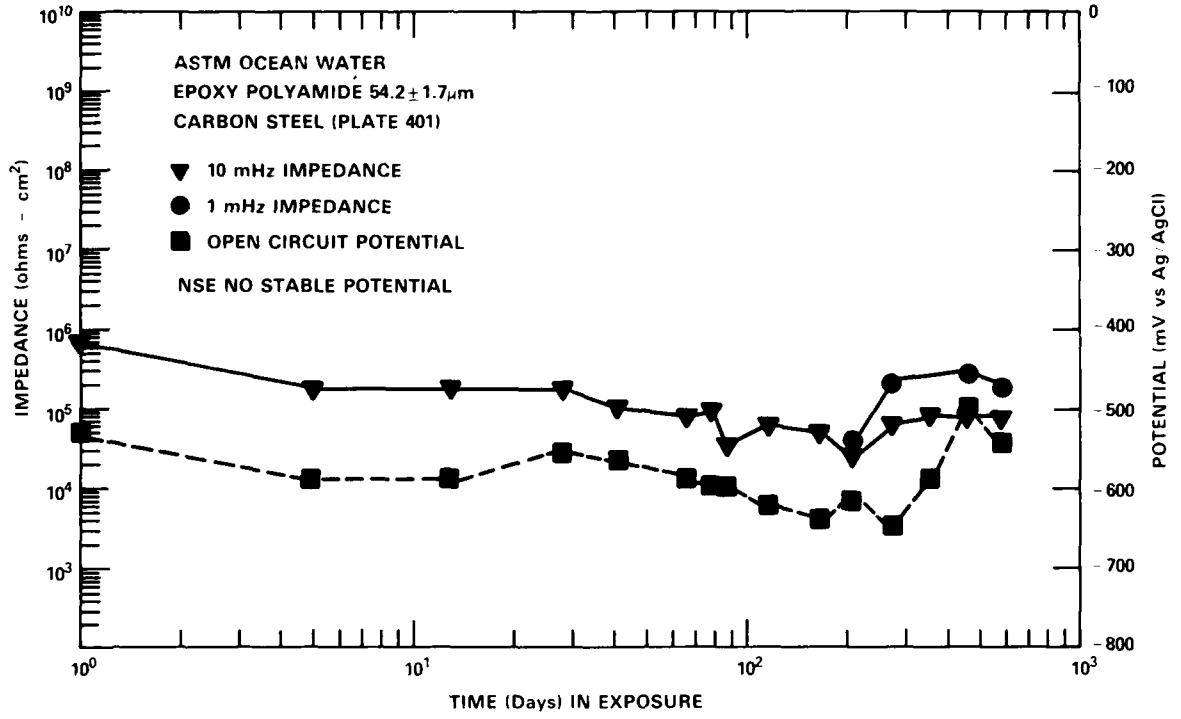

Fig. 18. Low frequency impedance behavior for 54-μm-thick epoxy polyamide coated steel.

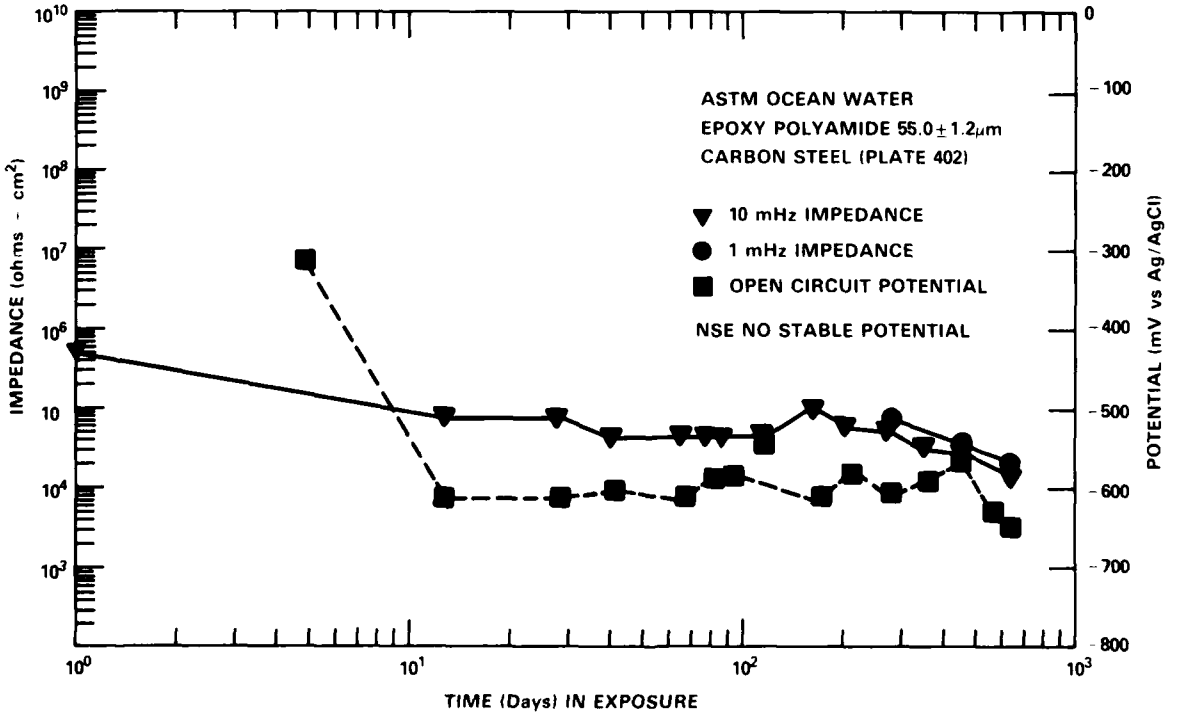

Fig. 19. Low frequency impedance behavior for 55-μm-thick epoxy polyamide coated steel.

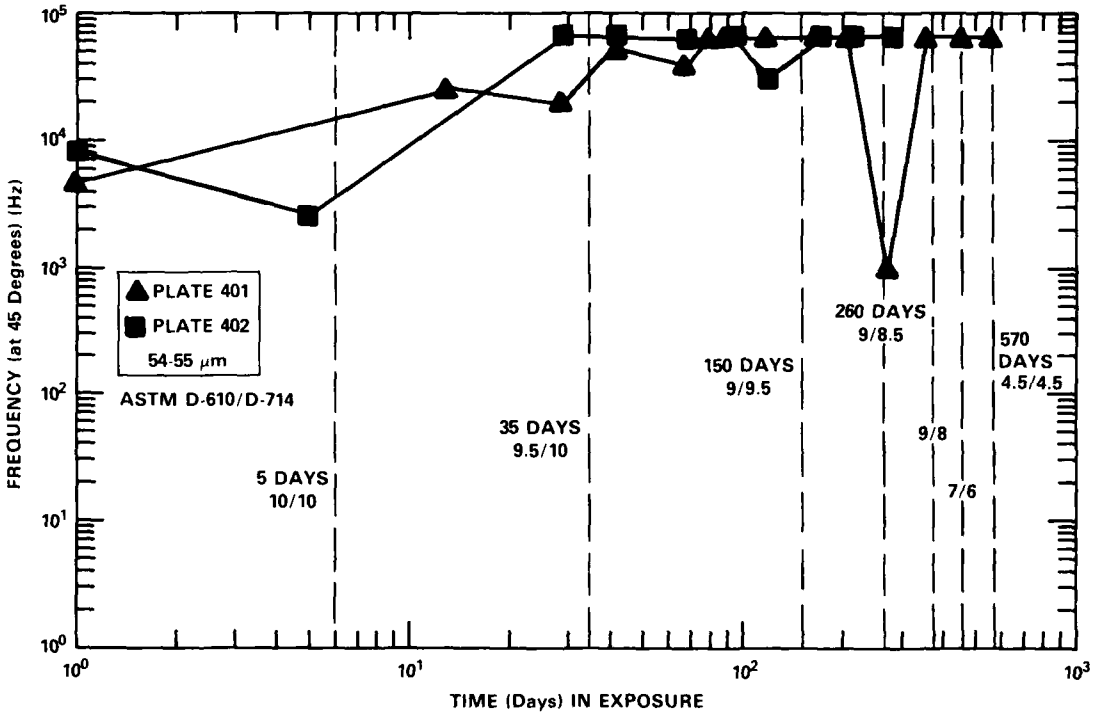

Fig. 20. Relative increases in electrochemically active area for 54-55-μm-thick epoxy polyamide coated steel.

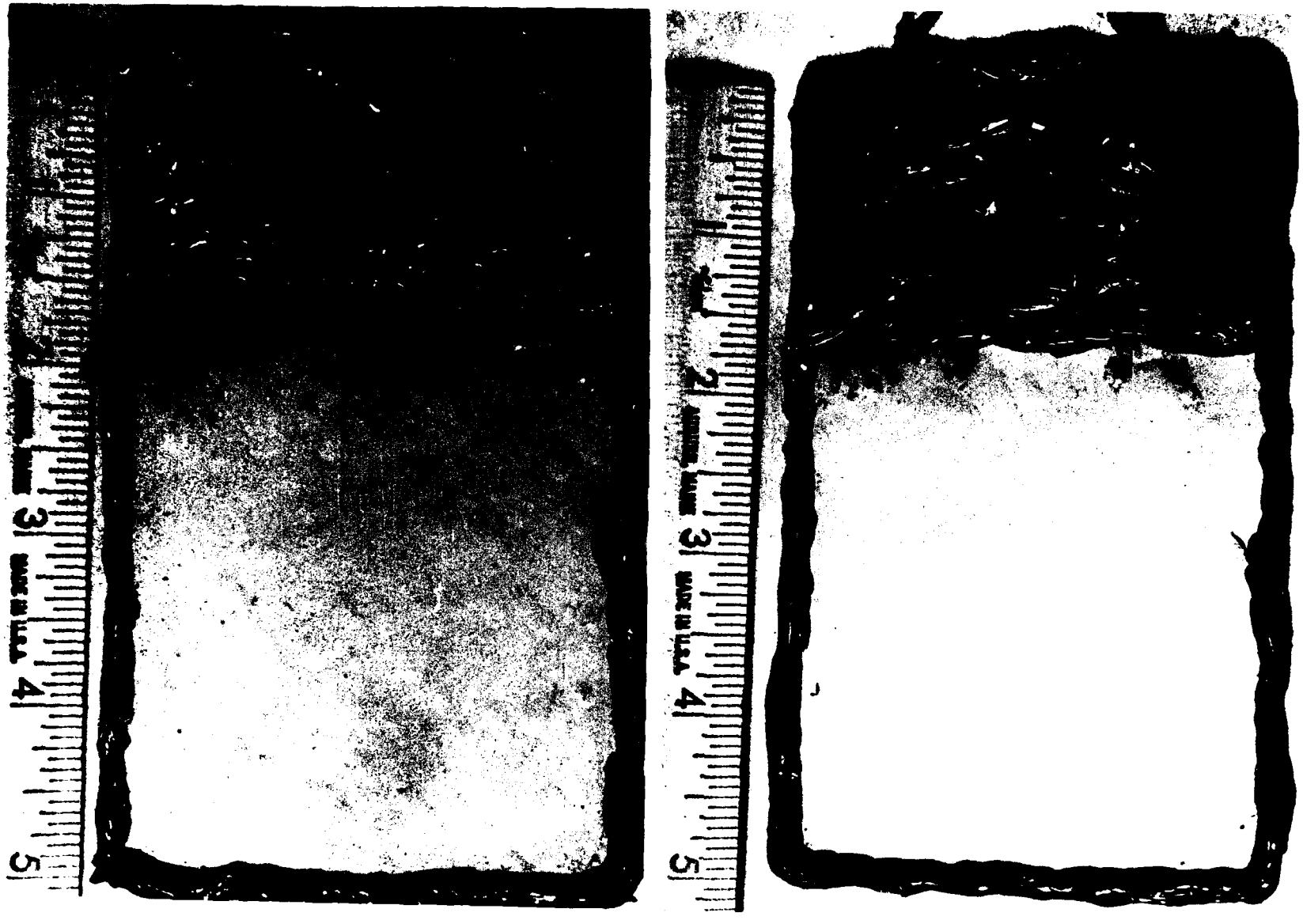

Fig. 21. Visual appearance of 54-55-μm-thick epoxy polyamide coated steel after 158-days exposure in ASTM artificial ocean water.

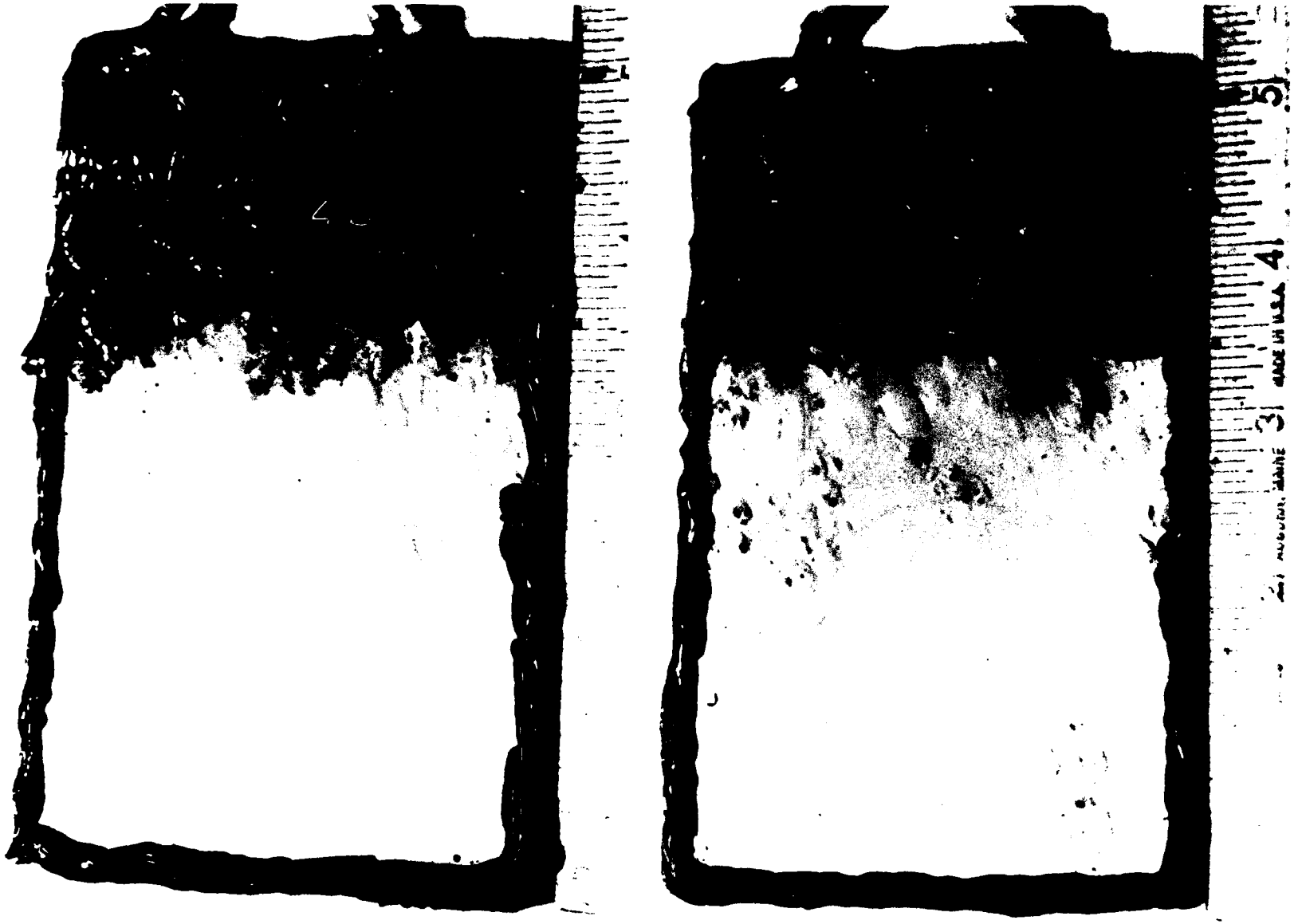

Fig. 22. Visual appearance of 54-55-μm-thick epoxy polyamide coated steel after 400-days exposure in ASTM artificial ocean water.

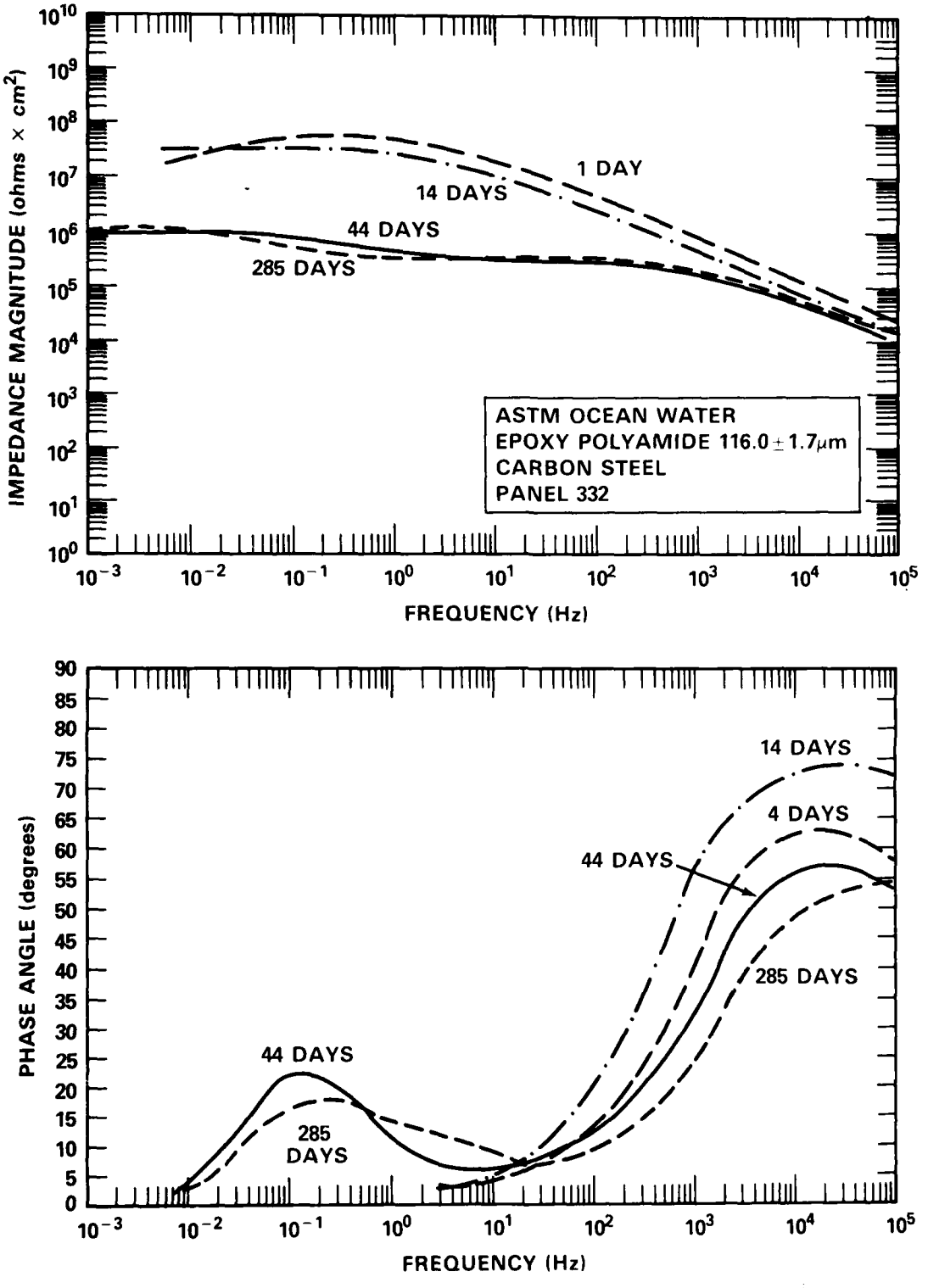

Fig. 23. Bode magnitude and phase data for 116-μm-thick epoxy polyamide coated steel.

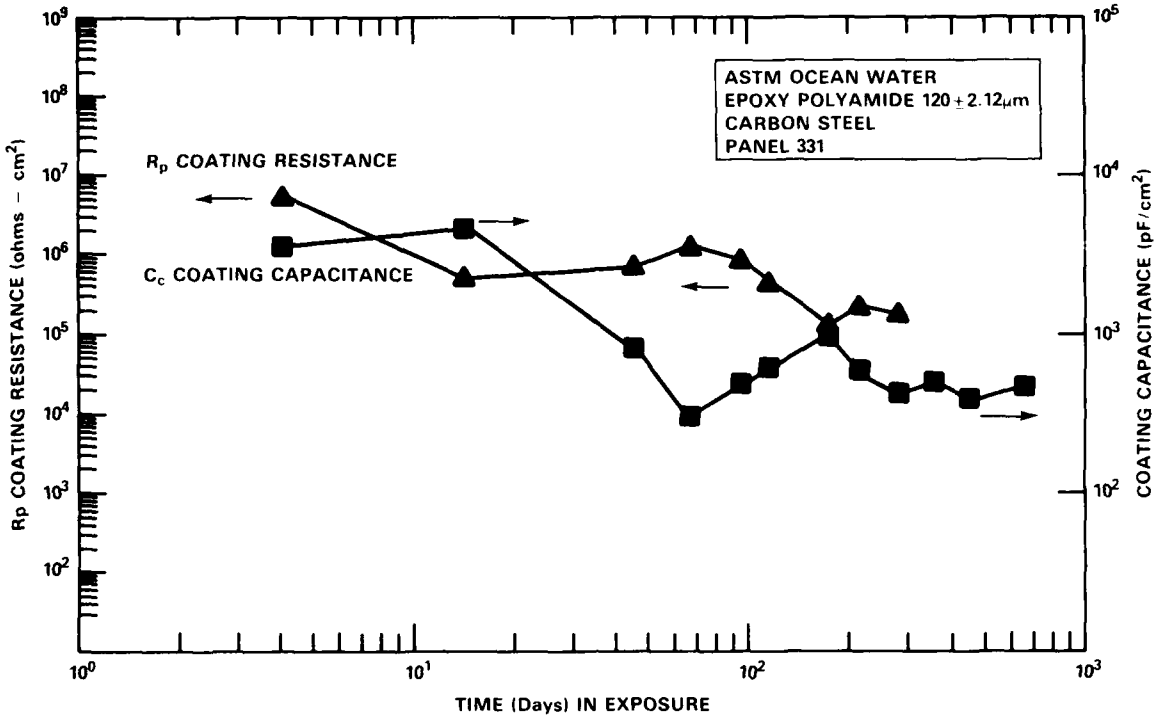

Fig. 24. Coating resistance and capacitance behavior as a function of exposure time for 121-μm-thick epoxy polyamide coated steel.

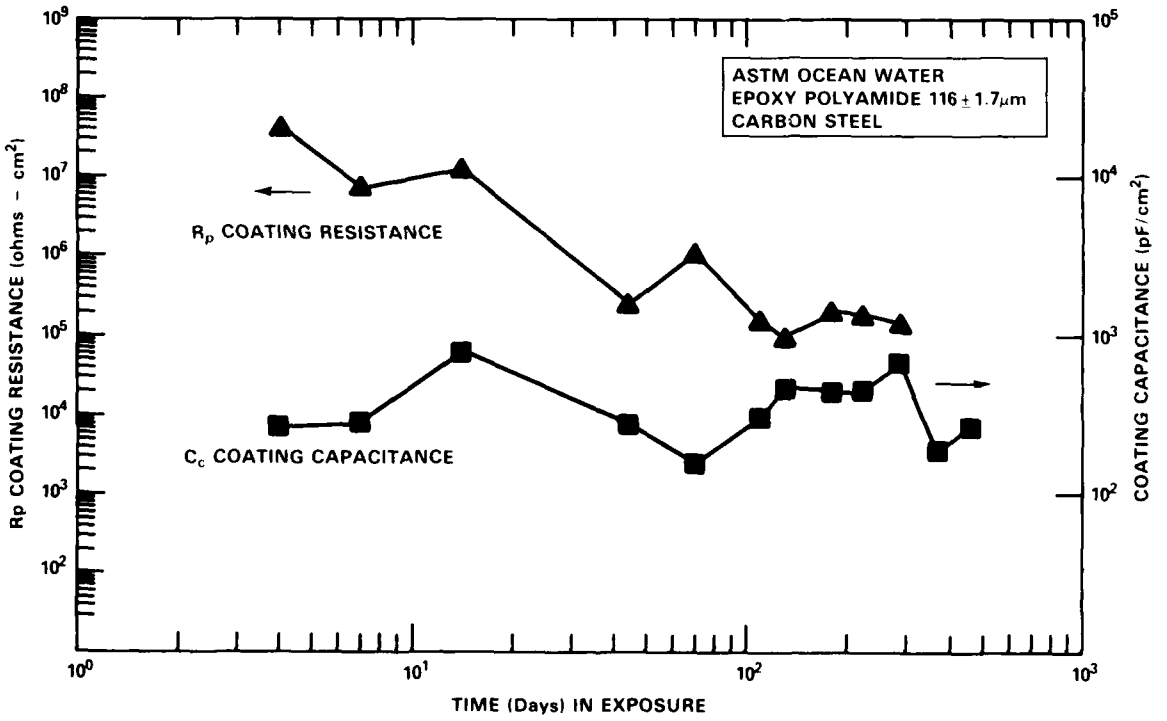

Fig. 25. Coating resistance and capacitance behavior as a function of exposure time for 116-μm-thick epoxy polyamide coated steel.

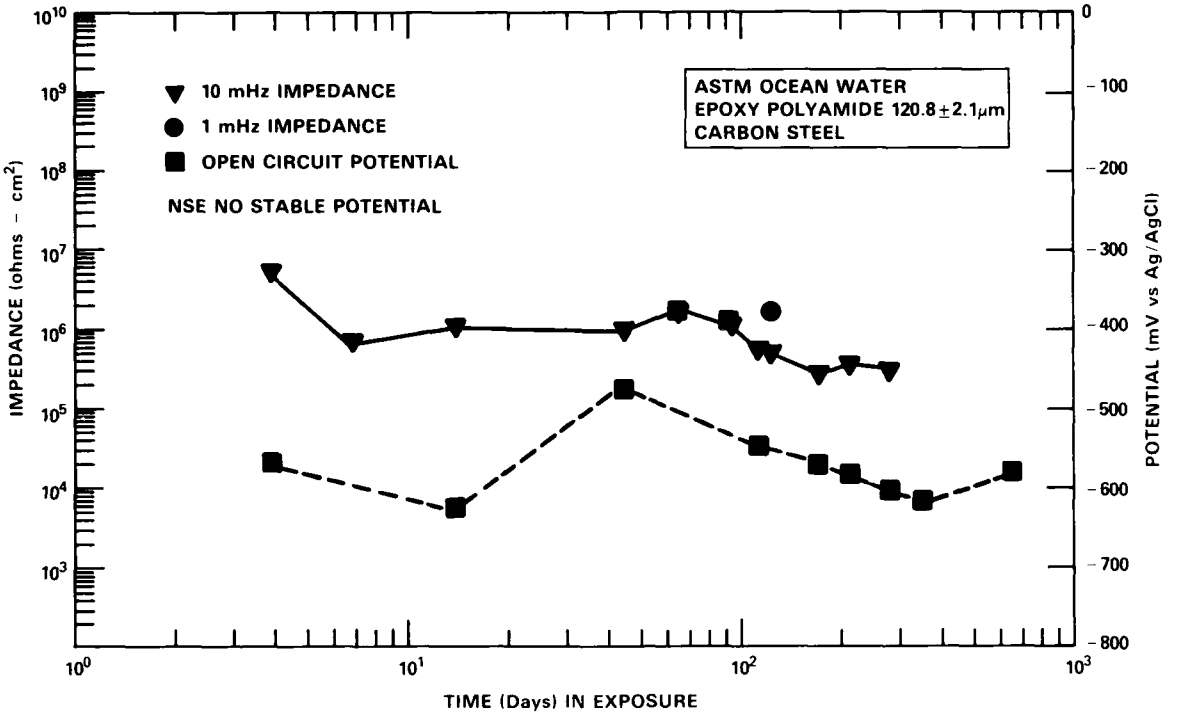

Fig. 26. Low frequency impedance behavior as a function of exposure time for 121-μm-thick epoxy polyamide coated steel.

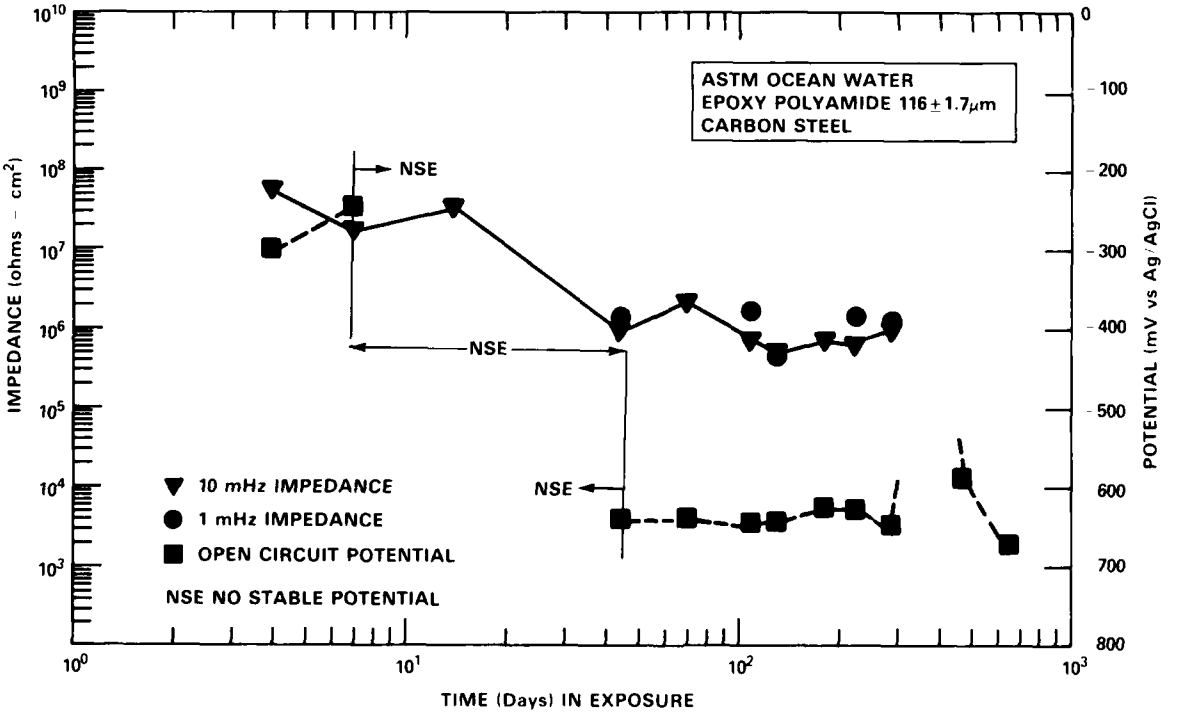

Fig. 27. Low frequency impedance behavior as a function of exposure time for 116-μm-thick epoxy polyamide coated steel.

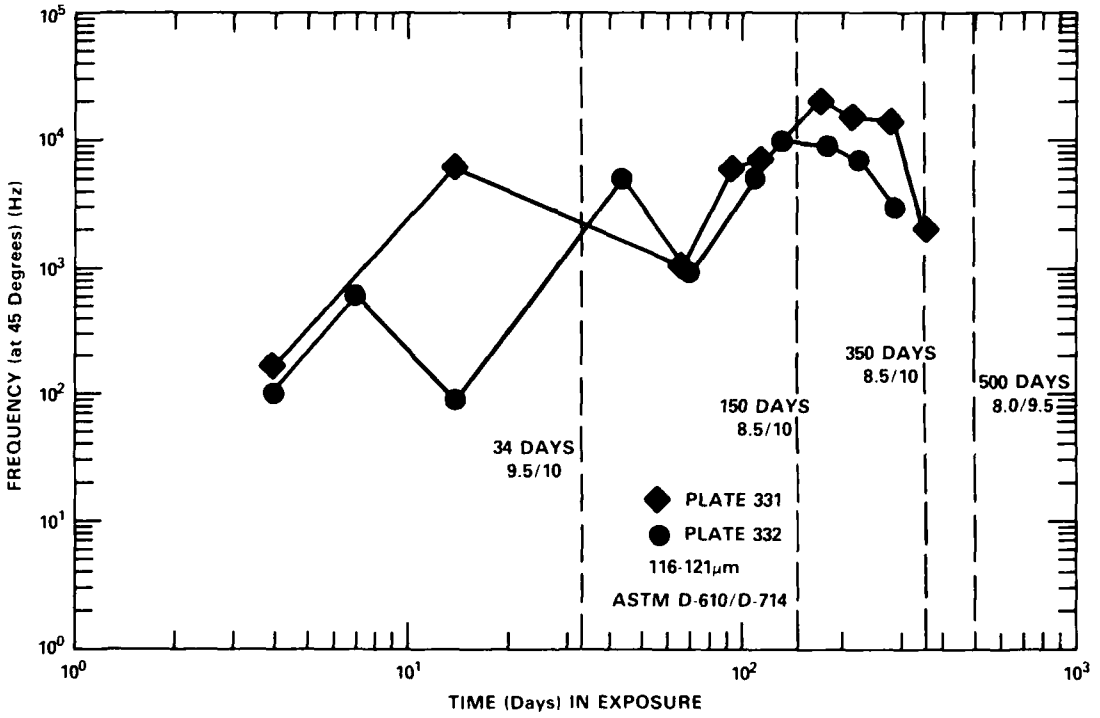

Fig. 28. Relative increases in electrochemically active area for 116-121-μm-thick epoxy polyamide coated steel.

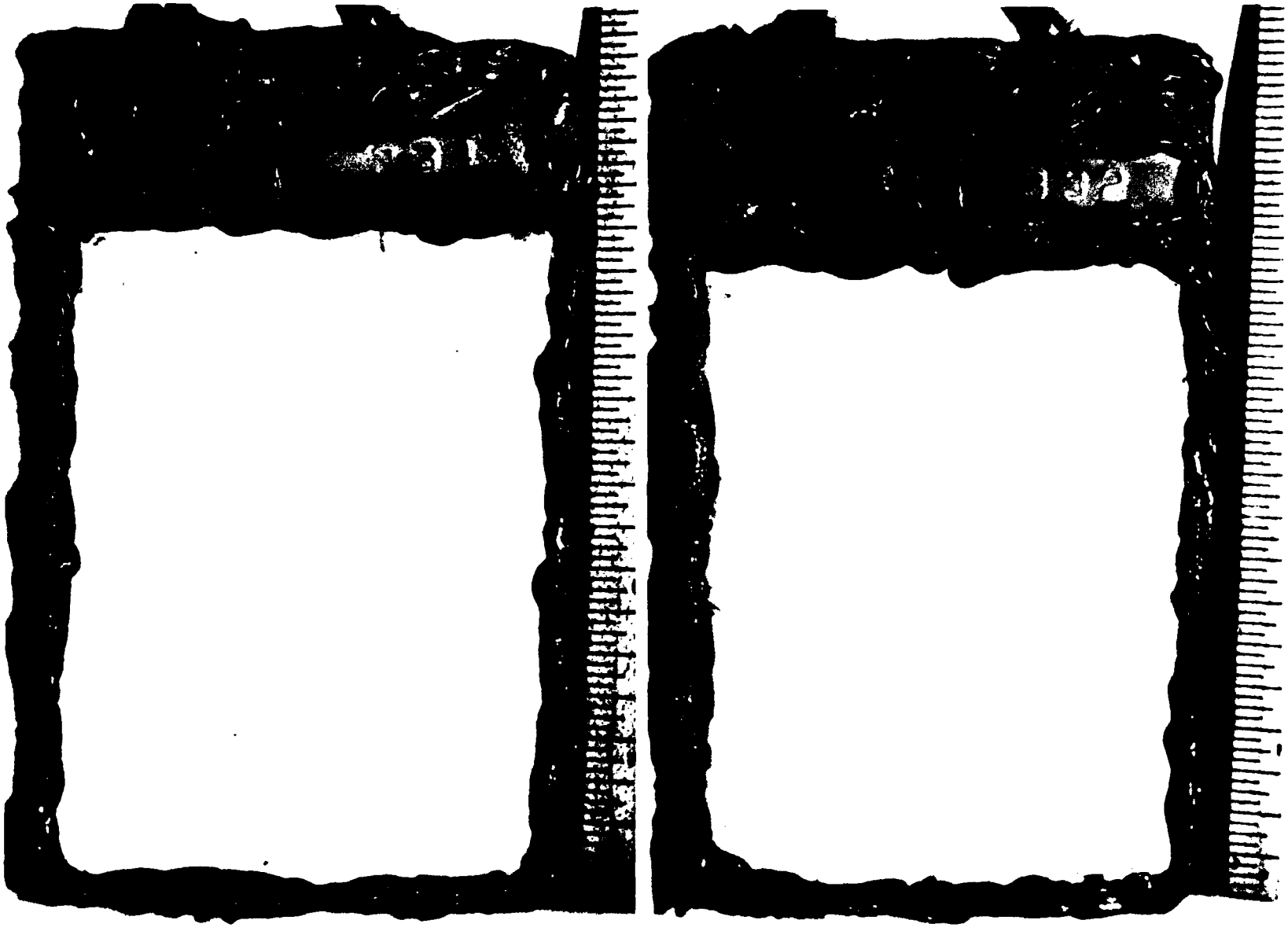

Fig. 29. Visual appearance of 116-121-μm-thick epoxy polyamide coated steel after 267-days exposure in ASTM artificial ocean water.

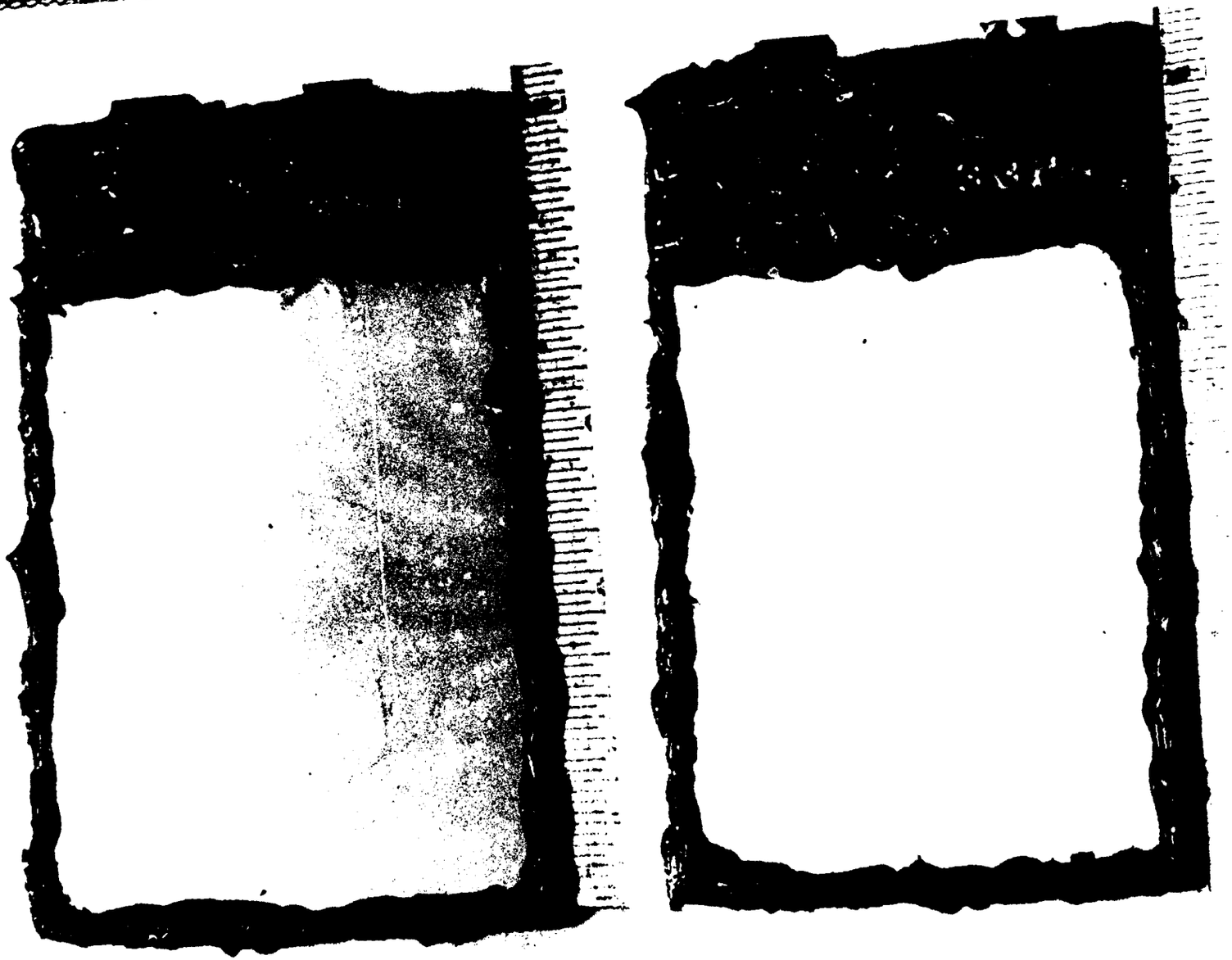

Fig. 30. Visual appearance of 116-121-μm-thick epoxy polyamide coated steel after 400-days exposure in ASTM artificial ocean water.

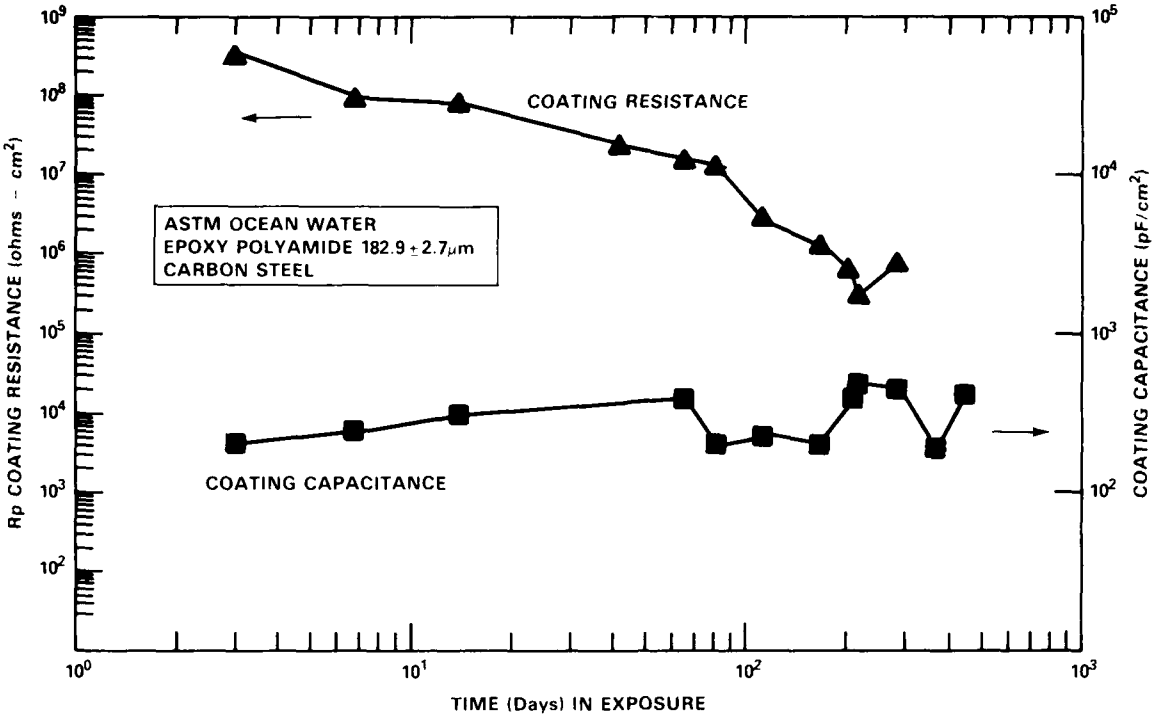

Fig. 31. Coating resistance and capacitance behavior as a function of exposure time for 183-μm-thick epoxy polyamide coated steel.

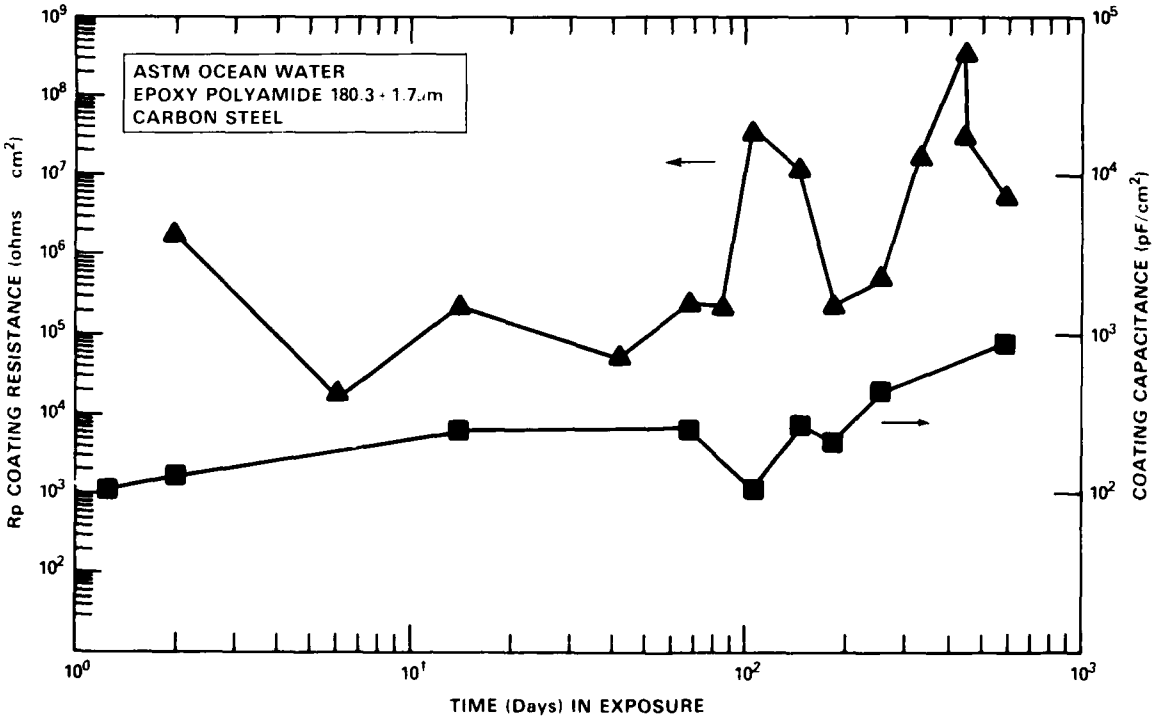

Fig. 32. Coating resistance and capacitance behavior as a function of exposure time for 180-μm-thick epoxy polyamide coated steel.

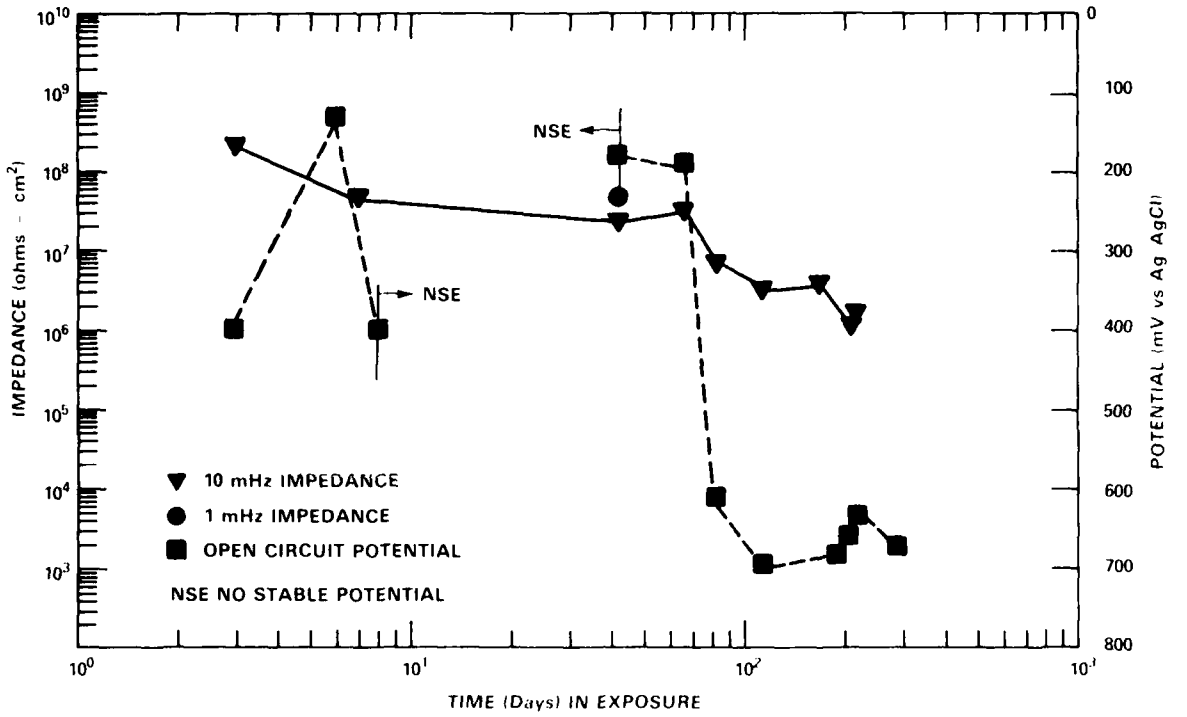

Fig. 33. Low frequency impedance behavior as a function of exposure time for 183-μm-thick epoxy polyamide coated steel.

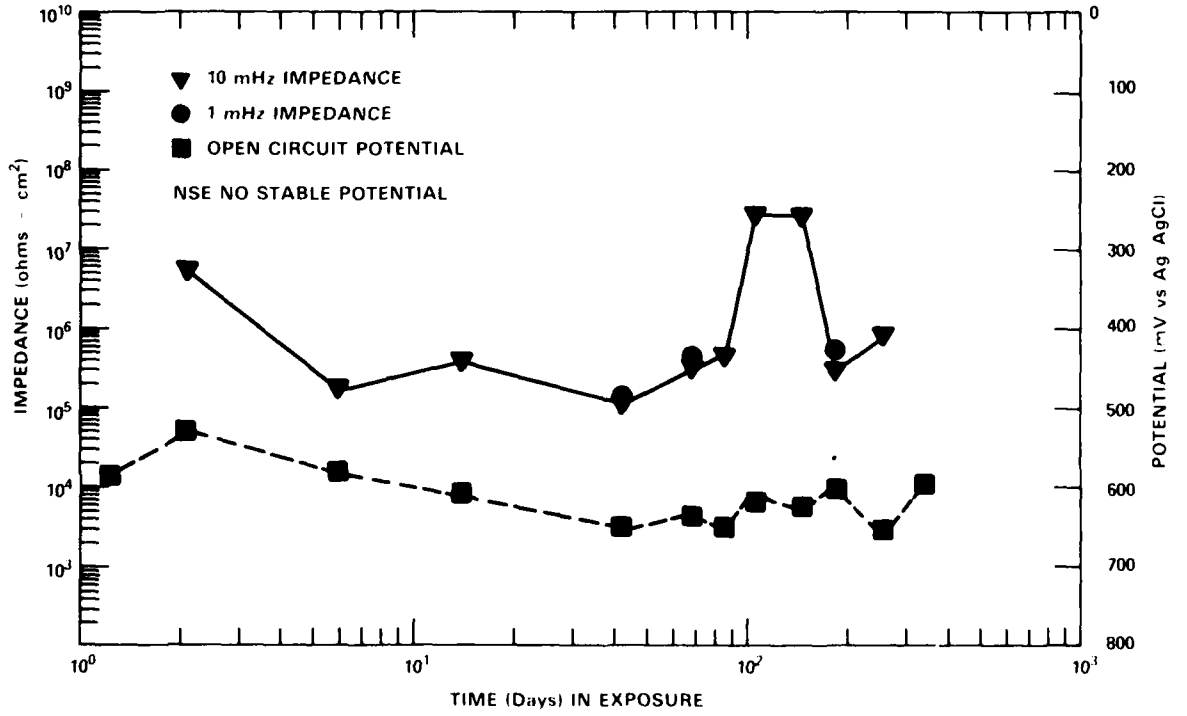

Fig. 34. Low frequency impedance behavior as a function of exposure time for 180-μm-thick epoxy polyamide coated steel.

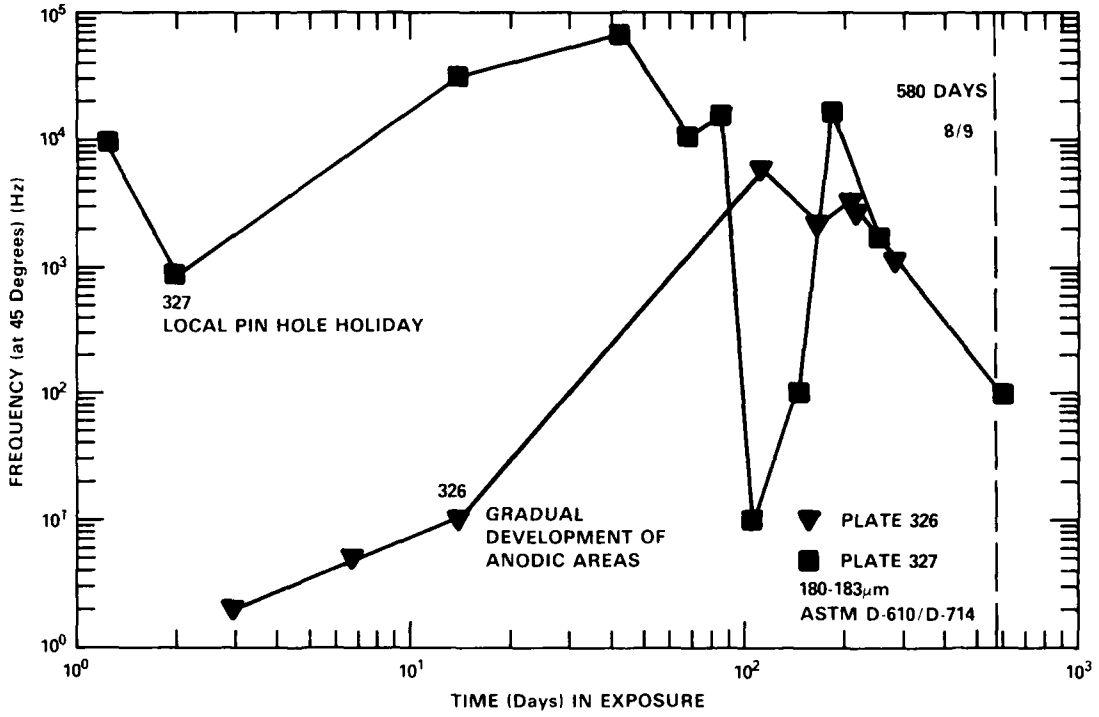

Fig. 35. Relative increases in electrochemically active area for 180-183-μm-thick epoxy polyamide coated steel.

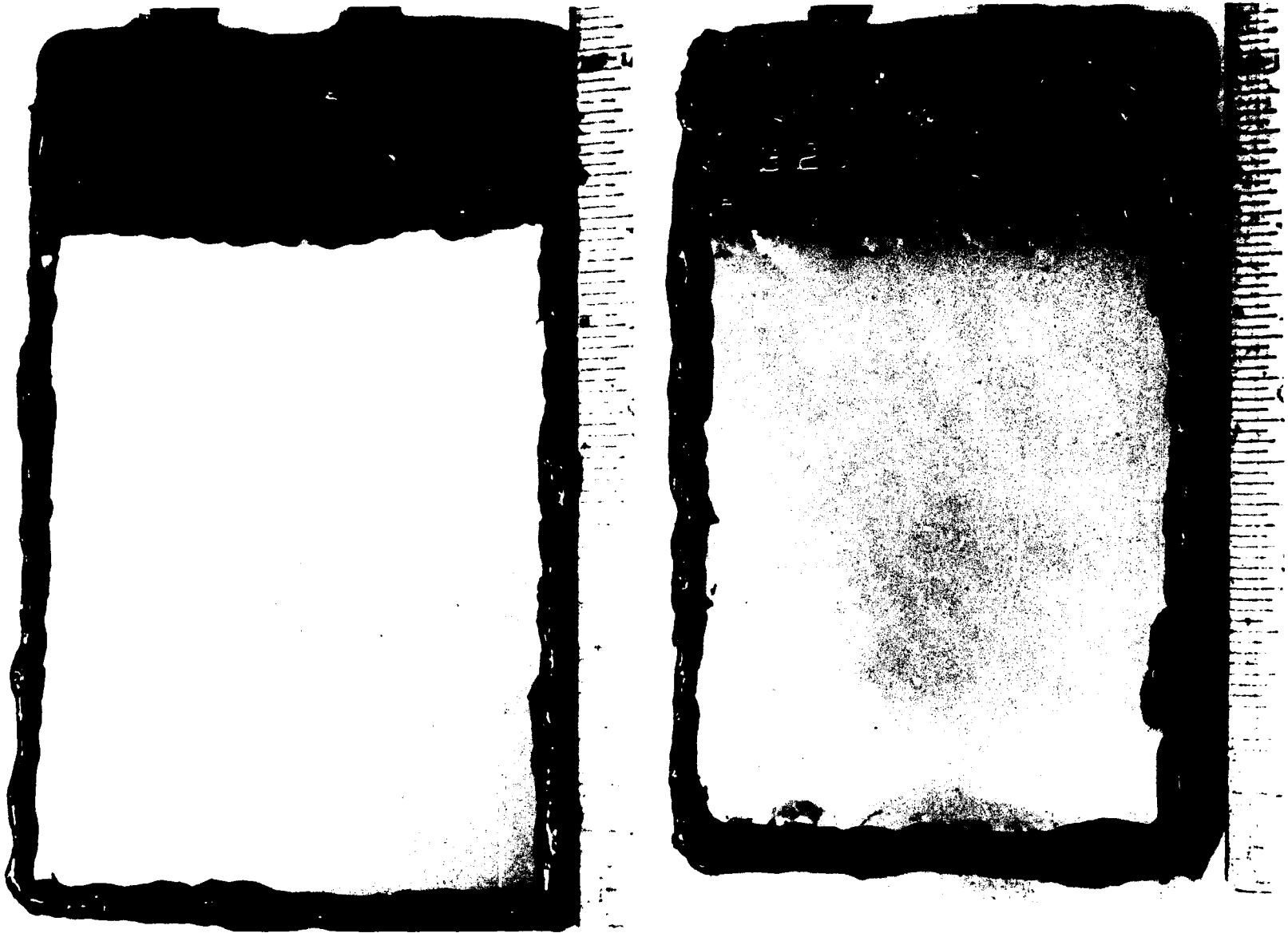

Fig. 36. Visual appearance of 180-180-µm-thick epoxy polyamide coated steel after 267-days exposure in ASTM artificial ocean water.

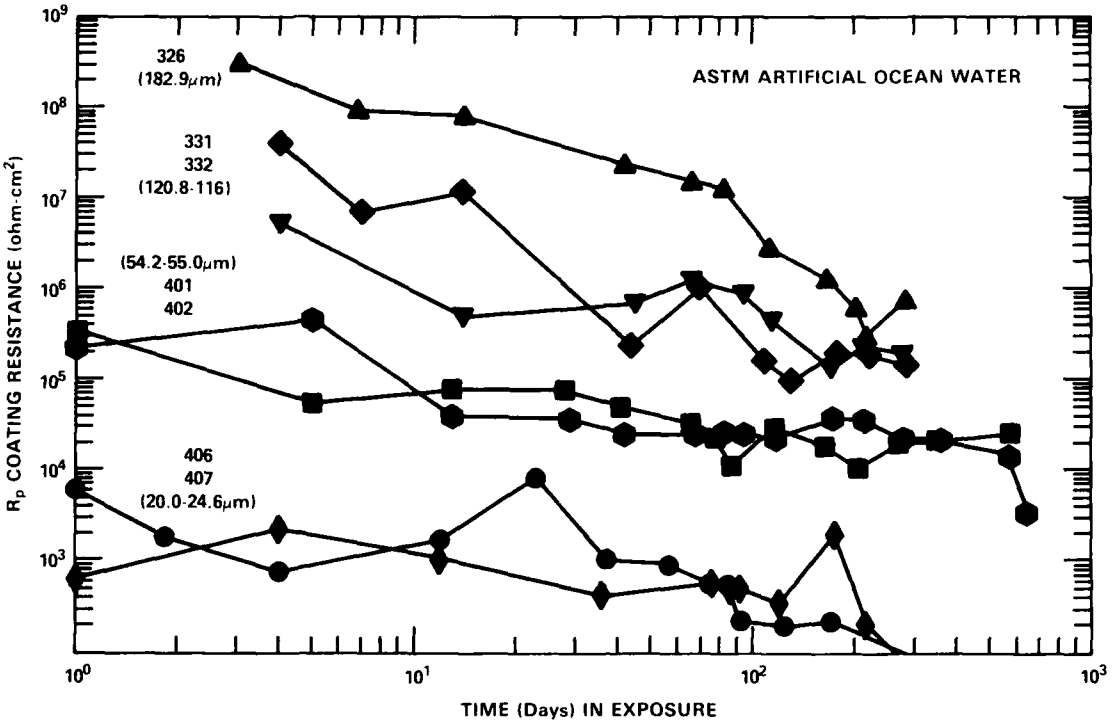

Fig. 37. Comparison of coating resistance behavior as a function of exposure time for various thicknesses of epoxy polyamide coated steel.

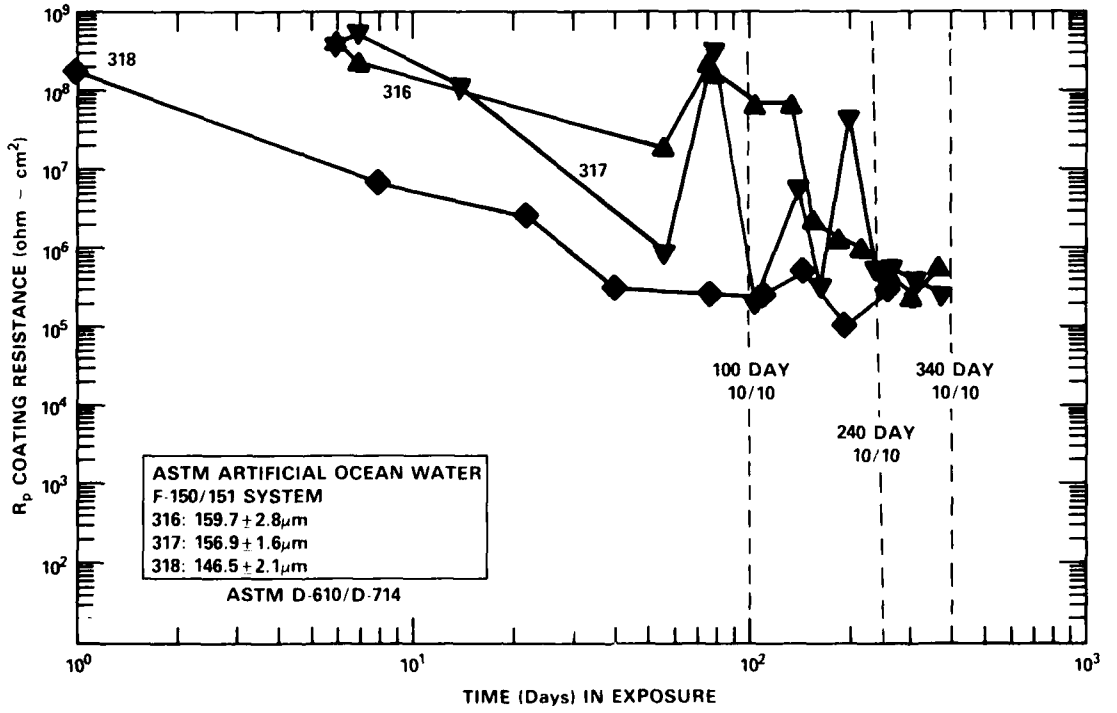

Fig. 38. Coating resistance as a function of exposure time for 146-160-μm-thick epoxy polyamide coated steel.

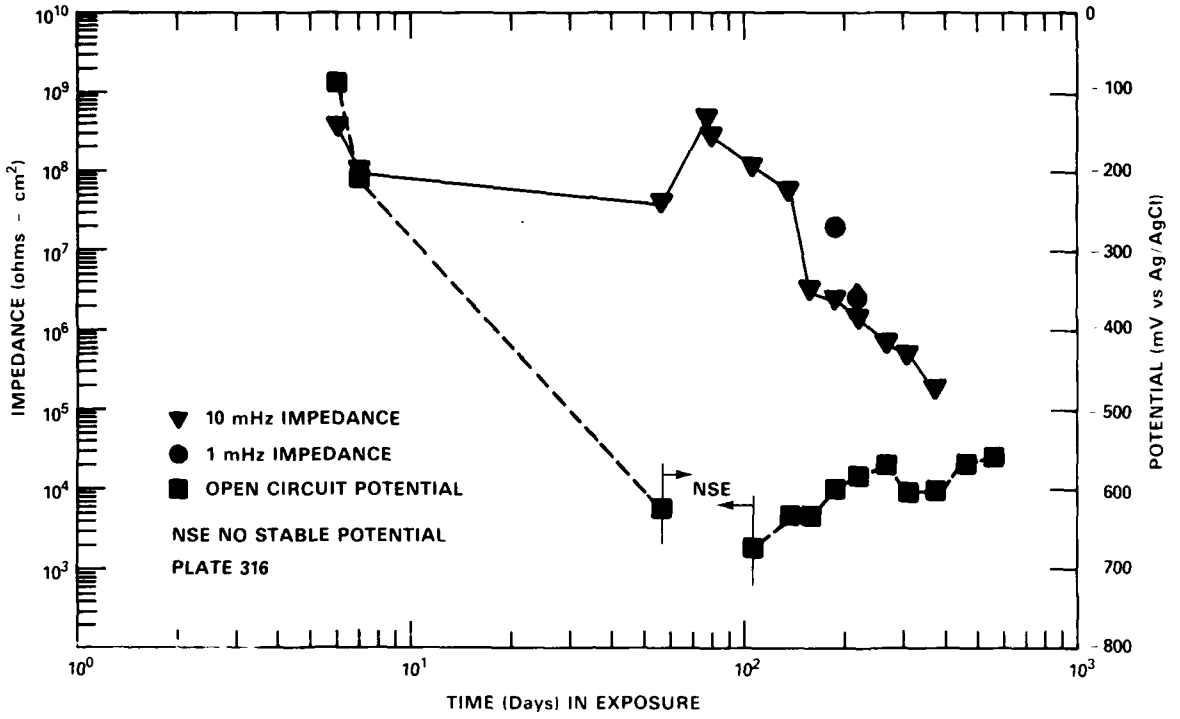

Fig. 39. Low frequency impedance behavior as a function of exposure time for 160-μm-thick epoxy polyamide coated steel.

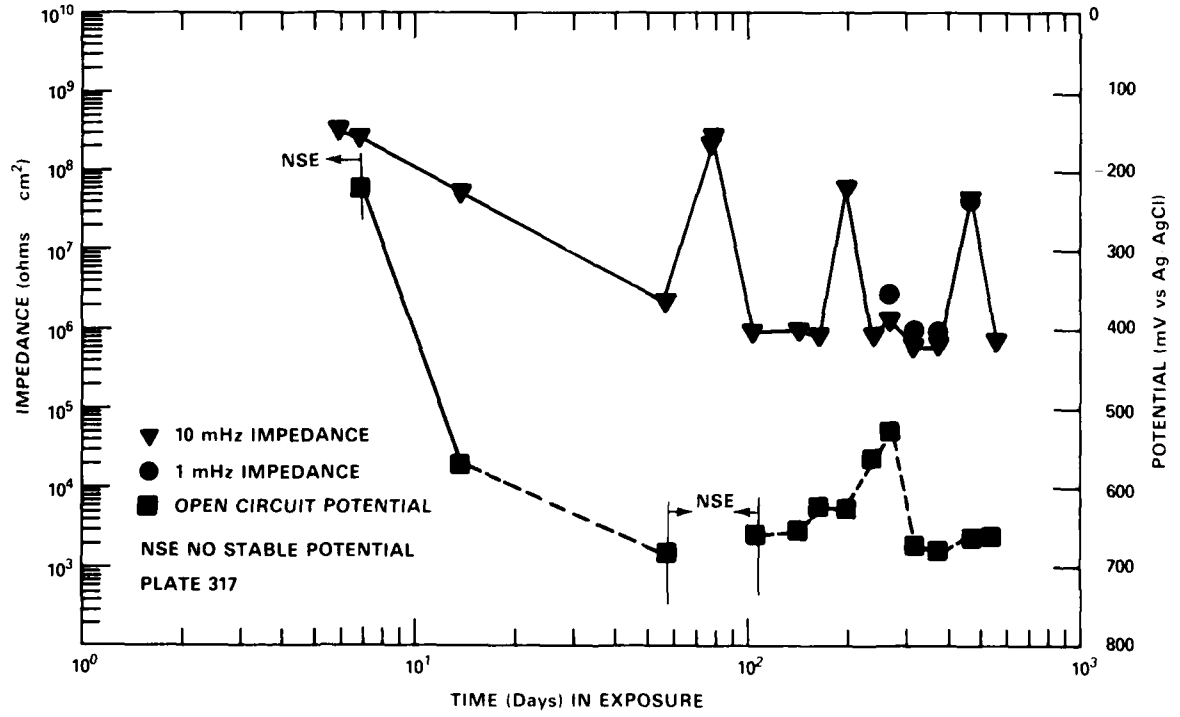

Fig. 40. Low frequency impedance behavior as a function of exposure time for 157-μm-thick epoxy polyamide coated steel.

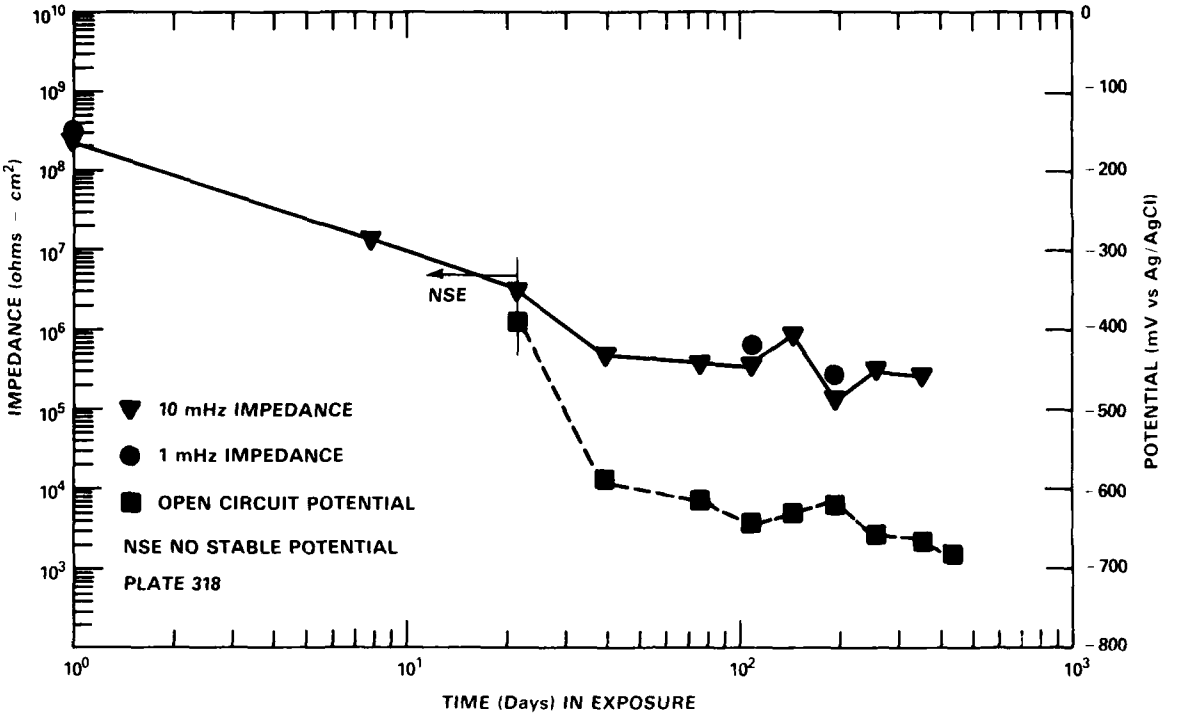

Fig. 41. Low frequency impedance behavior as a function of exposure time for 146-μm-thick epoxy polyamide coated steel.

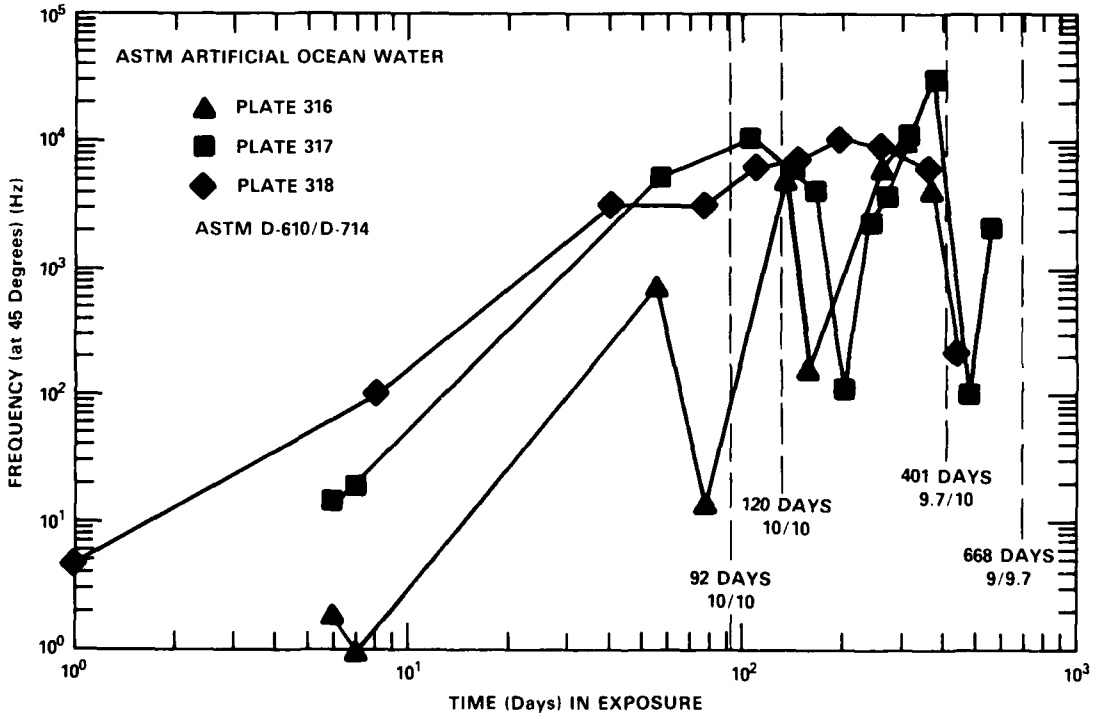

Fig. 42. Relative increases in electrochemically active area for 146-160-μm-thick epoxy polyamide coated steel.

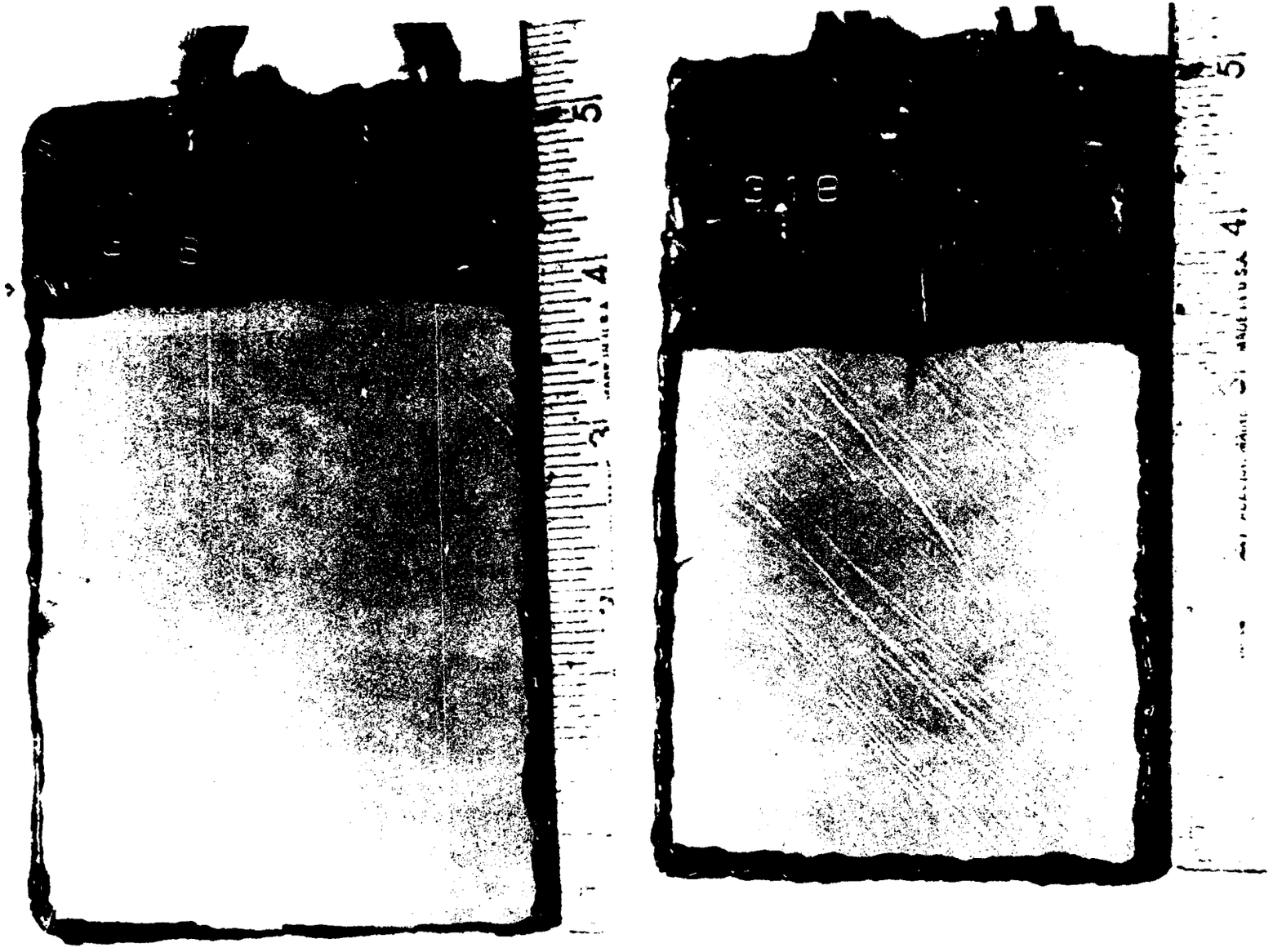

Fig. 43. Visual appearance of 146-160-μm-thick epoxy polyamide coated steel after 366-days exposure in ASTM artificial ocean water.

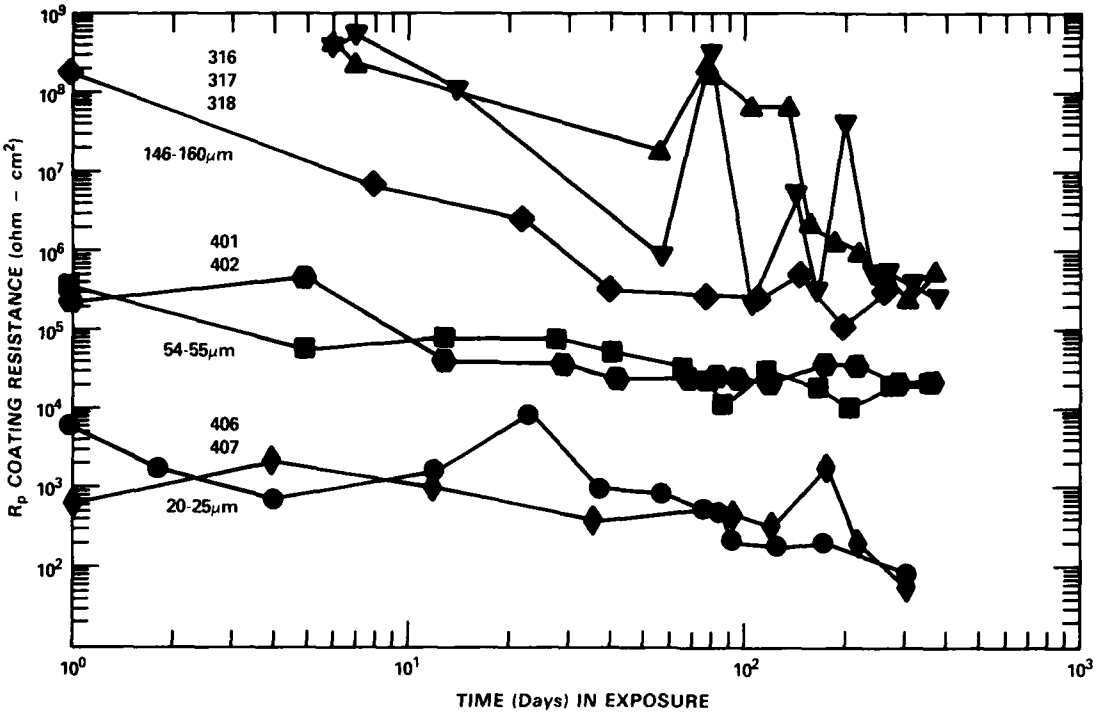

Fig. 44. Comparison of coating resistance behavior as a function of exposure time for various thicknesses of epoxy polyamide coated steel.

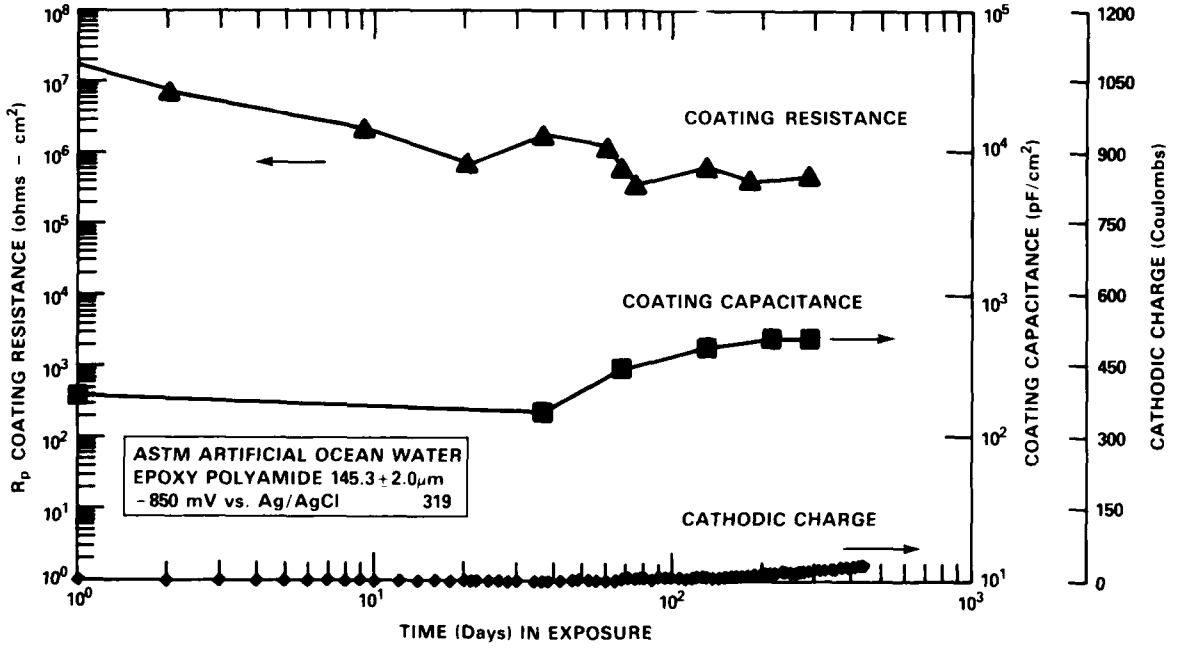

Fig. 45. Coating resistance, capacitance and total cathodic charge for cathodically polarized epoxy polyamide coated steel (-850 mV vs. SCE).

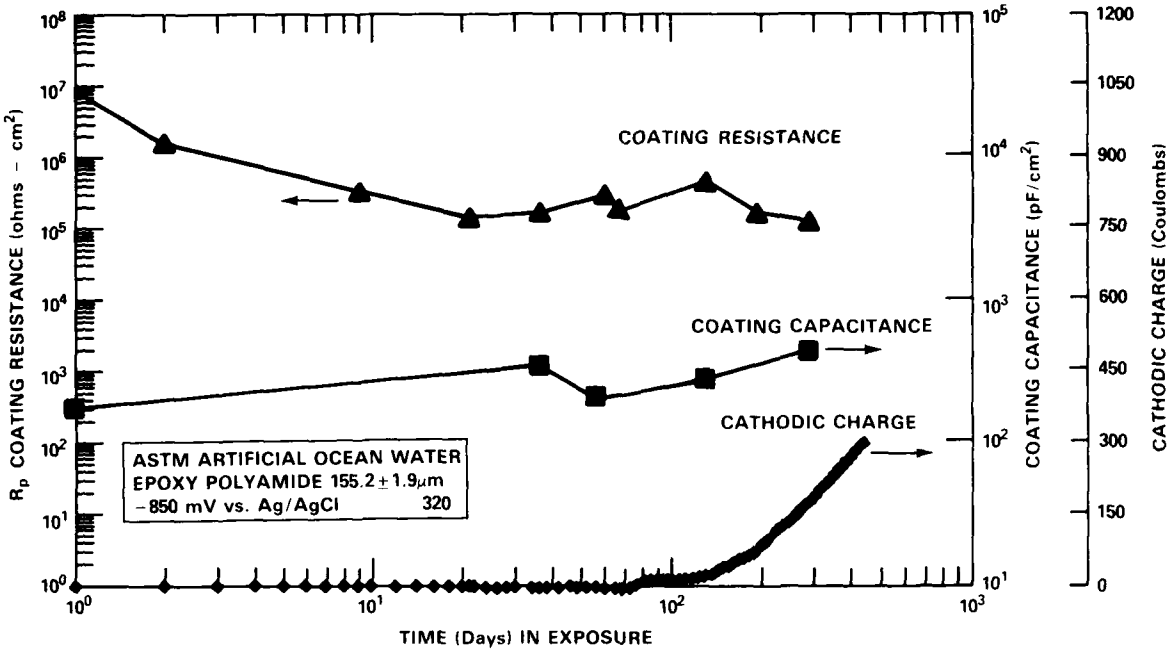

Fig. 46. Coating resistance, capacitance and total cathodic charge for cathodically polarized epoxy polyamide coated steel (-850 mV vs. SCE).

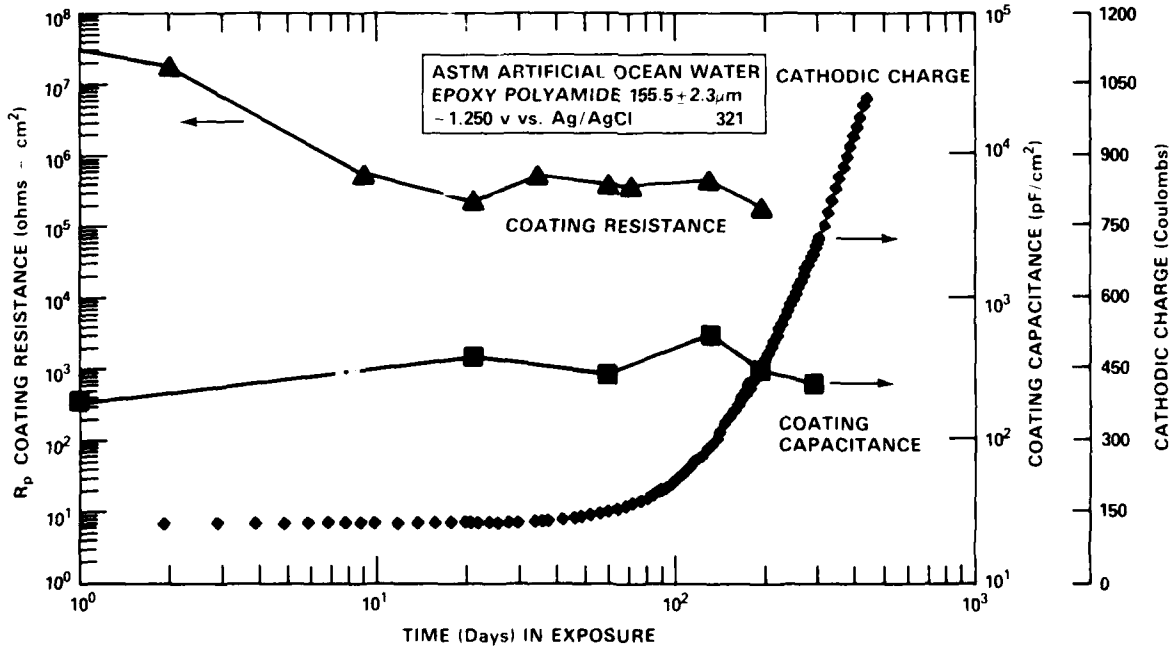

Fig. 47. Coating resistance, capacitance and total cathodic charge for cathodically polarized epoxy polyamide coated steel (-1250 mV vs. SCE).

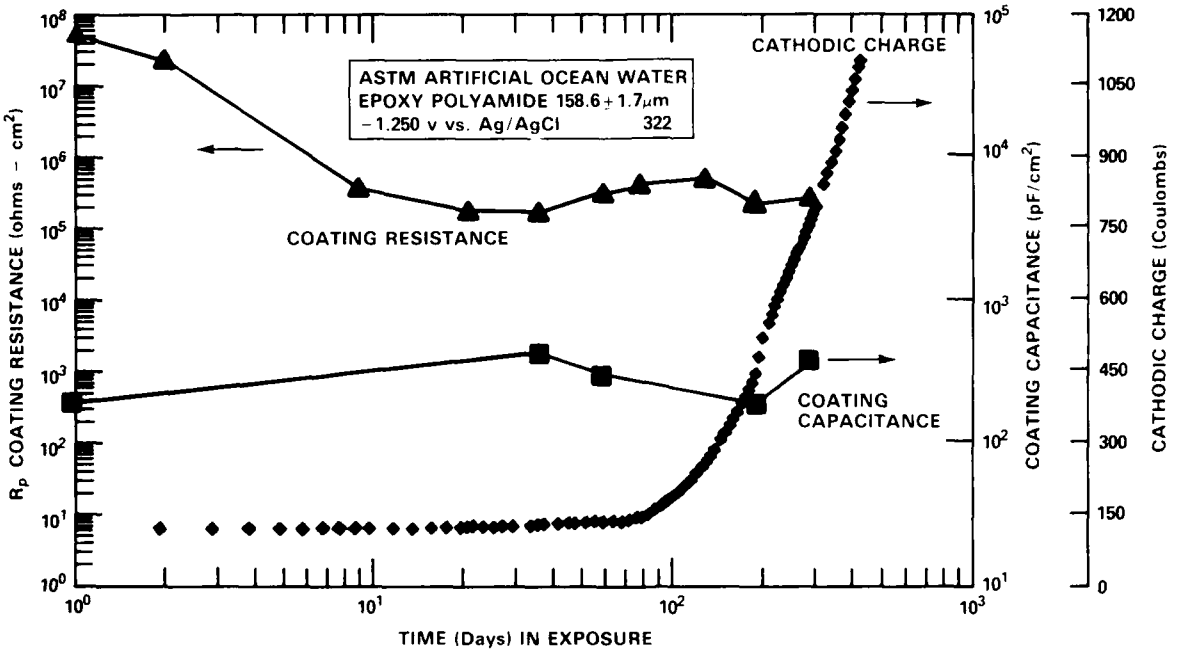

Fig. 48. Coating resistance, capacitance and total cathodic charge for cathodically polarized epoxy polyamide coated steel (-1250 mV vs. SCE).

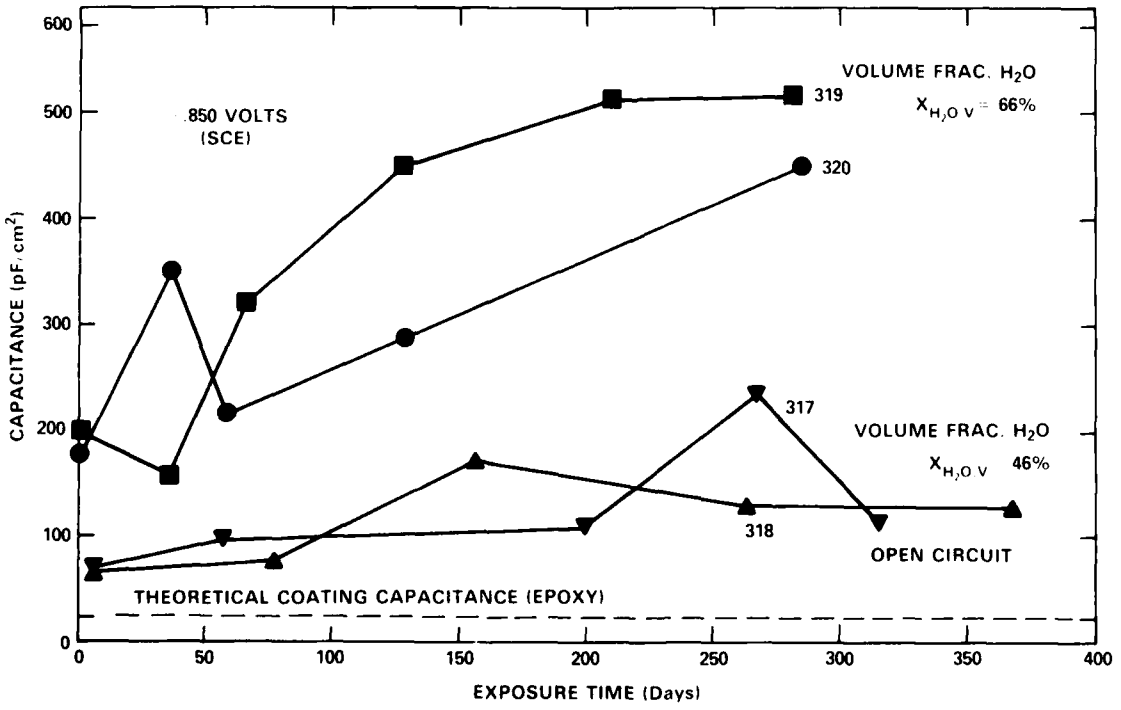

Fig. 49. Coating capacitance versus time.

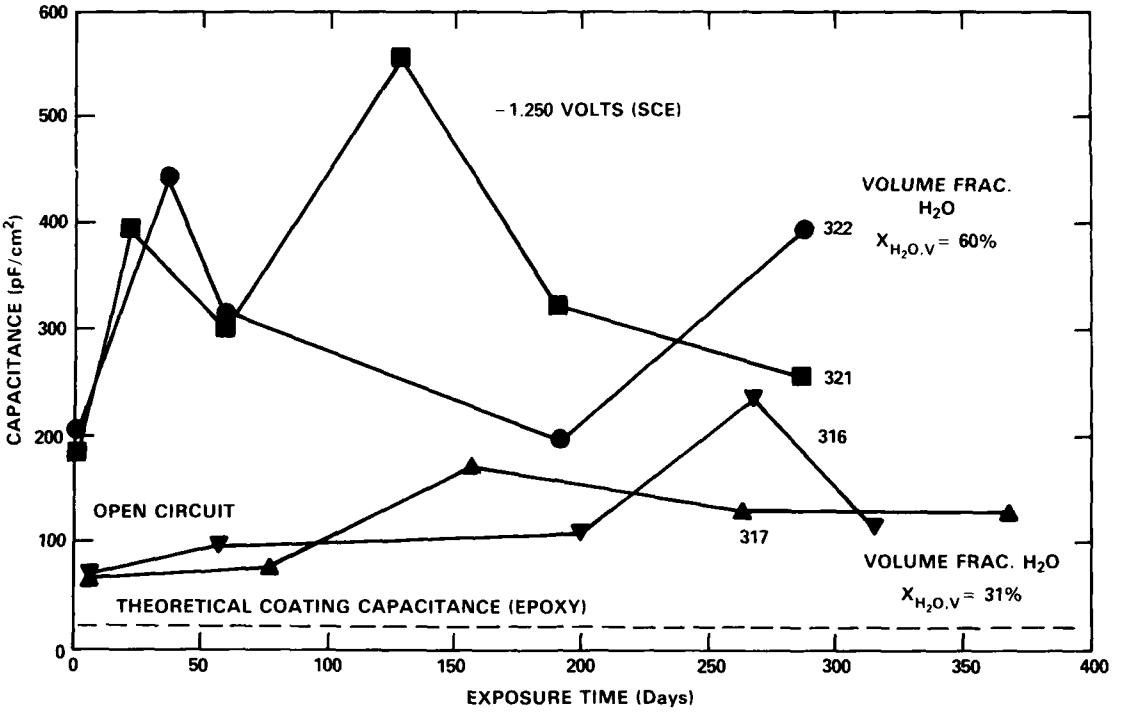

Fig. 50. Coating capacitance versus time.

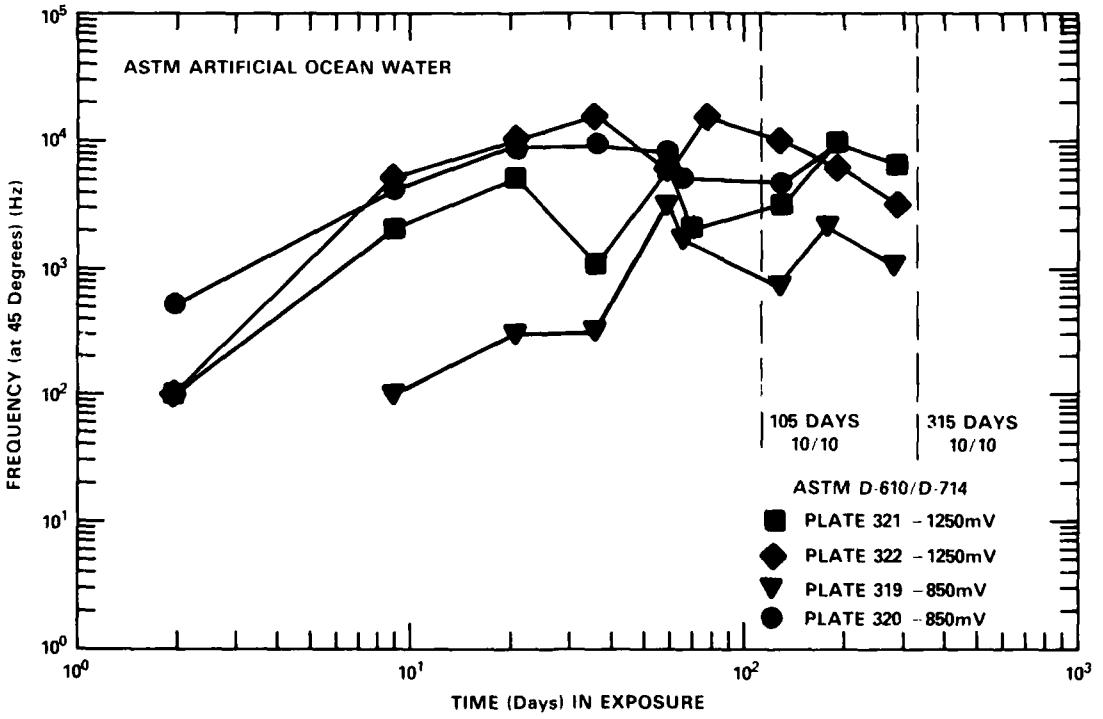

Fig. 51. Relative increases in electrochemically active area for cathodically polarized epoxy polyamide coated steel.

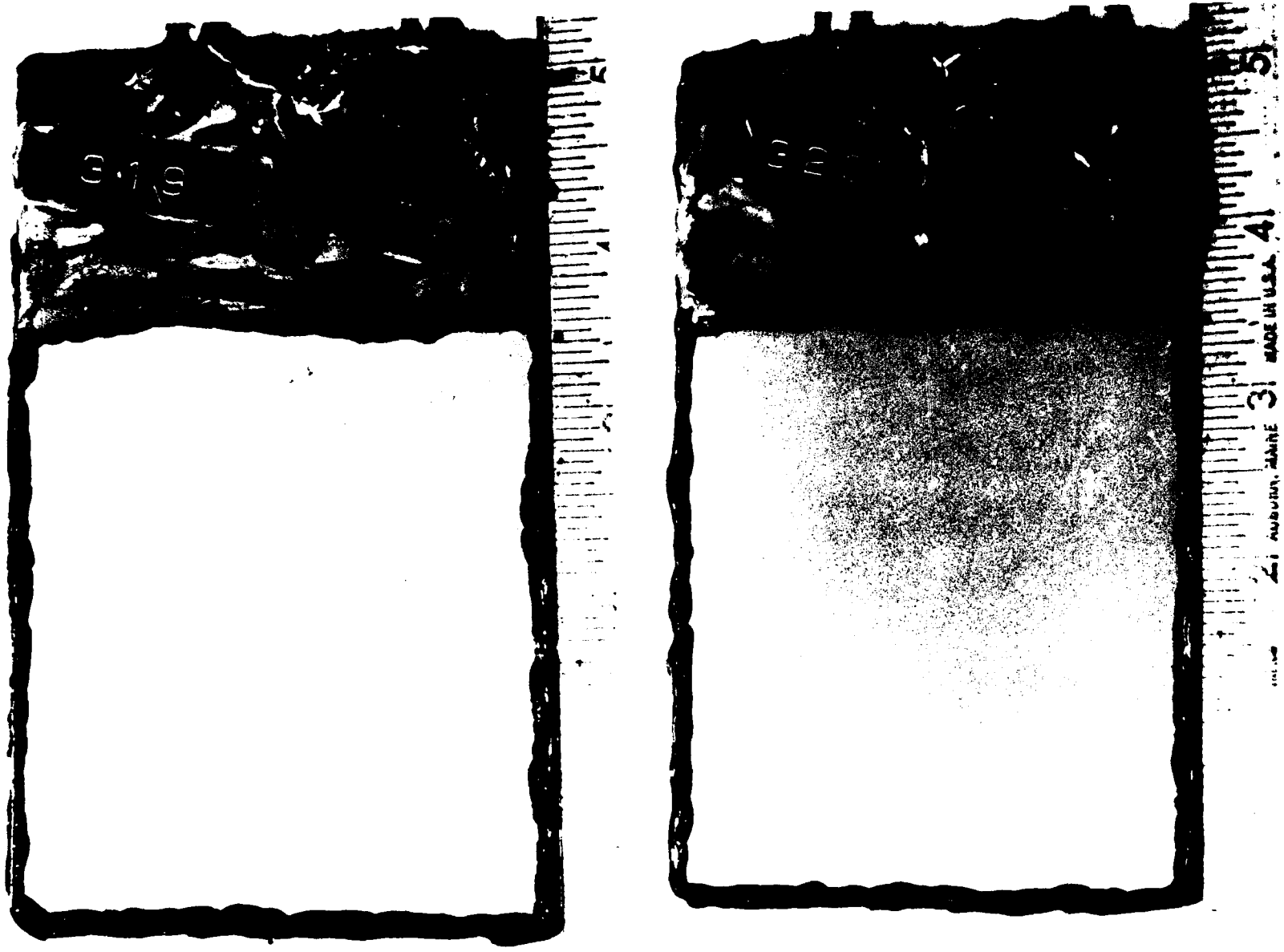

Fig. 52. Visual appearance of 145-155-μm-thick epoxy polyamide coated steel after 345-days exposure in ASTM artificial ocean water (-850 mV vs. SCE).

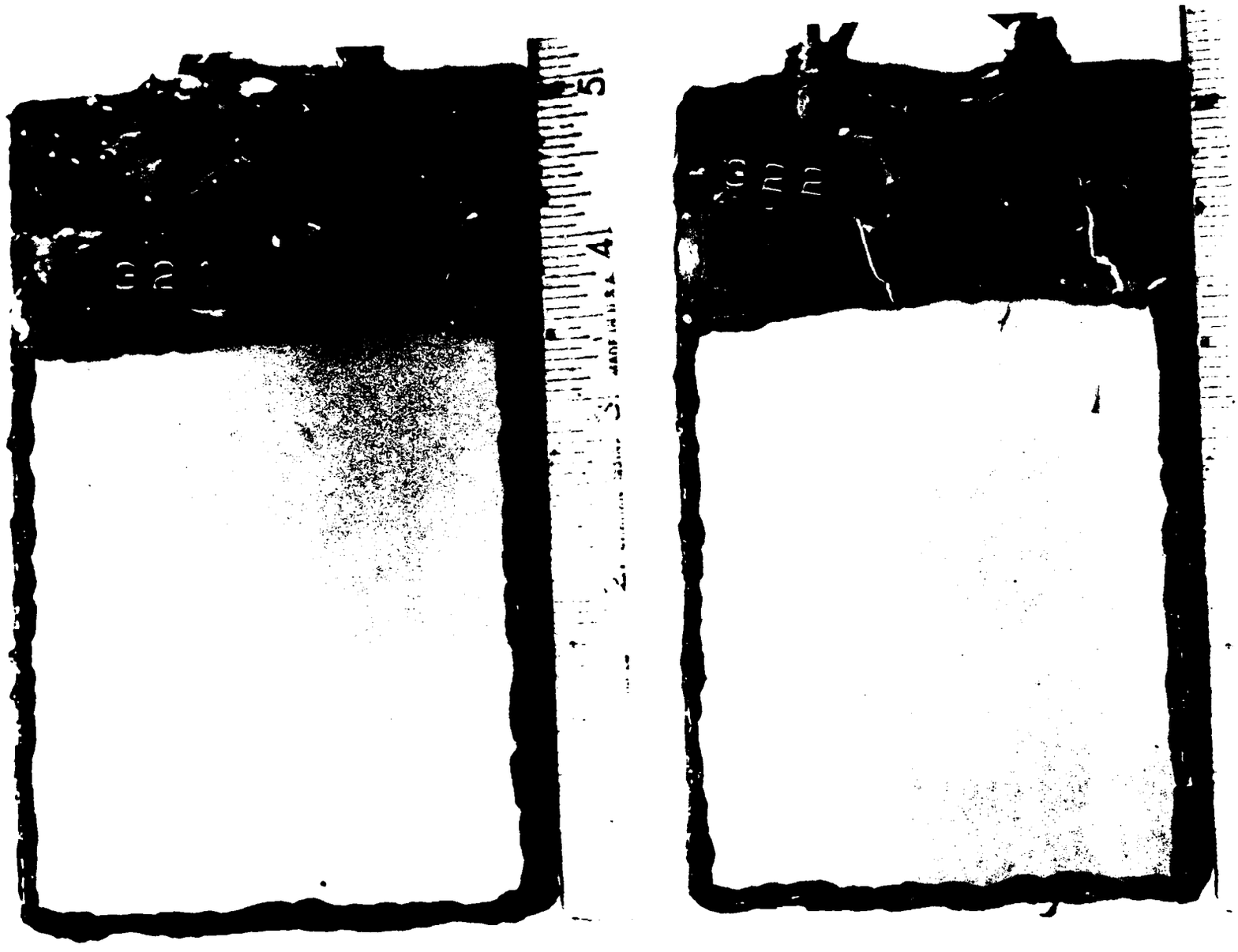

Fig. 53. Visual appearance of 155-160-μm-thick epoxy polyamide coated steel after 345-days exposure in ASTM artificial ocean water (-850 mV vs. SCE).

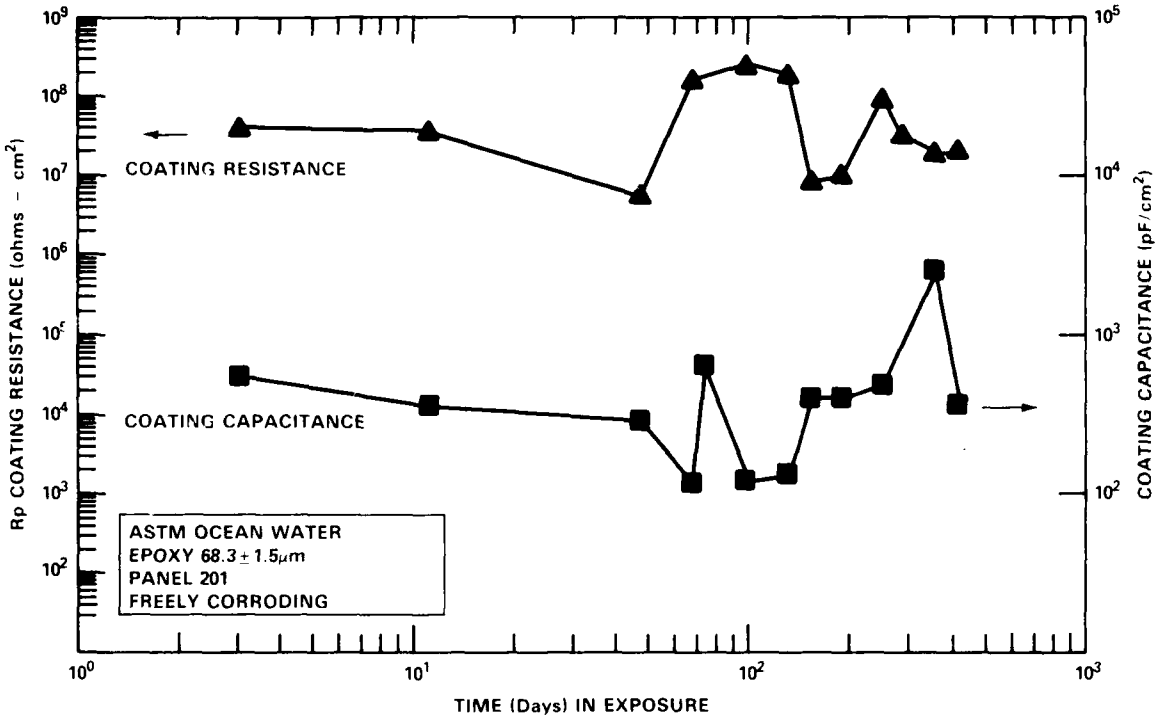

Fig. 54. Coating resistance and capacitance behavior as a function of exposure time for translucent epoxy coated steel.

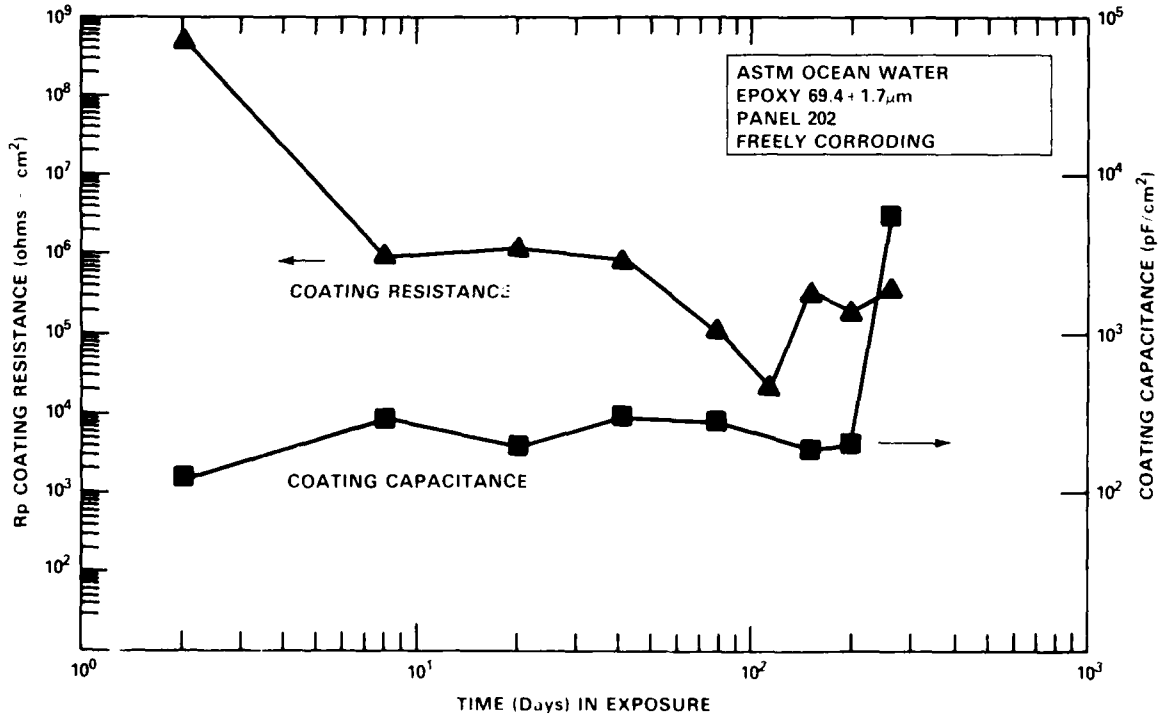

Fig. 55. Coating resistance and capacitance behavior as a function of exposure time for transluc nt epoxy coated steel.

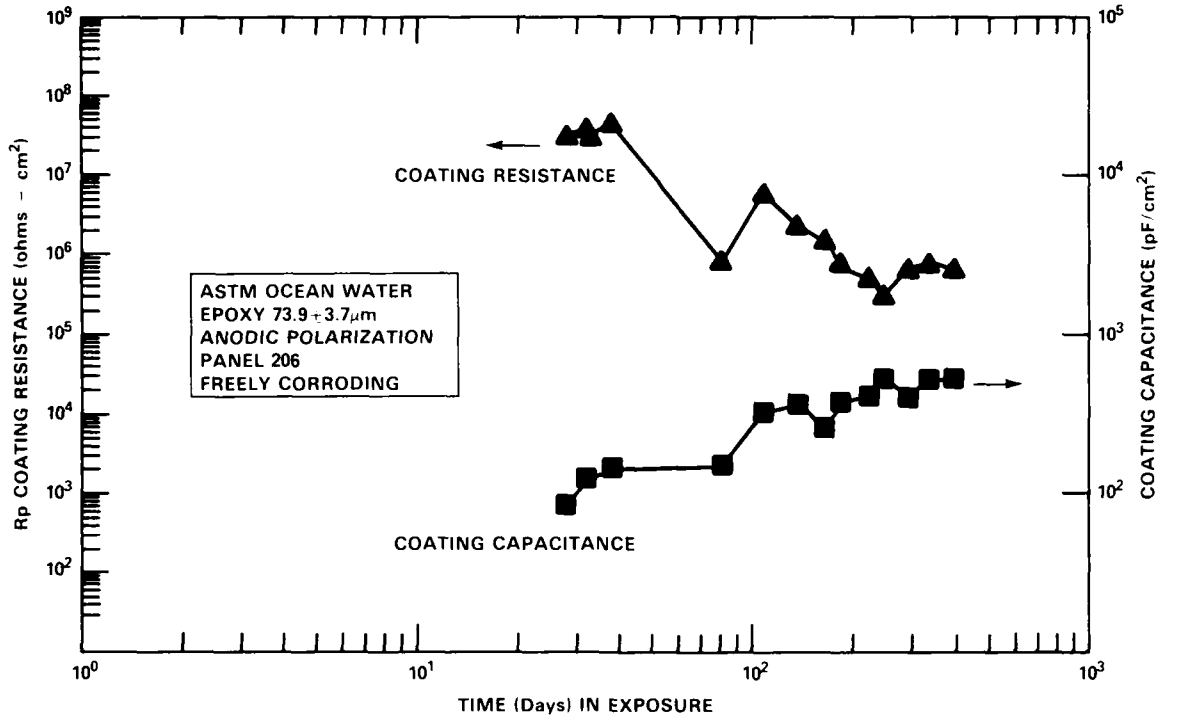

Fig. 56. Coating resistance and capacitance behavior as a function of exposure time for translucent epoxy coated steel.

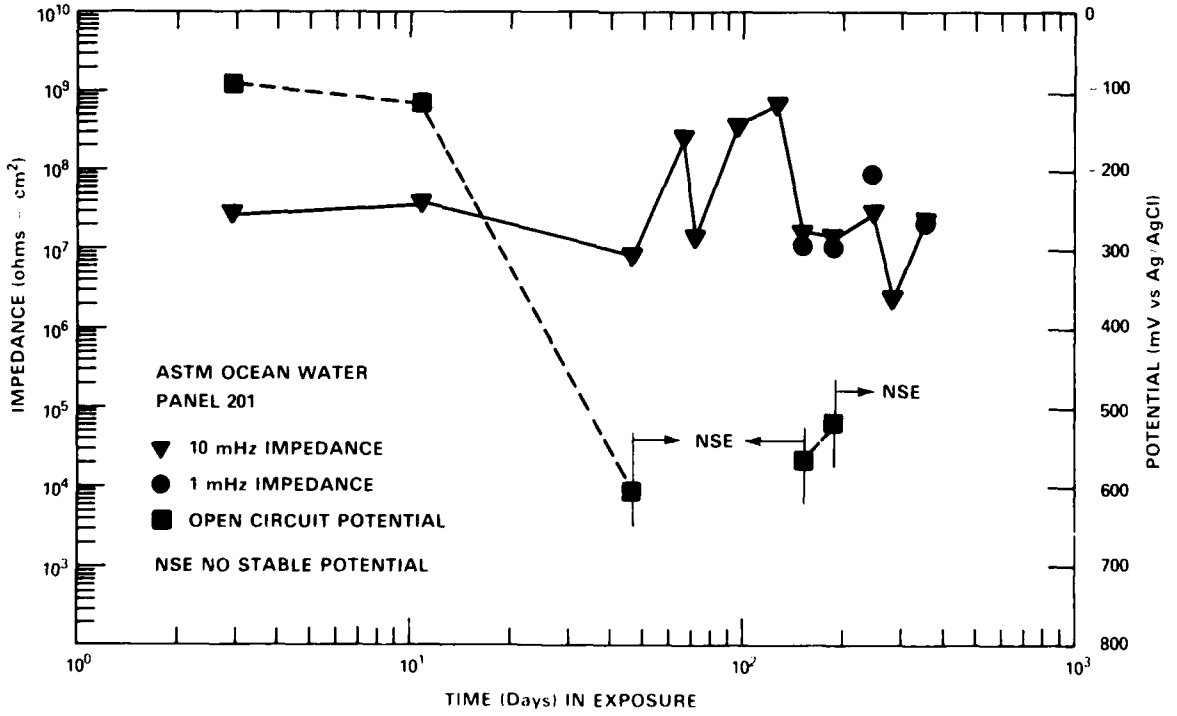

Fig. 57. Low frequency impedance behavior as a function of exposure time for translucent epoxy coated steel.

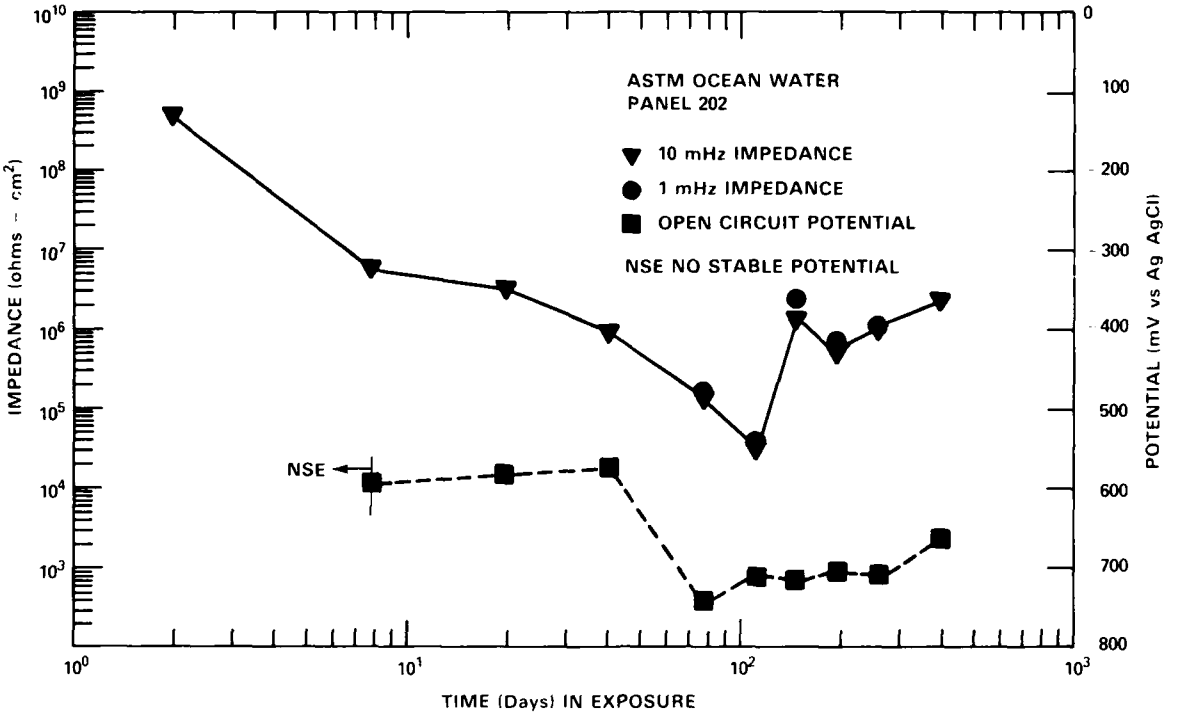

Fig. 58. Low frequency impedance behavior as a function of exposure time for translucent epoxy coated steel.

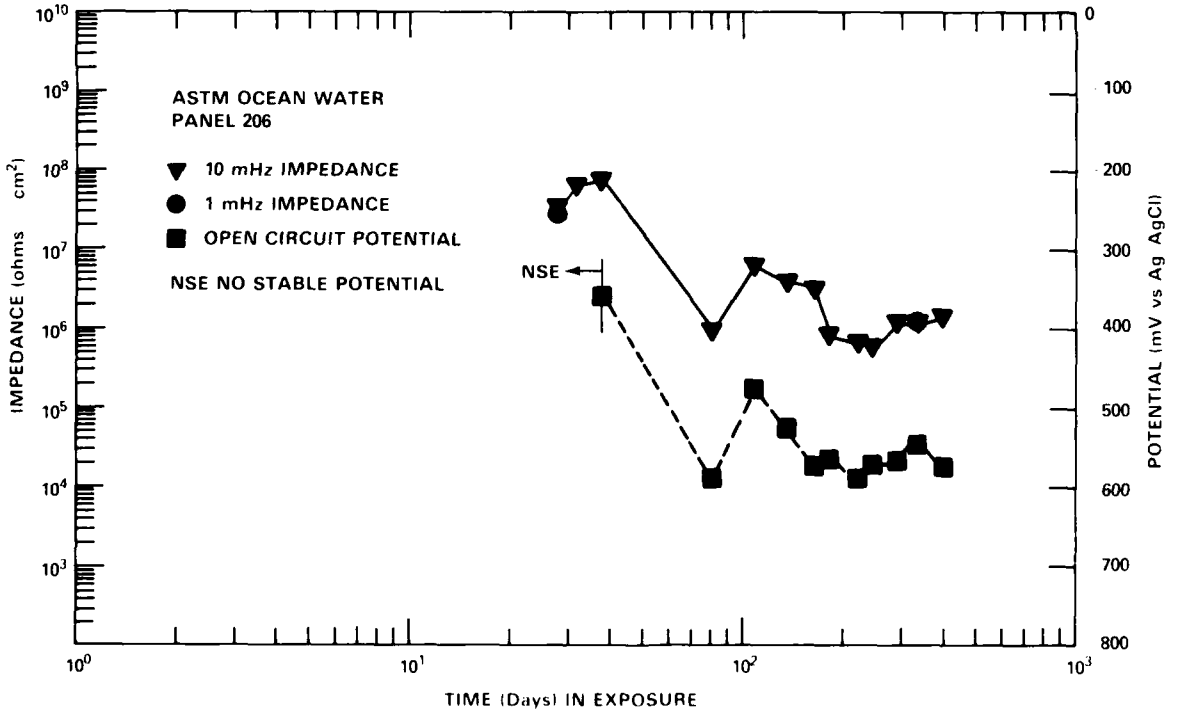

Fig. 59. Low frequency impedance behavior as a function of exposure time for translucent epoxy coated steel.

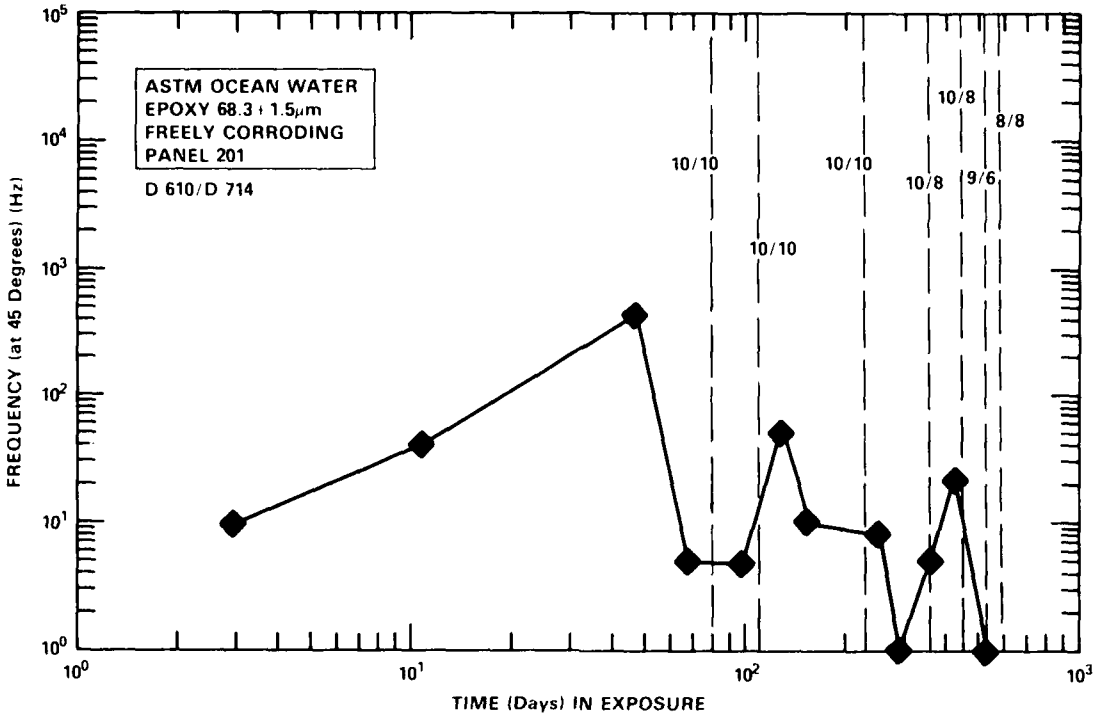

Fig. 60. Relative increases in electrochemically active area for translucent epoxy coated steel.

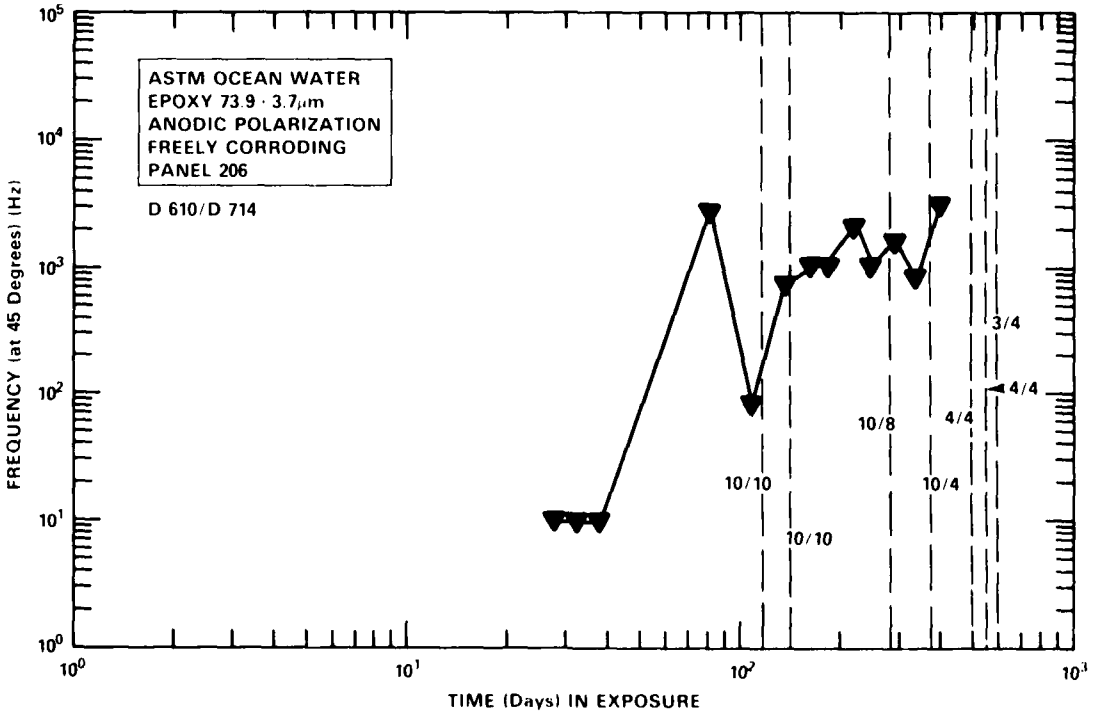

Fig. 61. Relative increases in electrochemically active area for translucent epoxy coated steel.

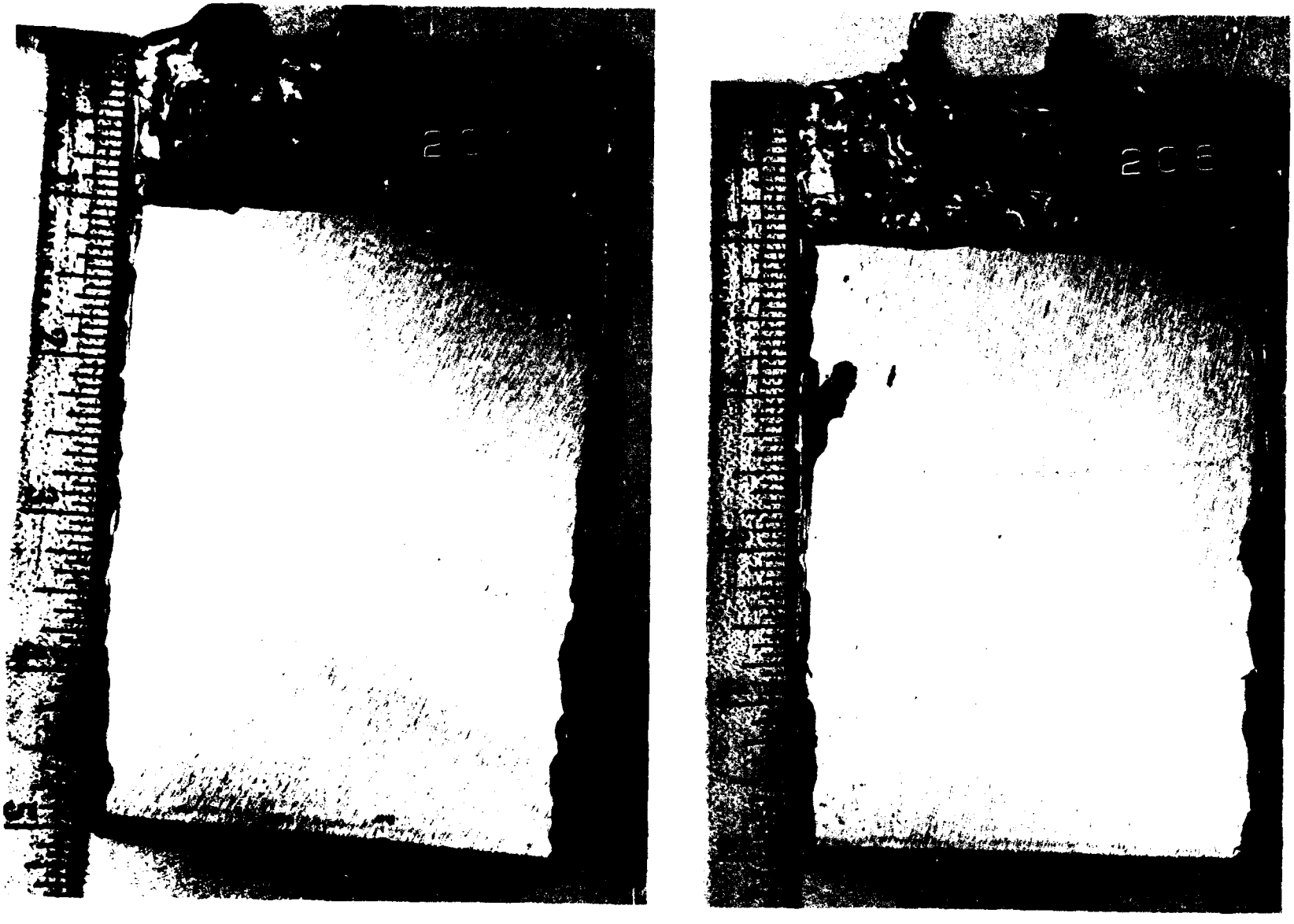

Fig. 62. Visual appearance of translucent epoxy coated steel after 110-days exposure in ASTM artificial ocean water.

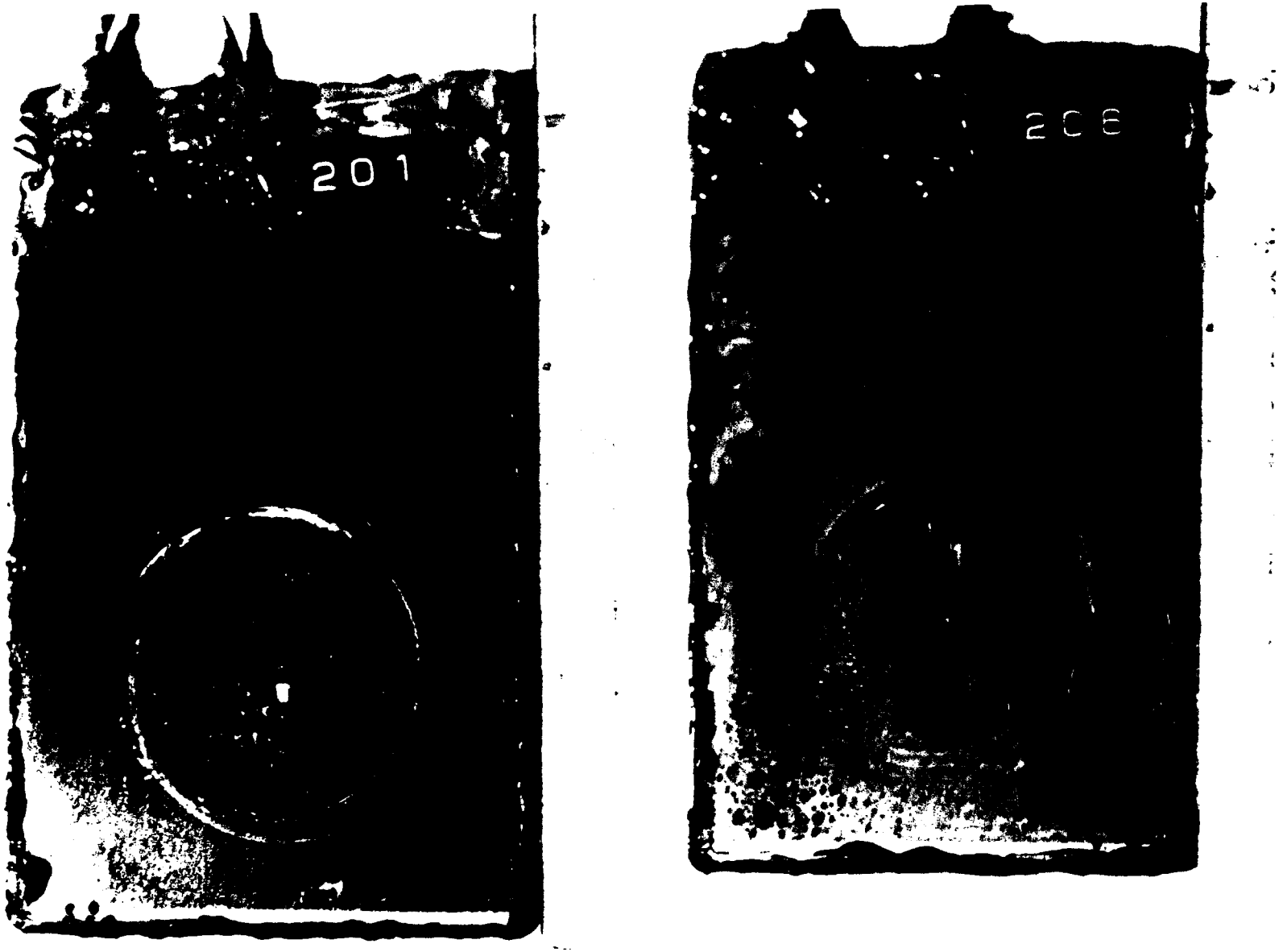

Fig. 63. Visual appearance of translucent epoxy coated steel after 475-days exposure in ASTM artificial ocean water.

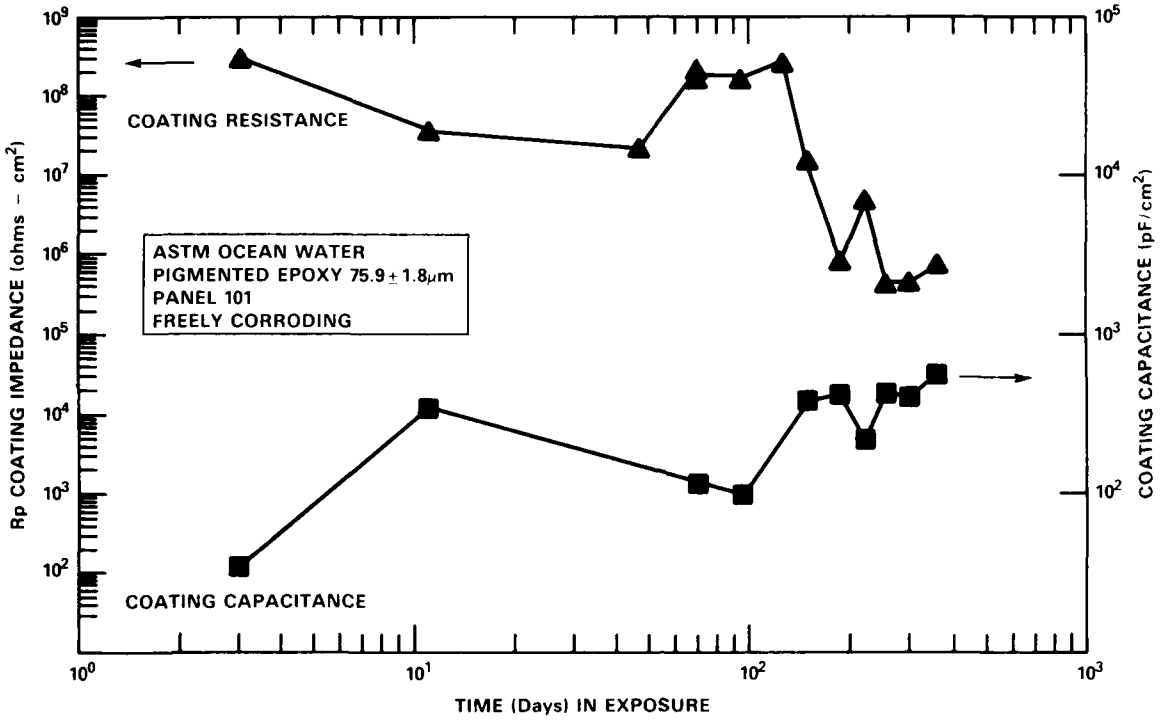

Fig. 64. Coating resistance and capacitance behavior as a function of exposure time for translucent pigmented epoxy coated steel.

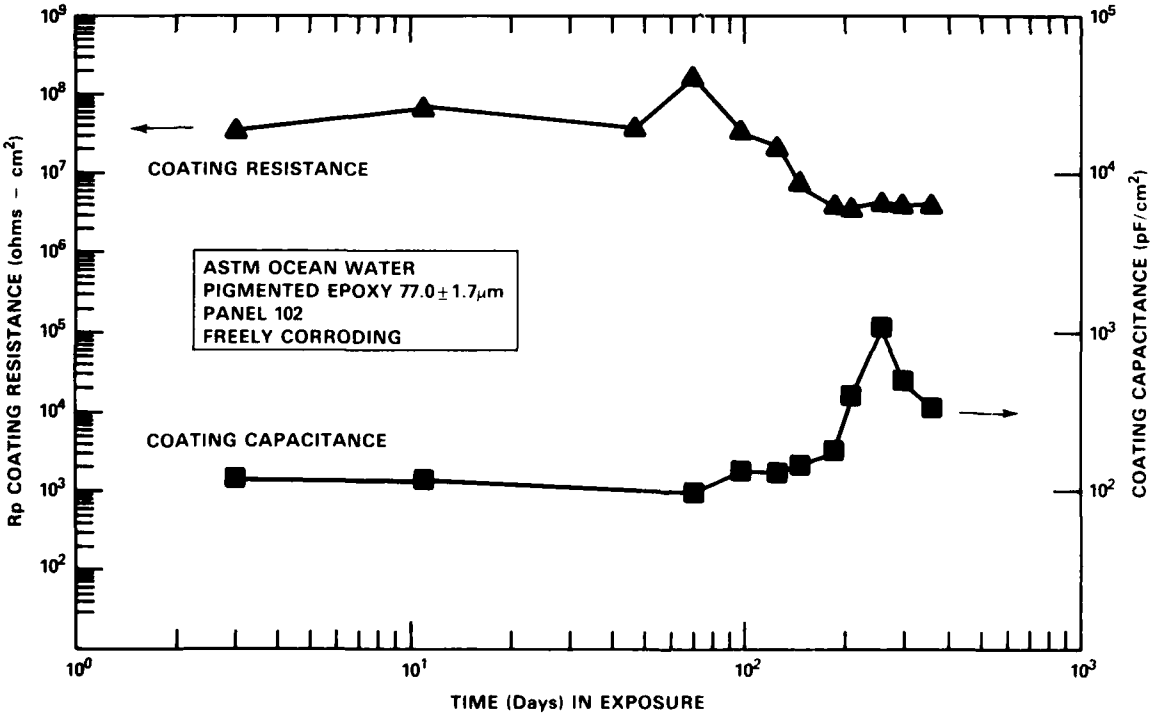

Fig. 65. Coating resistance and capacitance behavior as a function of exposure time for translucent pigmented epoxy coated steel.

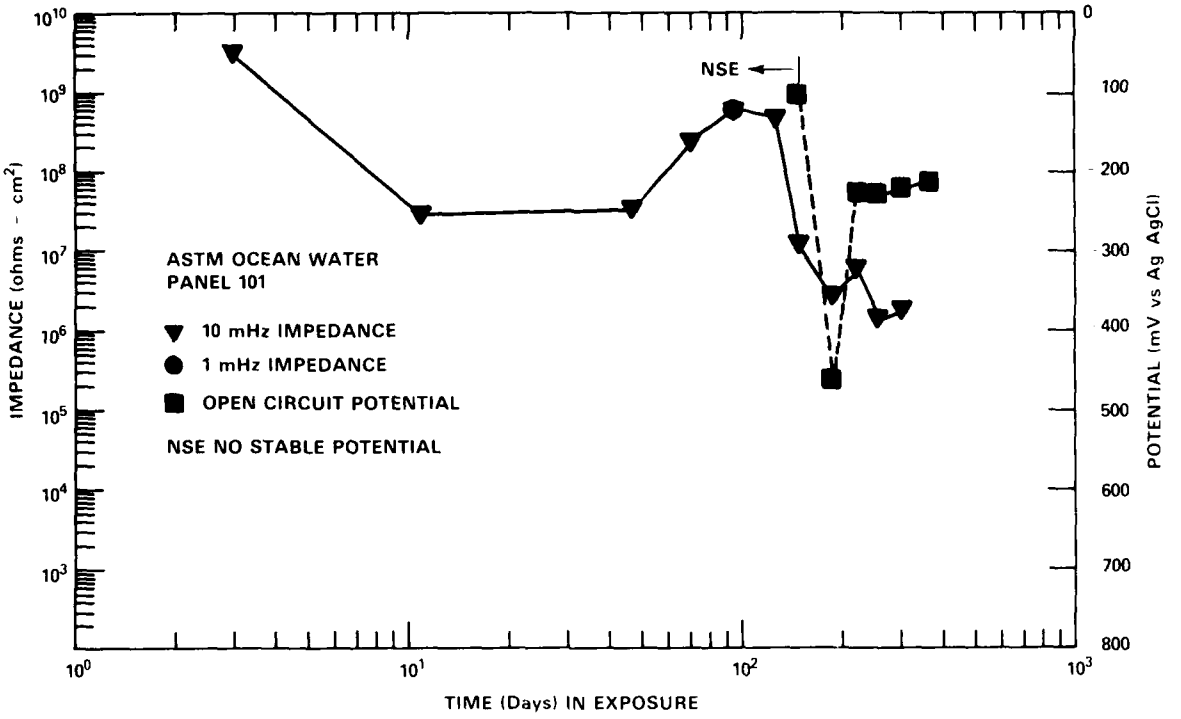

Fig. 66. Low frequency impedance behavior as a function of exposure time for translucent pigmented epoxy coated steel.

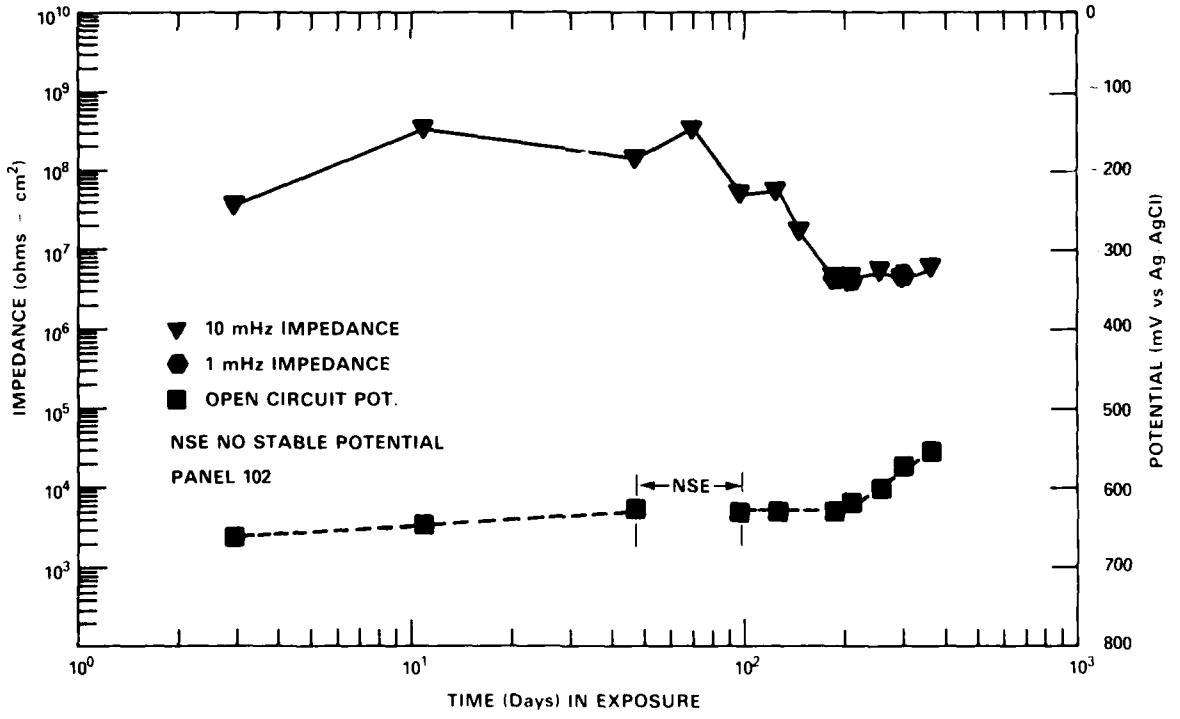

Fig. 67. Low frequency impedance behavior as a function of exposure time for translucent pigmented epoxy coated steel.

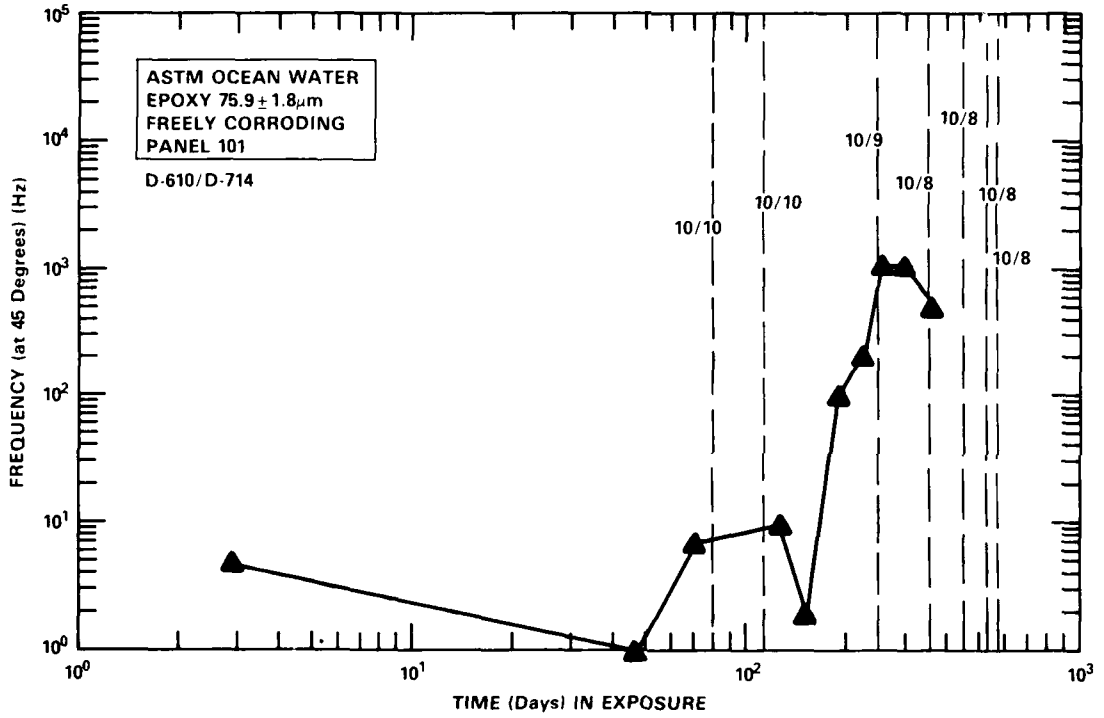

Fig. 68. Relative increases in electrochemically active area for translucent pigmented epoxy coated steel.

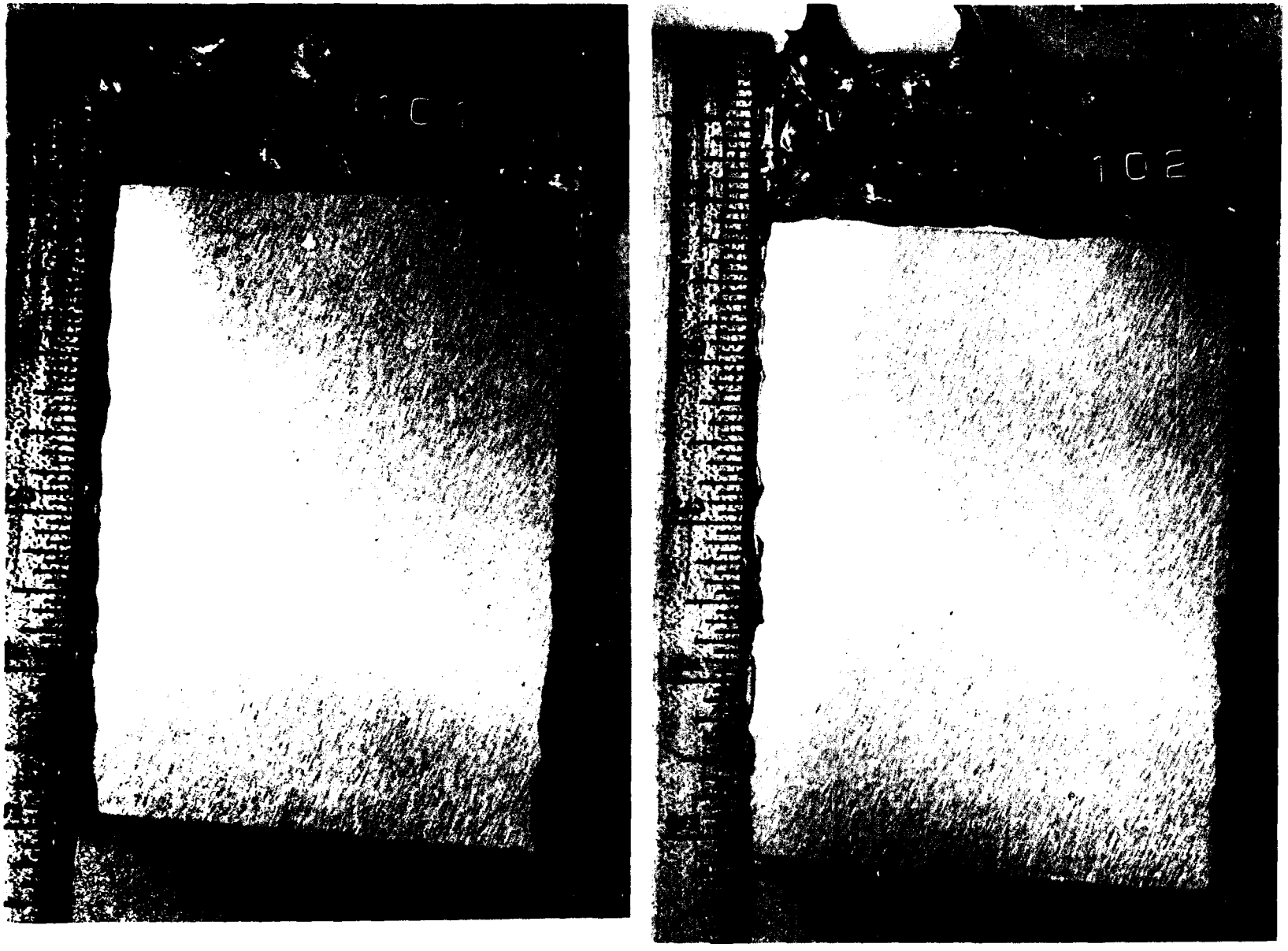

Fig. 69. Visual appearance of translucent pigmented epoxy coated steel after 110-days exposure in ASTM artificial ocean water.

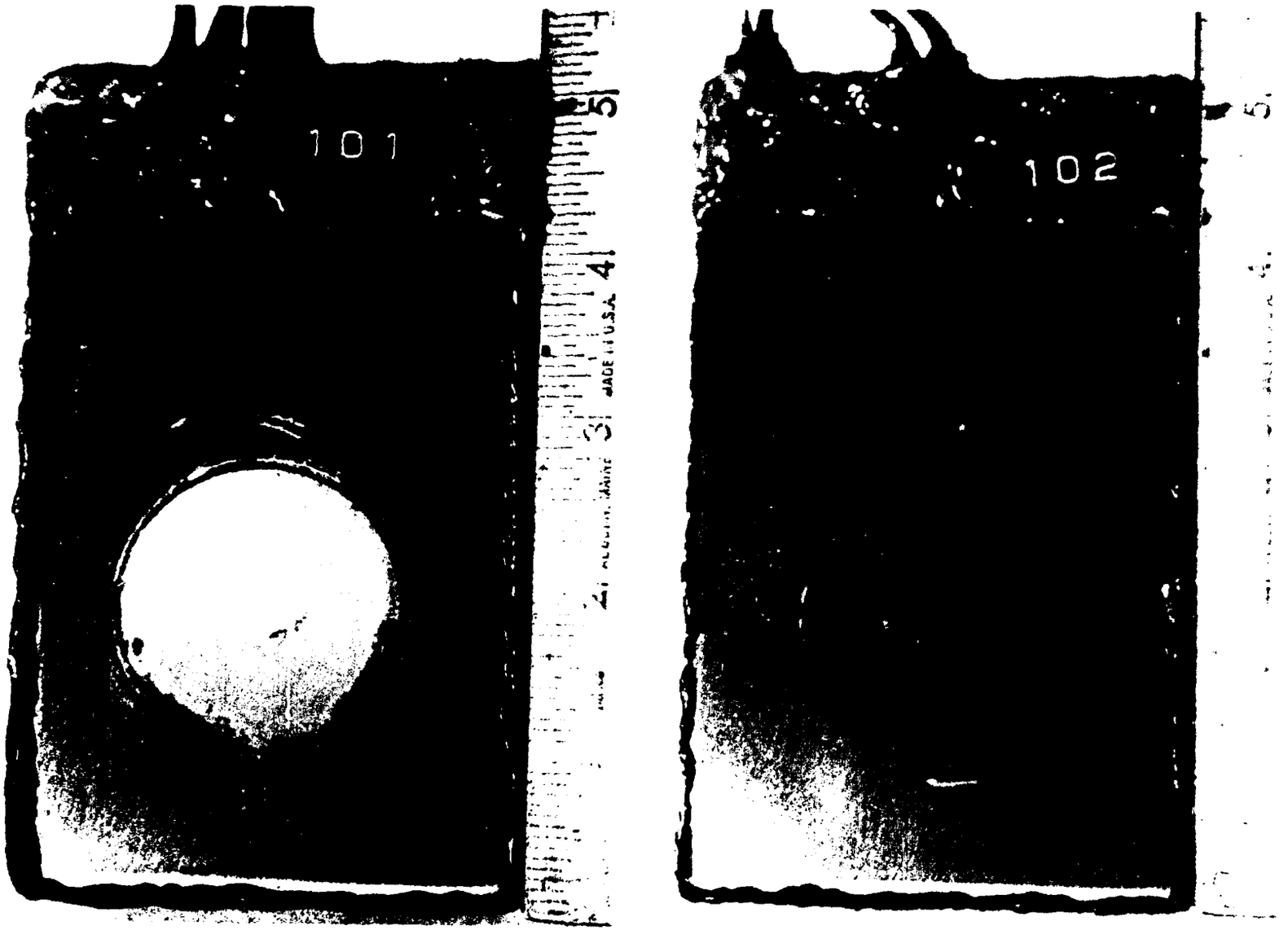

Fig. 70. Visual appearance of translucent pigmented epoxy coated steel after 475-days exposure in ASTM artificial ocean water.

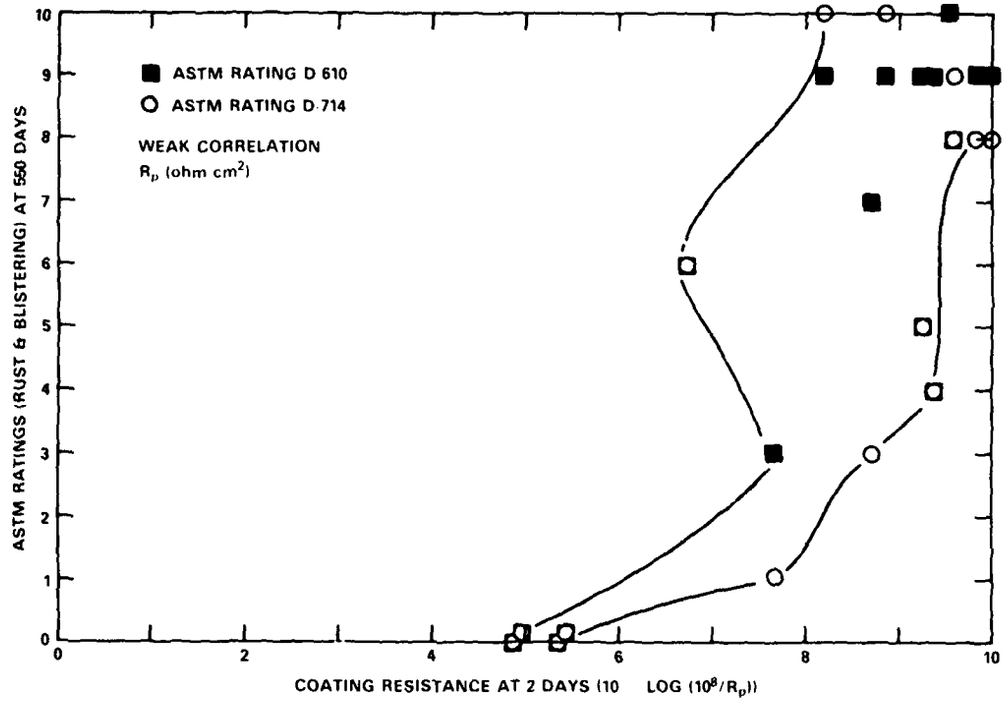

Fig. 71. Correlation between impedance data determined at short exposure time and 550-day ASTM visual evaluation: coating resistance at 2 days.

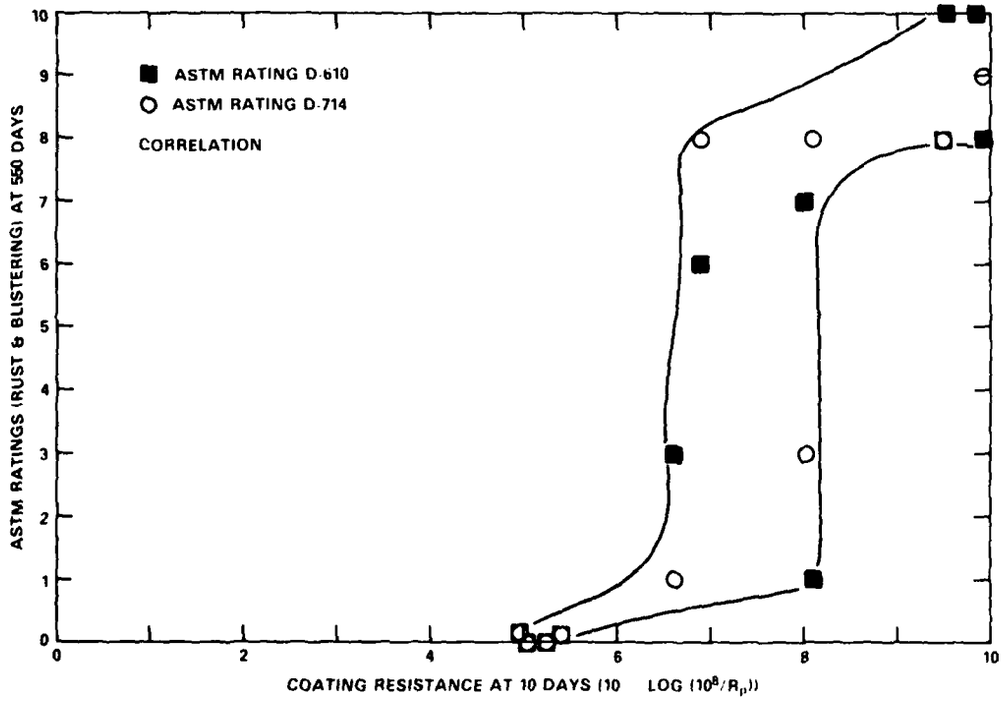

Fig. 72. Correlation between impedance data determined at short exposure time and 550-day ASTM visual evaluation: coating resistance at 10 days.

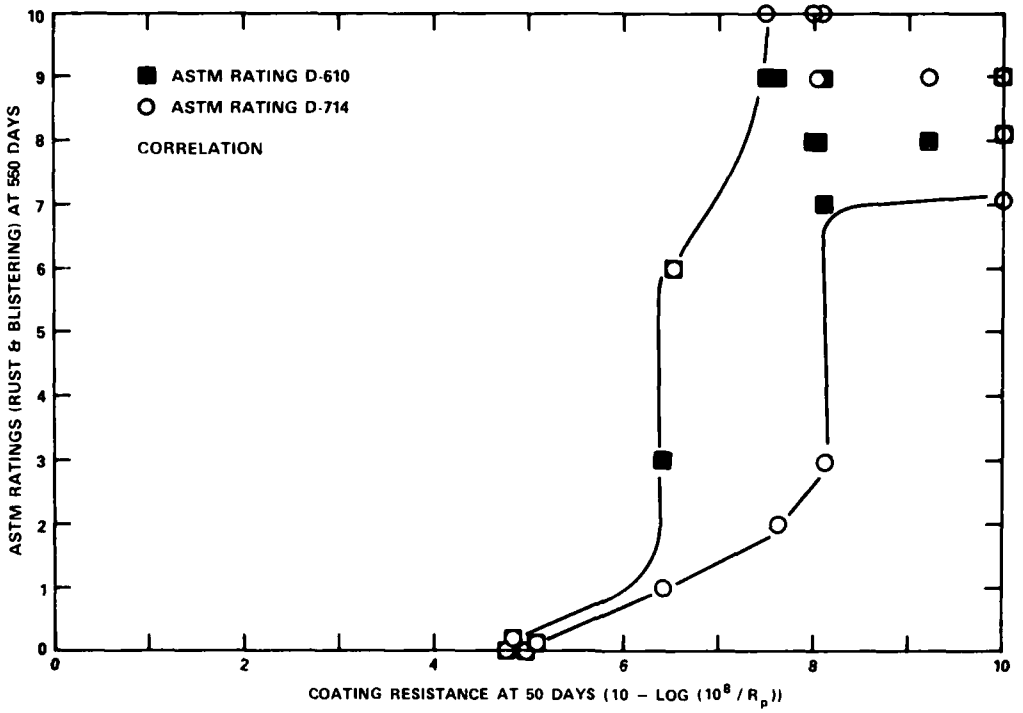

Fig. 73. Correlation between impedance data determined at short exposure time and 550-day ASTM visual evaluation: coating resistance at 50 days.

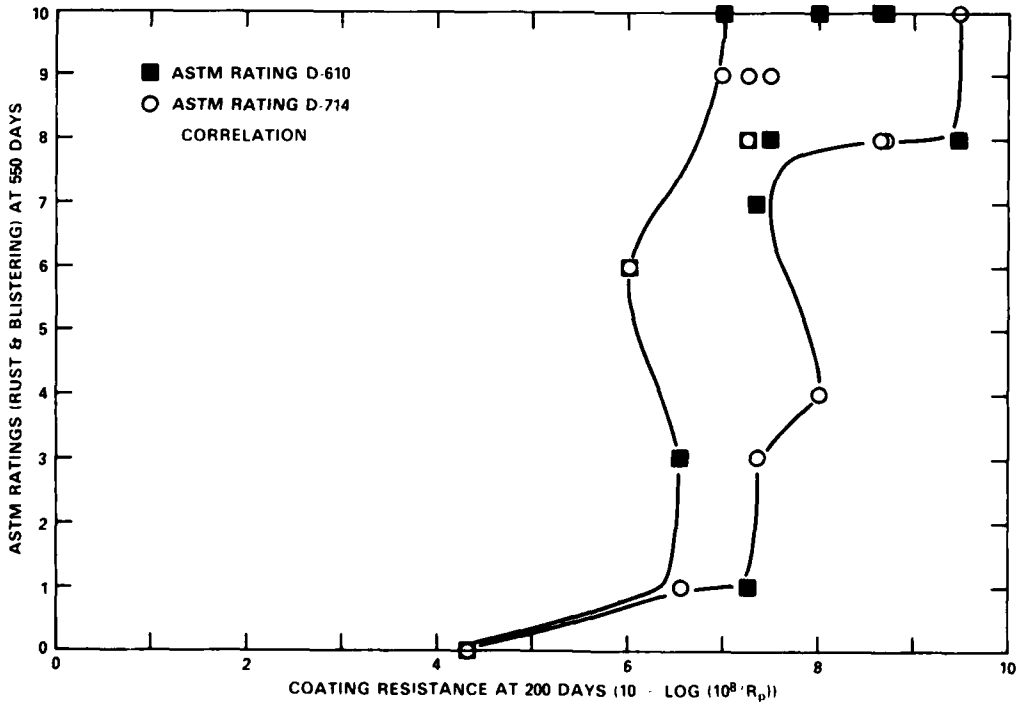

Fig. 74. Correlation between impedance data determined at short exposure time and 550-day ASTM visual evaluation; coating resistance at 200 days.

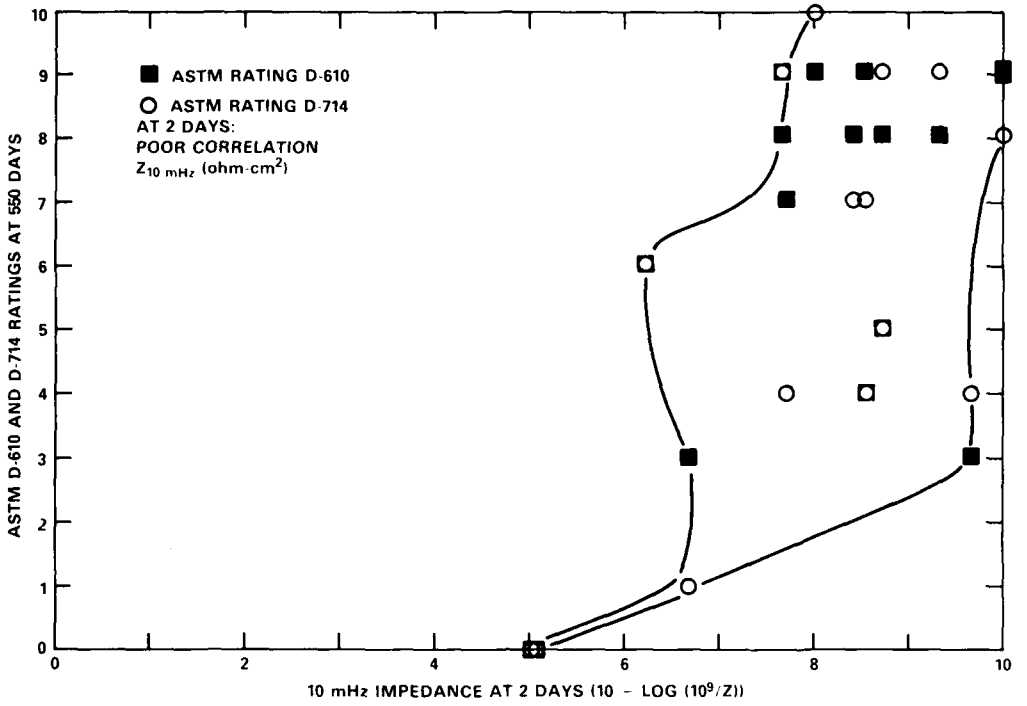

Fig. 75. Correlation between impedance data determined at short exposure time and 550-day ASTM visual evaluation: 10 mHz impedance at 2 days.

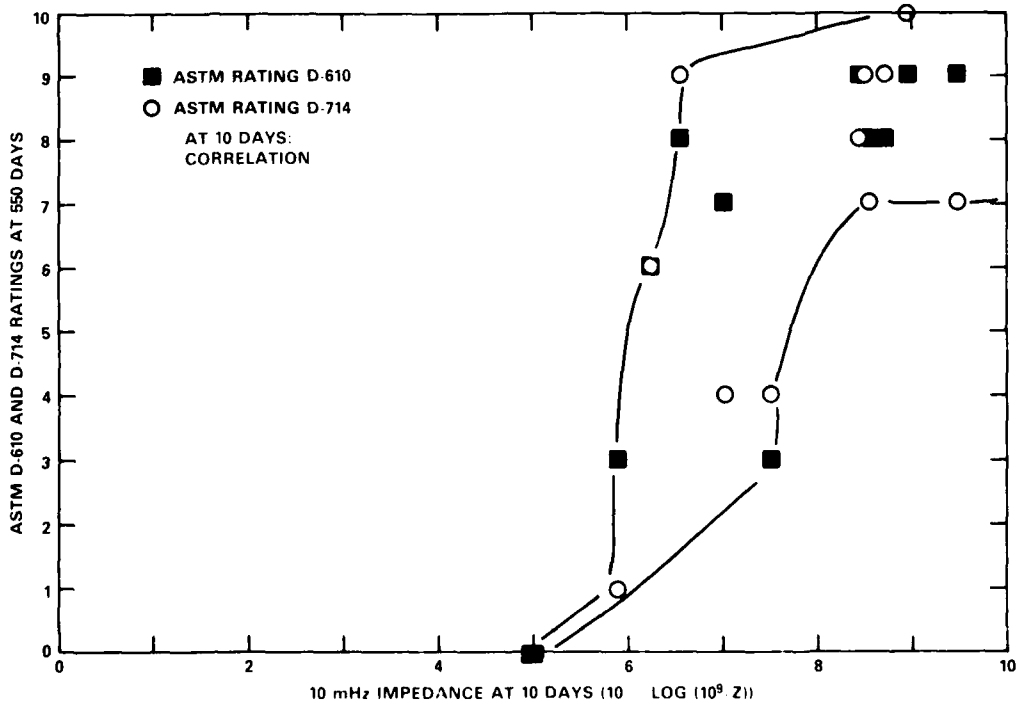

Fig. 76. Correlation between impedance data determined at short exposure time and 550-day ASTM visual evaluation: 10 mHz impedance at 10 days.

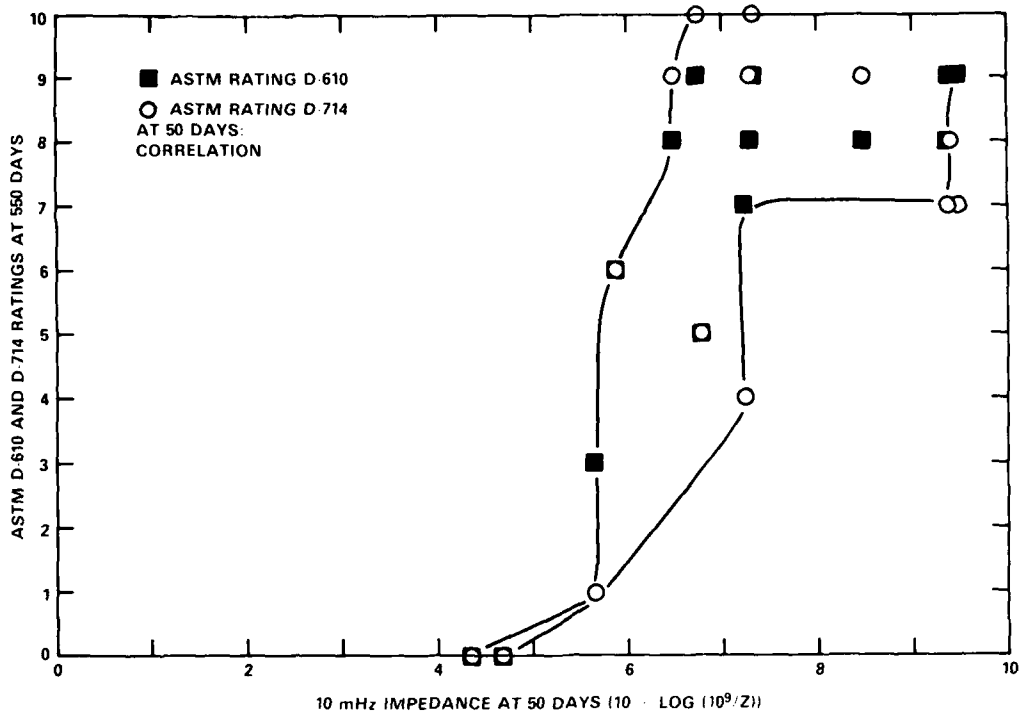

Fig. 77. Correlation between impedance data determined at short exposure time and 550-day ASTM visual evaluation: 10 mHz impedance at 50 days.

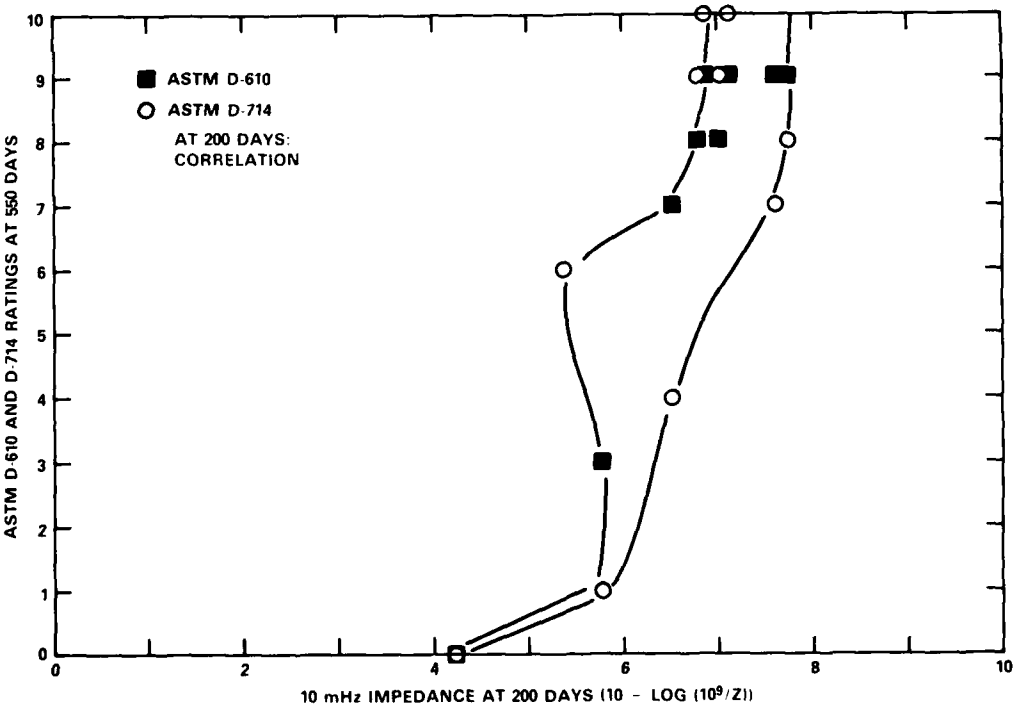

Fig. 78. Correlation between impedance data determined at short exposure time and 550-day ASTM visual evaluation: 10 mHz impedance at 200 days.

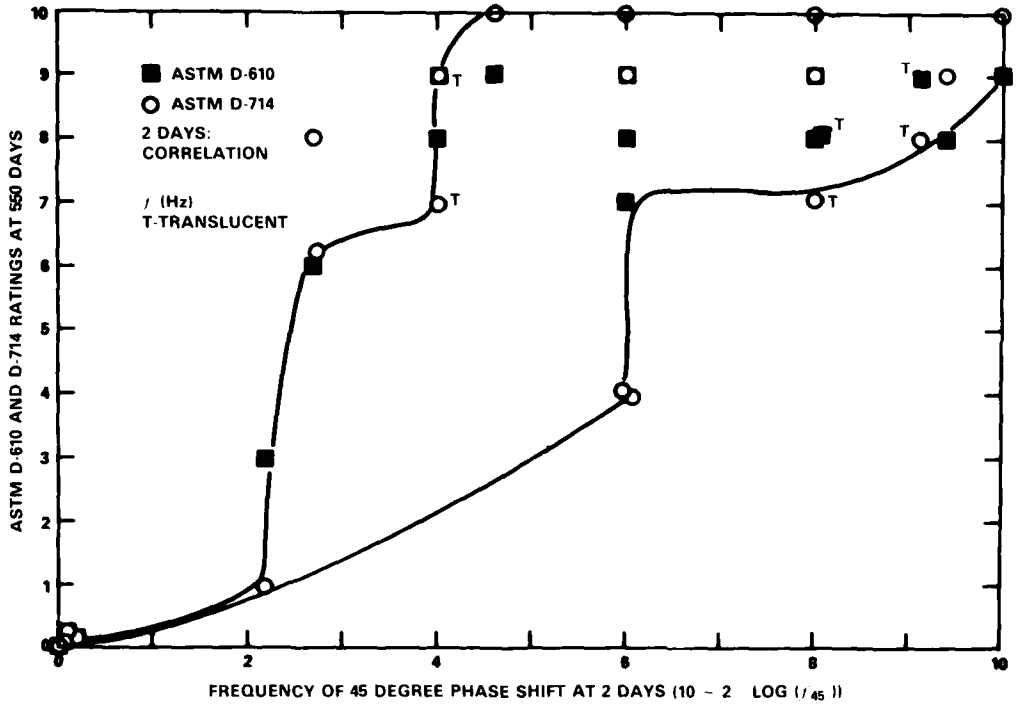

Fig. 79. Correlation between impedance data determined at short exposure time and 550-day ASTM visual evaluation: 45 degree phase shift frequency at 2 days.

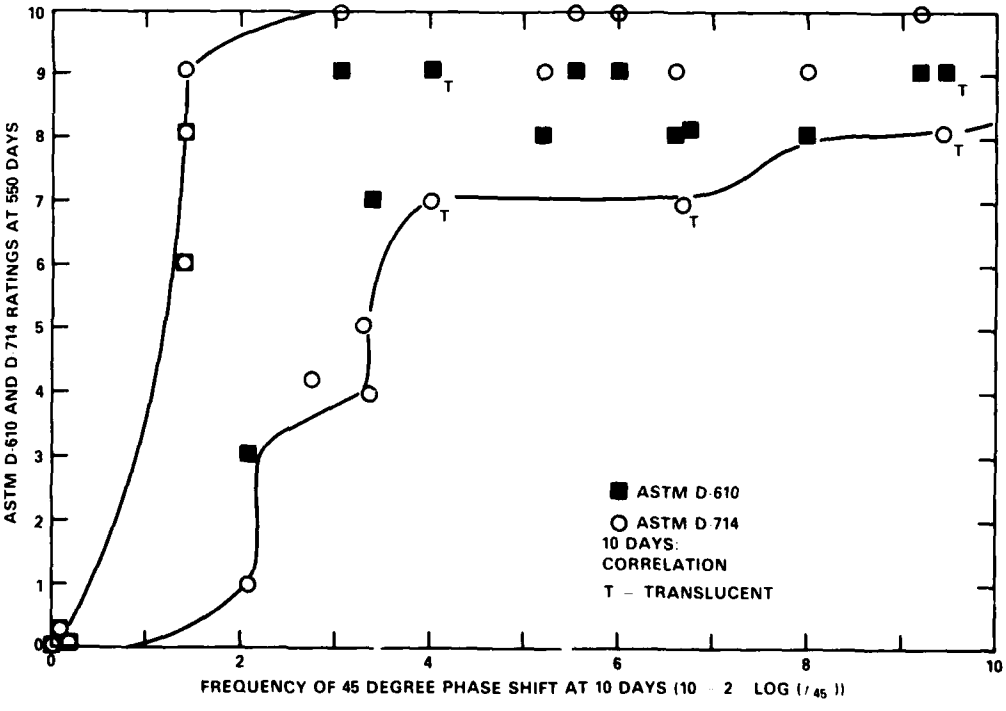

Fig. 80. Correlation between impedance data determined at short exposure time and 550-day ASTM visual evaluation: 45 degree phase shift frequency at 10 days.

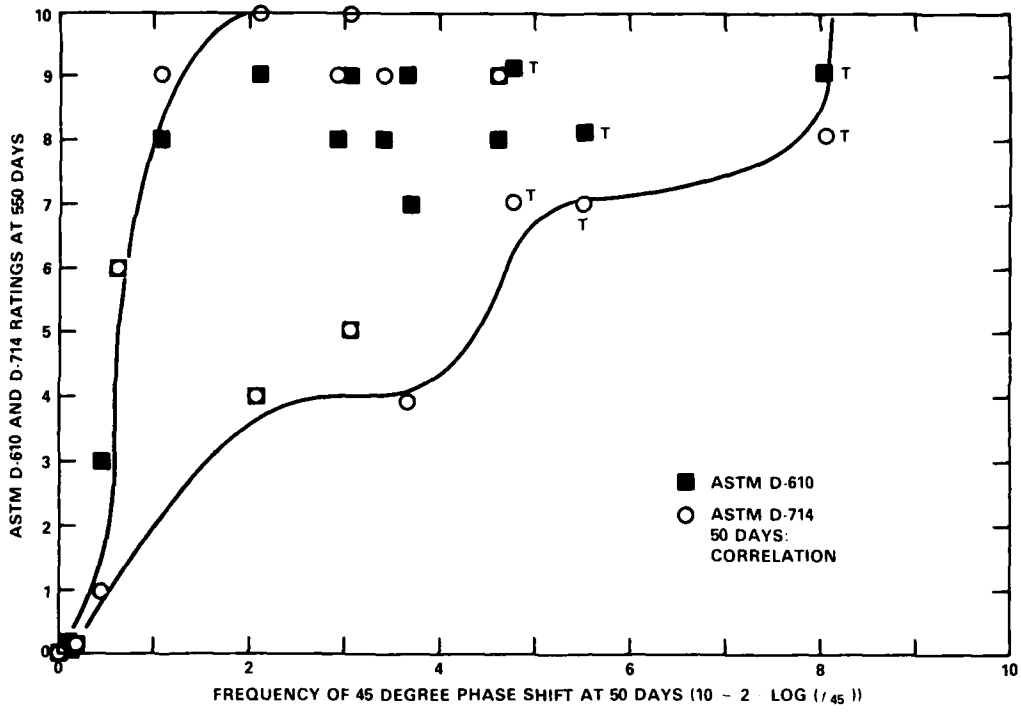

Fig. 81. Correlation between impedance data determined at short exposure time and 550-day ASTM visual evaluation: 45 degree phase shift frequency at 50 days.

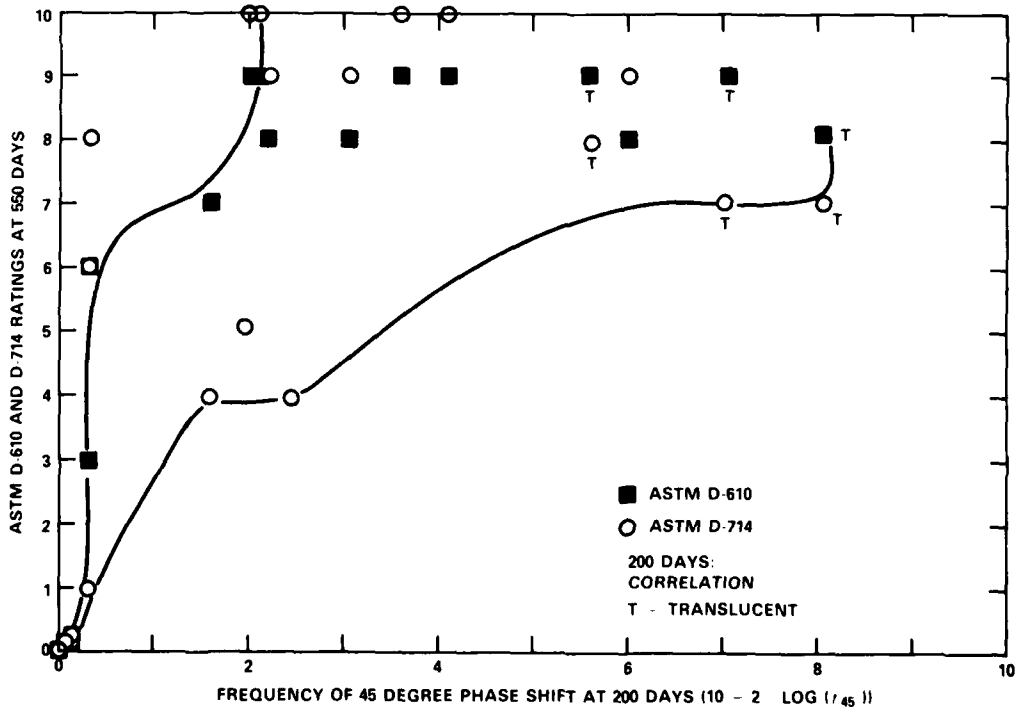

Fig. 82. Correlation between impedance data determined at short exposure time and 550-day ASTM visual evaluation: 45 degree phase shift frequency at 200 days.

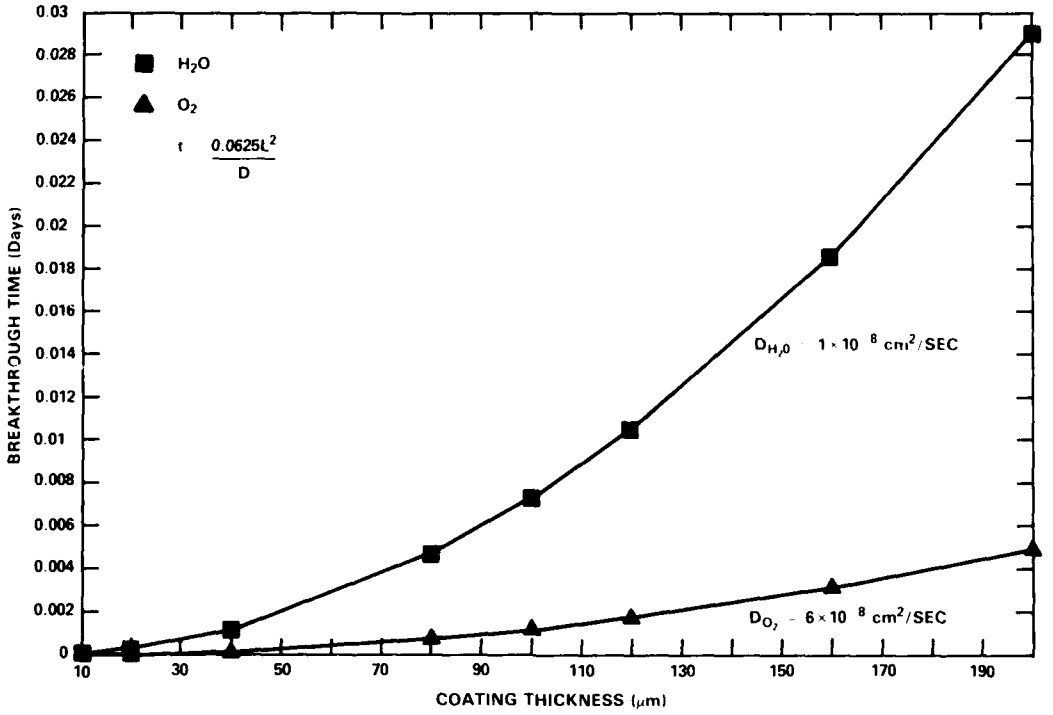

Fig. 83. Electrolyte permeation for epoxy polyamide coatings: H_2O, O_2.

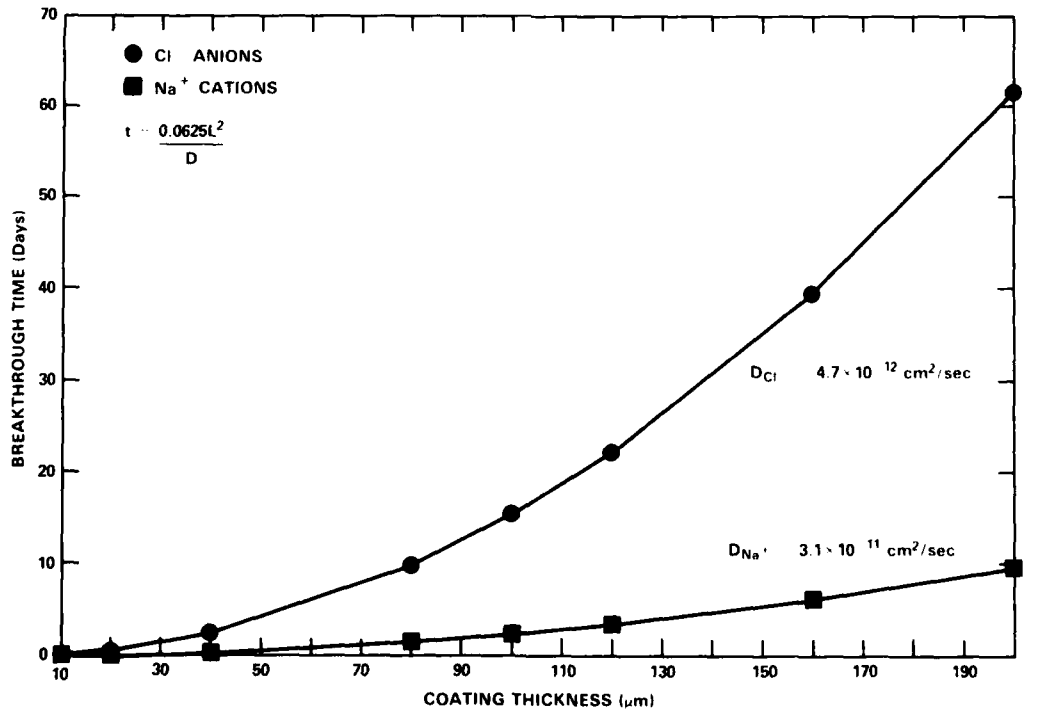

Fig. 84. Electrolyte permeation for epoxy polyamide coatings: Na^+, Cl^-.

REFERENCES

1. Scully, J.R., "Electrochemical Impedance Spectroscopy for Evaluation of Organic Coating Deterioration and Underfilm Corrosion--A State of the Art Technical Review," DTRC Rept SME 86/006 (Sep 1986).

2. Mansfeld, F. and M. Kendig, "Evaluation of Protective Coatings with Impedance Measurements," Presented at the International Congress on Metallic Corrosion, Toronto, Canada, Sponsored by The National Research Council, Canada, Vol. 3, p. 74, (June 1984).

3. Mansfeld, F., M. Kendig, and S. Tsai, Corrosion Science, Vol. 33, No. 4, pp. 317-329 (1983).

4. ASTM Standard D-823, 1986 ASTM Annual Book of Standards, Vol. 06.01, p.140, (Mar 1987).

5. McKubre, M.C., CORROSION 87, Paper No. 480, San Francisco, CA (Mar 1987).

6. Leidheiser, H., D.J. Mills, and W. Bilder, In: Corrosion Protection by Organic Coatings, M.W. Kindig and H. Leidheiser, eds., ECS Proceedings, Vol. 87-2, p. 31 (1987).

7. M. Sluyters-Rehbach, and J.H. Sluyters, In: Electroanalytical Chemistry, A.J. Bard, M. Dekker, eds., Vol. 4 (1970).

8. A.J. Bard, L.R. Faulkner, Electrochemical Methods, Fundamentals, and Application, John Wiley and Sons, NY (1980).

9. MacDonald, D.D. and M.C. McKubre, In Electrochemical Corrosion Testing, ASTN STP 727, F. Mansfeld, U. Bertocci, eds., ASTM, Philadelphia, PA, p. 110 (1981).

10. Juttner, K. and W.J. Lorenz, In: Proceedings of the Symposium on Computer Aided Acquisition and Analysis of Corrosion Data, Electrochem. Soc. Proc., Vol. 85-3, M.W. Kendig, U. Bertocci, and J.E. Strutt, eds., p. 75 (1985).

11. Bonnel, A., F. Dabosi, C. Deslouis, M. Duprat, M. Keddam, and B. Tribollet, J. Electrochem. Soc., Vol 130, No. 4, p.753 (1983).

12. Dawson, J.L. and D.G. John, J. Electroanal. Chem., Vol. 110, p. 37 (1980).

13. Buck, R.P., J. of Electroanal. Chem., Vol. 18, p.363,381,387 (1977).

14. Polymers Handbook, 2nd Edition, J. Bandrup and E.H. Immergut, eds., John Wiley and Sons, New York (1975).

15. Touhassent, R. and H. Liedheiser, Corrosion, Vol. 28, No. 12, p. 435 (Dec 1982).

16. Haruyama, S., M. Asari, and T. Tsuru, In: Proceedings of the Symposium on Corrosion Protection by Organic Coatings, Electrochem. Soc. Proc. Vol. 87-2 M. Kendig, H. Leidheiser, Eds., p. 197 (1986).

17. ASTM Standard D-610, 1986 ASTM Annual Book of Standards Vol. 06.01, p.98, (1986).

18. ASTM Standard D-714, 1986 ASTM Annual Book of Standards Vol. 06.01, p.124, (1986).

19. Leidheiser, H., R.D. Granata, and R. Turoscy, Corrosion, Vol. 43, No. 5, pp. 296 (1986).

20. Parks, J. and H. Leidheiser, Jr., Ind. Eng. Chem. Prod. Res. Dev., Vol. 25, No.1 (1986).

21. Ruggeri, R.T. and T.R. Beck, Corrosion, Vol. 39, No. 11, p. 452 (1983).

22. Glass, A.L. and J. Smith, J. Paint Technol, 39(511), p. 490-493 (1969).

INITIAL DISTRIBUTION

Copies

1 DARPA
1400 Wilson Blvd
Arlington, VA 22209
Attn: Dr. P. Parrish

1 Office of Deputy Under Secretary
of Defense for Research
Room 3D1089, Pentagon
Washington, DC 20301
Attn: Mr. Jerome Persh

1 U.S. Army Chemical R&D Center
Aberdeen Proving Ground, MD
21010-5423
Attn: Mr. Paul Cannan, Jr.

3 Department of the Army
AMTL
SLCMT-MCM-SB
Watertown, MA 02172
Attn: Mr. M. Levy
Dr. E. Wright

2 U.S. Army Research Office
Associate Director of
Metallurgy & Materials
Science Division
P.O. Box 1221
Triangle Park, NC 27709
Attn: Dr. John Hurt
Dr. Robert Rebar

1 U.S. Army Material Command
5001 Eisenhower Avenue
Alexandria, VA 22333
Attn: Mr. I. Smart

3 Naval Research Laboratory
Dr. R. Crowe (Code 6372)
Dr. J. Crooker (Code 6310)
Dr. E. McCafferty (Code 6310)

2 Office of Naval Research
800 N. Quincy Street
Arlington, VA 22217
Dr. J. Sederiks (Code 1131)
Dr. S. Fishman (Code 1131)

Copies

2 Commander
Naval Surface Weapons Center
Silver Spring, MD 20910
Attn. Dr. C. Dacres (Code R33)
Dr. J. Tydings (Code R32)

1 Commander
Naval Surface Weapons Center
Dahlgren, VA 22448
Attn: Dr. S. Bettadapur (Code G53)

4 Commander
Naval Civil Engineering Laboratory
Port Hueneme, CA 93043
Attn: Dr. R. Drisko, Dr. P. Hearst
Mr. J. Jenkins, Mr. Brunner

1 Commander
Naval Ocean Systems Center
San Diego, CA 92152
Attn: Mr. Gordon Chase (Code 932)

12 Defense Technical Information Center
Cameron Station
Alexandria, VA 22314

3 Commanding Officer
Air Force Materials Laboratory
Wright-Patterson AFB
Dayton, OH 45433
Attn: Mr. F. Meyer (Code MLSA)

1 Air Force Office of Scientific
Research
Bolling Air Force Base
Washington, DC 20332
Attn: Dr. A. Rosenstein

1 NASA Headquarters
600 Independence Avenue
Washington, DC 29546
Attn: Dr. G. Deutsch

2 National Bureau of Standards
Washington, DC 20234
Attn: Dr. N.E. Pugh and
Dr. U. Bertocci

Copies

1 Monsanto Company
800 N. Lindbergh Blvd.
St. Louis, MO 63167
Attn: Dr. David Silverman

4 Center for Surface and Coating Research
Sinclari Laboratory 7
Lehigh University
Bethlehem, PA 18015
Attn: Dr. Richard Granata and
Dr. H. Leidheiser

3 EG&E
Princeton Applied Research
P.O. Box 2565
Princeton, NJ 08540
Attn: Mr. Marc Rothstein,
Mr. Robert S. Rodgers,
Mr. Bill Eggers

1 Martin-Marietta Laboratories
1450 South Rolling Road
Baltimore, MD 21227-3898
Attn: Dr. J. Ahearn and
Dr. W. Moshier

1 S.C. Johnson & Son
Racine, WI 53403
Attn: Mr. David A. Tomkins

1 FMC Corporation
Central Engineering Labs
1185 Coleman Ave., Box 580
Santa Clara, CA 95052
Attn: Mr. Manual Mekhijan

1 The Proctor & Gamble Company
Winton Hill Technical Center
6300 Center Hill Road
Cincinnati, OH 45224
Attn: Mr. George W. Coates

1 Columbia Gas Systems Service Corporation
1600 Dublin Road
P.O. Box 2318
Columbus, OH 45224
Attn: Mr. Arthur Eberle

Copies

1 Electrical Technology Corp.
1601 Dexter Avenue
N. Seattle, WA 98109
Attn: Dr. Theodore Beck

1 Department of Physics
Case Western Reserve University
Cleveland, OH 44106
Attn: Philip Taylor

1 Chemistry Department
Kent State University
Kent, OH 44242
Attn: Dr. Carl Knauss

1 Polymers and Coatings Department
North Dakota State University
Fargo, ND 58105
Attn: Dr. Marek Urban

1 Department of Chemistry
University of Missouri
Rolla, MO 65401
Attn: Dr. James Stoffer

1 University of Nevada
Reno, NV 89557
Attn: Dr. Denny Jones

1 Georgia Tech Research Institute
Georgia Institute of Technology
Atlanta, GA 30332
Attn: Dr. Thomas Starr

1 Sherwin-Williams Company
Research Center
10909 South Cottage Grove Ave.
Chicago, IL 60628
Attn: Dr. Gordon Bierwagen

1 Rockwell Science Center
1049 Camino Dos Rios
Thousand Oaks, CA 93160
Attn: Dr. Martin Kendig

1 National Bureau of Standards
Center for Building Technology
Gaithersburg, MD 20899
Attn: Dr. J.W. Martin

Copies

1 Steel Structures Painting Council
4400 Fifth Avenue
Pittsburgh, PA 15213
Attn: Dr. Bernard Appleman

3 The Johns Hopkins University
Corrosion & Electrochemistry Research
Center
Charles & 34th Street
Baltimore, MD 21218
Attn:. Dr. J. Kruger, Dr. P.J. Moran
and Dr. G. Prentice

CENTER DISTRIBUTION

Copies

1 012 (Moran)

1 0115 (Caplan)

1 28

1 2801

1 2803

5 281

20 2813 (Morton)

30 2813 (Scully)

1 2814 (Montemarano)

1 284

5 2841 (Montemarano/Ross/Laster/Loeb

1 522.2 (TIC)

2 5231 (Office Services)

☆U.S. G.P.O. 1988-202-270:80001